by Anhalt University of Applied Sciences and Perm National Research Polytechnic University

Proceedings of the 5th International Conference on Applied Innovations in IT

Volume 5

EDITION
Hochschule Anhalt

Proceedings of the 5th International Conference on Applied Innovations in IT

Volume 5

Koethen , Germany
16 March 2017

Editors:

Prof. Dr. Eduard Siemens* (editor in chief),
Dr. Bernd Krause*,
Dr. Leonid Mylnikov**

(*Anhalt University of Applied Sciences,
** Perm National Research Polytechnic University)

This volume contains publications of the International Conference on Applied Innovations in IT (ICAIIT), which took place in Koethen March 16th 2017. The conference is devoted to problems of applied research in the fields of automation and communications. The research results can be of interest for researchers and development engineers, who deal with theoretical base and the application of the knowledge in the respective areas.

ISBN: 978-3-96057-024-0 (Online)
ISSN: 2199-8876

Additional copies of this publication are available from:
FB6 Anhalt University of Applied Sciences
Postfach 1458
D-06354 Koethen, Germany
Phone: +49 3496 67 2327
Email: eduard.siemens@hs-anhalt.de
Web: http://icaiit.org

Content

Section 3. Automation and algorithms

Section 4. Data processing and data analysis

Fraud Attacks in VoIP-Based Communications Systems
Risk Analysis, Prevention, Protection, Detection

Benedikt Machens[1], Olaf Gebauer[2] and Diederich Wermser[1,2]
[1]*IANT - International Applied NGN Technologies GmbH, Salzdahlumer Str. 46/48, D-38302, Wolfenbüttel, Germany*
[2]*Research Group IP-Based Communication Systems, Ostfalia University of Applied Sciences, Salzdahlumer Str. 46/48, D-38302, Wolfenbüttel, Germany*
benedikt.machens@iant.de, {ola.gebauer, d.wermser}@ostfalia.de

Keywords: Fraud, VoIP, PBX, Honey Pot, SIP, SIPX, SBC.

Abstract: This paper explains how fraud on modern VoIP-Systems works and which attacks are executed. This was examined practically by the example of a honey pot PBX, which ran for about 3 months and was monitored accordingly. Furthermore, this paper presents possibilities of how to protect productive VoIP systems against Fraud and to examine the fraud vulnerability.

1 INTRODUCTION

Fraud in general is the attempt to obtain a paid service. In the times of the analogue- or ISDN telephony, the obtained service often was a subscription or a simple telephone Advertisement like e-mail spam. By shutting down ISDN and the newly wide use of VoIP-Technologies, every telephone system is now affected by this danger. The user must be aware of the fact that he must accept losses in security due to the better availability of the VoIP-Service and thus become a fraud target. The communication system is now also vulnerable, similar to e-mails or websites. At the technical level, the conversion from ISDN to VoIP means that a previously closed system, which could only be attacked by physical manipulation or by the provider, is now more or less accessible on a logical level. The main goal of VoIP fraud is thereby the billing of a telephone call at the expense of the fraud victim, in order to make as much profit as possible for an Attacker.

The type of profit generation in VoIP that is the Obtainment of a chargeable service (telephone conversation) is a unique feature of VoIP compared to other IP services. As a result, VoIP systems, in addition to the usual threats to IP services, require a special way of thinking. The permanent availability of the system transfers the problems of a service provider on the Internet to every user of a VoIP system. Regardless of whether this user is a provider, a company or a private individual.

This paper addresses the topics of risk, prevention, detection, analysis and defense of fraud in VoIP and intends to uncover the danger for VoIP systems. The aim of this paper is to examine the risks and the expected costs of fraud-attacks in the field of VoIP systems. Therefore, a honey pot was set up for several months, which monitored most of the incoming attacks. In addition to these results, this paper shows which attacks can be repelled without hindering the normal operation of a VoIP infrastructure.

2 FRAUD IN VOIP-SYSTEMS

In the case of a fraud experiment, different participants are involved together as shown in Figure 1. On the one hand, there is the VoIP user with his system, which is typically connected to the VoIP provider via a WAN. On the other hand, there is the attacker, who looks for an access to the VoIP system and finally the internet service provider (ISP). No detailed statement can be made about the connection of the attacker, since he can make a fraud attempt at every point in the system.

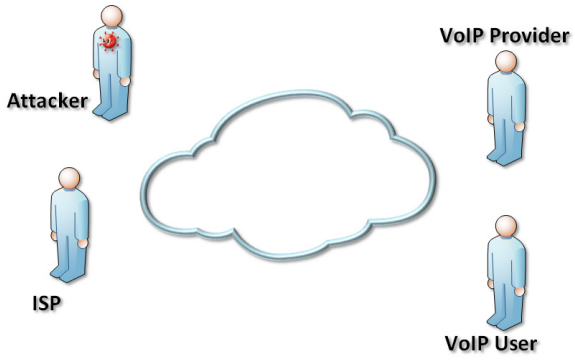

Figure 1: General fraud environment in VoIP.

In this consideration, the network service provider has a small influence on the VoIP level since the service is limited to the transport of IP packets and the possibilities only extend to OSI layer 3. Typical VoIP-Protocols are shown in Figure 2 (Sisalem, et al., 2009).

In the specific case of VoIP, an economic motive can be clearly defined, which consists in the negotiation of conversations without paying the costs for these. In this scenario, the attacker is someone who is himself a VoIP provider for another person. This untrustworthy Provider tries to arrange the handling of his calls through another VoIP system in order to let this fraud Victim pay the costs of the VoIP Call. In the same way, the fraud VoIP Provider keeps the cash from his subscriber. For this purpose, the surroundings are extended by Subscriber A and B, see Figure 3.

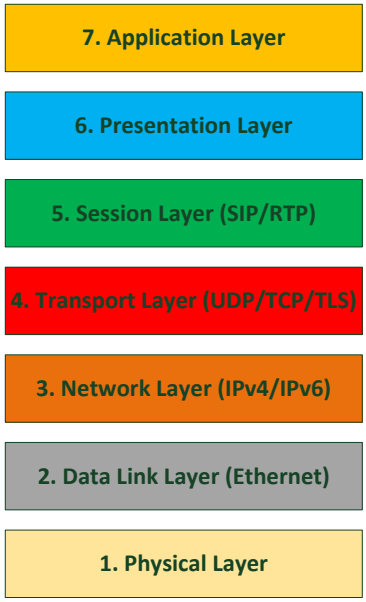

Figure 2: OSI layer with some VoIP protocols.

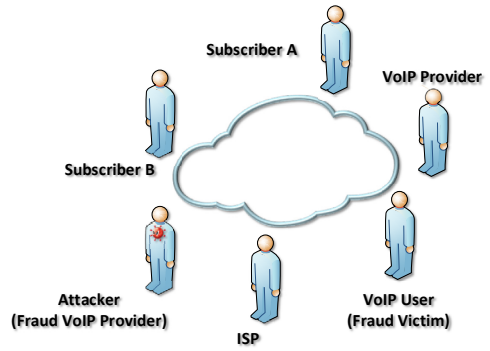

Figure 3: Extended fraud environment with all involved instances in VoIP.

The cost is very low for the attacker because of the IP-based communication. The fraud Provider just needs e.g. a virtual server, which can be hosted in any data center and manages the SIP communication. In general, this works with every call, but international calls are much more attractive in terms of the margin.

Figure 4 shows the path from subscriber A to subscriber B through the different SIP elements in the fraud scenario. The call is routed through the system of a fraud victim. In the legal case, the calls would be charged to the subscriber of the fraud victim but this does not apply to the fraud case. Here, the cash flow between fraud provider an fraud victim is not existent.

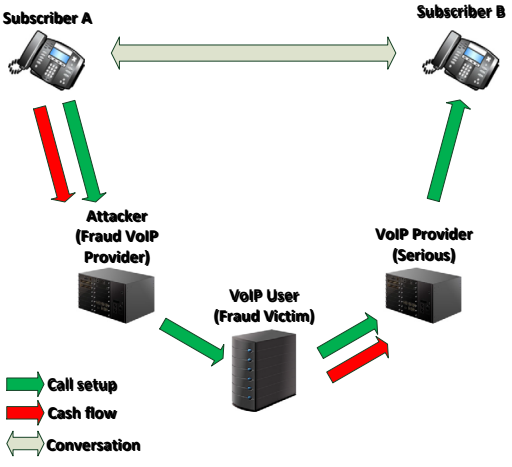

Figure 4: Cashflow in VoIP fraud.

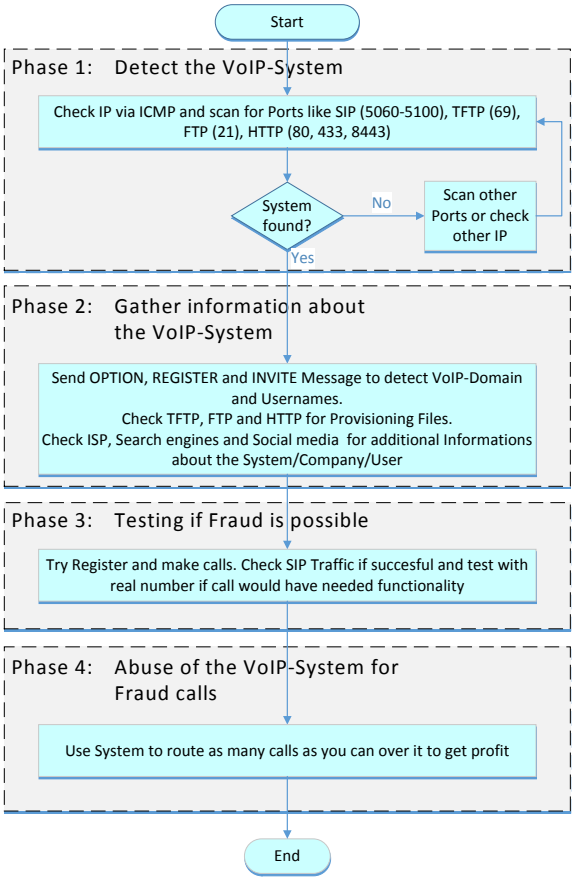

Figure 5: Fraud phase model.

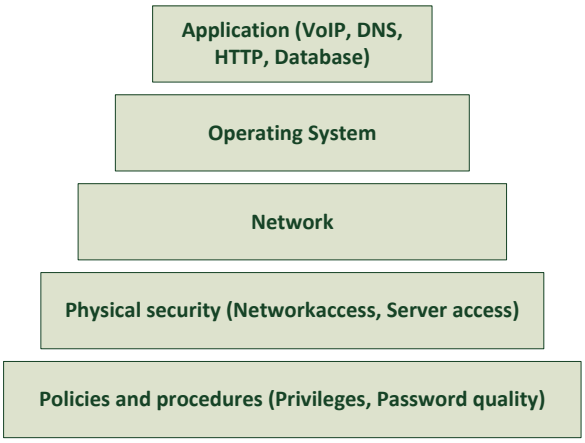

Figure 6: IP service security pyramid.

Technically a fraud attack on a VoIP system can be divided into several phases as shown in Figure 5. The aforementioned switching chain corresponds to the flow of information and cash within phase 4.

The attack scenarios on VoIP systems are similar to other IT services, such as DNS or HTTP. Figure 6 shows the different levels on which an attack can occur (Brennecke, 2009). If, for example, the password quality is poor at the lowest level or the authorization concept is insufficient or not available, safety precautions on higher levels are almost ineffective.

A general overview of the attack methods and threats typically affecting a VoIP system is shown in Figure 7. Many of these methods of attack are used in fraud experiments, and one has to protect the VoIP system against each of these.

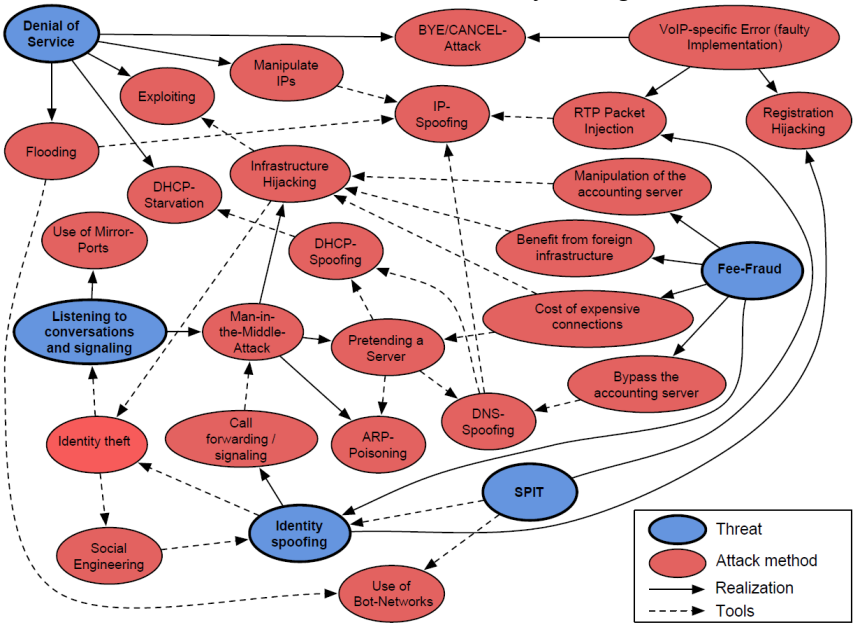

Figure 7: Overview of attack methods in VoIP systems (Brennecke, 2009).

3 HONEY POTS

In order to analyze attacks on VoIP systems more closely, the use of a honey pot is a good idea. This method is widely used in IP services, e.g. for e-mail systems. In that case e-mail addresses are provided, which receive spam mails in order to evaluate them. After a SPAM mail has been detected, the global lists of the mail providers are updated and can be used to protect the regular e-mail accounts.

The main difference in the detection of unwanted e-mails and unwanted telephone calls is that content analysis is much easier with e-mails than with calls because of a better pattern recognition. There are only a few parameters for deciding whether a connection request is a "fraud call" (Endler & Coller, 2007).

- Caller
- Callee
- Time of the request
- Frequency of the request

The use of honey pots as a productive counterpart in addition to a running PBX is basically possible, but the expected benefits do not cover the resources and configuration costs. All the information that the honey pot could collect can be detected by a session border controller (SBC). Furthermore, the handling of traffic on the edge of VoIP systems mitigates the effects of DoS attacks.

In this case open-source solutions were used for the honey pot. The core is a SipX (http://www.sipxcom.org), which provides all services and functions of a modern VoIP PBX as seen in Table 1 (ProQuest, 2016).

Table 1: Relevant services of a SipX honey pot system.

Dienst	Beschreibung
SIP Proxy	Exchange of SIP-packets
SIP Registrar	Management of registered SIP-Users
Call-Queue	ACD-Solution
TFTP	Provisioning of Telephones
HTTP	Platform for Management
DNS	Nameresolution for Services (e.g. SRV-Records)
NTP	Timeserver for Local Telephony
SNMP	Log-Server for Telephony
XMPP (OpenFire)	Instant Messaging Service

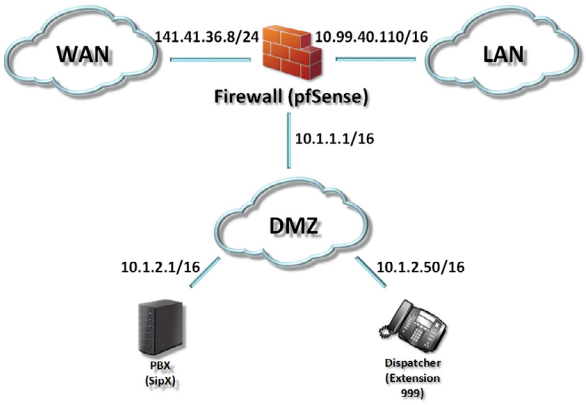

Figure 8: Architecture of the honey pot.

In order to create a controllable and manageable environment, it is necessary to place the SipX behind a firewall. For this, a pfSense (https://www.pfsense.org) was used. With appropriate firewall rules, the PBX is made completely accessible via the external IP. The only exception is port 22 for SSH access. An overview of the network structure is shown in Figure 8. The demilitarized zone (DMZ) network contains all the necessary components of the honey pot, while the LAN segment is intended for administrative access to the DMZ.

4 RESULTS

The goal of the first filtering of the raw data is to remove the internal traffic of the SipX and the internal network. This traffic plays a subordinate role for the search for fraud attempts and must only be taken into account in special cases. The recorded data shows that accessibility via ICMP is a critical point because attackers first check the general availability. After enabling ICMP and the external availability of UDP and TCP, approximately 90 minutes have elapsed until the first IP packet from an unknown source were received. This short time shows it is likely that a variety of port scanners and bots are looking for systems with security weaknesses.

The daily traffic summaries were scanned for external IP addresses and checked with the help of an online API (http://ip-api.com) to determine IP information. This data is from a database that is updated monthly. Therefore, the full validity of the information is not given. Dynamic IP addresses are not provided with the correct global position, but the

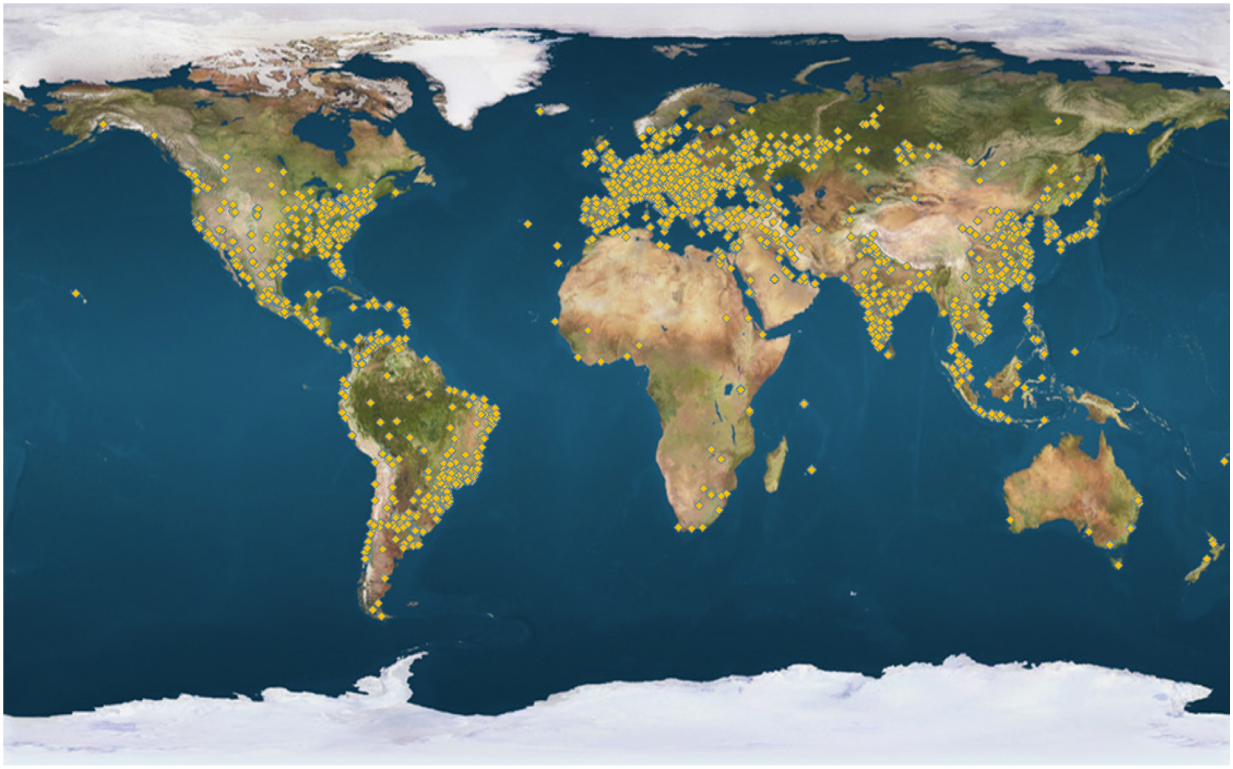

Figure 9: Location of the attacker's IP addresses.

IP ranges are usually assigned to an ISP and are thus located within a specific region. Static IP addresses, on the contrary, are indicated with the presumed current position.

Another critical point is the IP address itself. From the point of view of the honey pot, the IP is the last layer 3 device from which the packet was received. However, this does not necessarily have to be the attacker, but could be a pirated PC, a router or a spoofed IP. Considering the restrictions mentioned above, a world map with the potential attacker positions was drawn as seen in Figure 9.

The different IP addresses are evaluated, but not how often packets were received from these IP addresses. For a system which is connected in Germany, external IP addresses from Germany, for example NTP servers, should appear predominantly. The following Table 2 and Table 3 show the top 20 countries and Cities of the IP addresses. A total of 11956 IP addresses (as of 12.07.2016) were recorded.

Table 2: List of external IP addresses by country that communicated with the honey pot.

Number of Different IP Addresses	Country
1805	USA
1482	China
1113	Taiwan
568	Russia
559	Brazil
502	Venezuela
379	Germany
379	France
371	India
267	Vietnam
264	South Korea
218	Netherlands
216	Canada
204	Mexico
187	United Kingdom
173	Turkey
172	Italy
167	Argentinia
150	Indonesia
149	Romania

Table 3: List of external IP addresses by town that communicated with the honeypot (The World Bank, 2016).

Number of Different IP Addresses	Town
751	Taipei
237	Fremont
184	Peking
172	Hanoi
169	Roubaix
145	Ann Arbor
138	Montreal
137	Moscow
111	Fen-chi-hu
110	Nanjing
101	Guangzhou
100	Caracas
98	Paris
96	Seoul
95	Shanghai
94	São Paulo
93	St. Louis
92	Caracas (Los Palos Grandes)
89	Maracay
88	San Francisco (Financial District)

The evaluation of cities (Table 3) shows that Taipei leads the list by far. On closer examination of the background, the IPs can be traced back to the "Data Communication Business Group". This is the Asia Pacific Network Information Center (APNIC), which is responsible for IP management for the Asia and Pacific region. Since APNIC is a central administration, the identity of the attacker is probably concealed here or the WHOIS entries in the APNIC database are not completely maintained.

The configuration of the honey pot allows to monitor the SIP behavior, especially the SIP calls. Figure 11 shows the time course of the SIP requests recorded by the honey pot. In addition to the daily OPTION messages with which attackers are looking for a potential target, several INVITE and REGISTER brutforce attacks were registered. The analysis of SIP traffic per day shows that attacks are independent of the daytime. The attacks from 30th of May to the 7th of June were continuous inquiries with about a few hundred requests per minute. In contrast to this, the data of June 24th shows 200,000 SIP REGISTER requests during the lunch time within 200 minutes. In general, the assertion is that attacks occur primarily outside of business hours, e.g. on holidays or on weekends. However, this can not be confirmed by the recorded data. Thus, in a VoIP system which is reachable 24 hours a day and 7 days a week, fraud attempts should always be expected.

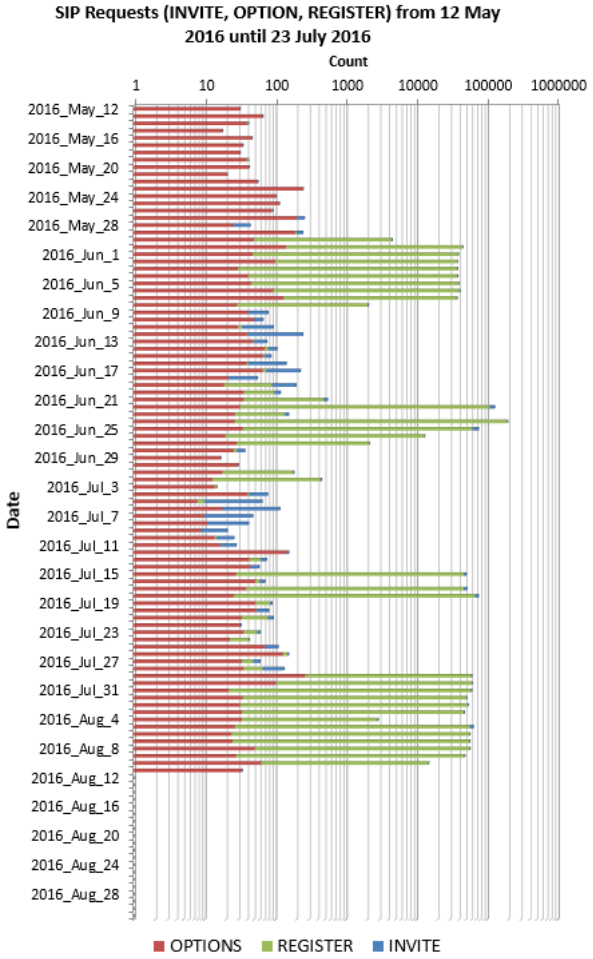

Figure 10: SIP requests of the honey pot from 12th of may until 23rd of july 2016.

5 FRAUD-VULNERABILITY

The verification of a VoIP system on its strength against fraud attacks can not be summarized in a single scenario. There is a large amount of attack points and various factors depending on the used PBX solution as well as the architecture and the specific installation. These points make it difficult to develop an automated tool that would allow people with no significant knowledge of the subject to check their own VoIP system.

There are several Linux-variants, which are good for fraud testing. For example "Kali" can be used . This distribution is freely available and specifically designed to perform "penetration testing" on IT systems. Kali provides hundreds of programs to perform attacks that target the goal of cracking passwords, manipulating DNS servers, or intercepting data as a “man-in-the-middle”.

A test plan should be based on the fraud-phase model (Figure 5) and be tested against a system, which is directly accessible. This scenario represents the greatest possible failure of firewall and SBC and offers a variety of possible attacks. In the first Phase, the goal is to detect the VoIP-System. Therefore, Tools like “nmap” for ICMP- and UDP/TCP-Port-scanning can be used. Especially the Port 5060 is important. In the next phase, the system under test should be confronted with several SIP messages. The information in the answers are essential for the next steps. This information can include details like the branch of the User Agents, the VoIP domain and the location of a TFTP server. Tools like “cURL” can now be used to download configuration data from a TFTP-Server. This is possible with the knowledge of the MAC addresses of the manufacturer. With the configuration file, it is often possible to register phones at the VoIP System. The tasks in the last phase is to get to know the necessary format of actually making calls. Therefore, “SIPp” test cases can be used to detect the prefix with a brutforce like method. Another possible way to get the format for making calls is to receive incoming calls because in most cases a recall is directly possible. After making an active outgoing call the fraud calls can be started.

6 CONCLUSION

The attempt to implement fraud over telephony is not a phenomenon of VoIP. It was already present with analog and ISDN telephones and as VoIP extended these old technologies, the fraud problem was also extended. The use of an open and strong network like the Internet requires new considerations of securing your own telephone system. The past thinking of the ISDN world is not sufficient in the security scenario and must be combined with already established methods of the IP services, such as layer 7 firewalls (SBCs), in order to be able to effectively protect against fraud (Wallingford, 2005).

The architecture of the VoIP system is decisive for the realizable degree of control. With an open structure and easy accessibility, the comfort factor is very high and easy to use. This applies to both, the administrator and the users, but unfortunately also to the attacker. Network severing (e.g., VoIP and data LAN) creates hurdles and ways to build control without massively reducing usability. It is irrelevant whether the separation takes place at the physical or the logical level.

For the establishment of a secure VoIP system, it is useful to consider all levels of the system and to decide whether and how services of the PBX should be used. From a technical security perspective, the construction of an ISDN system is secure. It is completely self-contained and can only be compromised in a few places. In combination with firewalls, SBCs and the PBX it is possible to get this state also in VoIP systems. The VoIP trunk can not be built into this old construct due to the public connection. For the design decision, you can choose between these two extremes (complete shutdown or direct public connection) in order to achieve the desired usability / security ratio.

The honey Pot experiment has shown how the impact on a directly to the Internet connected VoIP system is. The plant is under massive and permanent attacks and is therefore strongly endangered. The registered attacks show that it can be considered as negligent to operate an installation with such an architecture. This paper has shown how easy and quick a VoIP system can be analyzed and abused for fraud. If there are no corresponding backup measures or a preventive maintenance system is used to alert an administrator to an ongoing attack in case of an emergency, it is possible to hack a VoIP system and execute fraud attacks within a day. Depending on whether there is a limit for outgoing calls or not, the potential damage, even for such a short period of time is enormous.

REFERENCES

Brennecke, S., 2009. *Literaturgestützte und experimentelle Untersuchung zur Sicherheit vin Voice over IP in Unternehmensnetzwerken - Diploma Thesis.* Institute for communication and technologies - Ostfalia - Wolfenbüttel: s.n.

Endler, D. & Coller, M., 2007. *Hacking Exposed VoIP: Voice over IP Security - Secrets & Solutions. ISBN: 978-0072263640.* s.l.:Mc Graw Hill Professional.

ProQuest. *Products & Services - SIPX.* [Online] Available from: http://www.sipx.com/products/ 2016.10.19.

Sisalem, D., 2009. *SIP Security. ISBN: 978-0-470-51636-2.* s.l.:John Wiley & Sons Ltd..

The World Bank. *Data | The World Bank.* [Online] Available from: http://data.worldbank.org/ 2016.07.12.

Wallingford, T., 2005. *Switching to VoIP: A Solutions Manual for Network Professionals. ISBN: 978-0596008680.* 1. Hrsg. s.l.:O'Reilly Media.

QoS Characteristics Providing in Network Traffic Balancing

Irina Strelkovskaya, Irina Solovskaya and Nikolay Severin
Education and Research Institute for infocommunication and software engineering, Odessa National A.S. Popov Academy of Telecommunications, Kuznechnaya Str., Odessa, Ukraine
i.strelkovskaya@inbox.ru, *i.solovskaya@onat.edu.ua*, *n_severin@ukr.net*

Keywords: Nodal Tensor Method, Coordinate System of Branches and Nodes Pairs, Tensor, Traffic, Bypass Routes of Traffic Transmission, Traffic Balancing, Packets Delay Time, QoS Characteristics.

Abstract: Solving of the problem of quality characteristics providing QoS in MPLS-TE network with bypass routes of traffic transmission is proposed. By the nodal tensor method the value of packet delay along a traffic transmission route for the network with bypass routes of traffic transmission and without them is received and the results comparison of traffic balancing is conducted. It is shown, that in the network with the bypass routes of traffic transmission less time of packets delay is received. In this connection the balanced load of available network resources and its resiliency is provided.

1 INTRODUCTION

Modern transport packet network of multiprotocol switching according to the labels of MPLS-TE (Multiprotocol Label Switching Traffic Engineering) provides service packet traffic with the support for quality of service QoS (Quality of Service). MPLS-TE network functioning is based on the efficient use of available network resources, which is achieved by choosing the optimal route of traffic, procedures application of resource reservation and distribution network load, traffic balancing and application of mechanisms of preventing overloading and fault tolerance.

Ensuring the regulatory quality characteristic values of QoS in MPLS-TE network is performed by selecting the optimal route of traffic transmission by unidirectional tunnel TE-tunnel in the conditions of the rational application and downloading of network resources.

One of the solutions, that allows to ensure balanced load of network resources and its resiliency is the organization of bypass routes of traffic routing. This is due to the fact that during the operation of the network there is often a need to discharge certain routes, which loading is too significant.

Then, in order to balance traffic and in order to provide the required level of quality of service QoS, it is possible to use bypass (additional) pre-configured transmission route of traffic transmission.

Unlike fast rerouting of packages Fast ReRoute (FRR), which in the case of route failure allows in the network MPLS-TE to direct traffic to another pre-configured tunnel – TE-tunnel, chosen by the criterion of minimum packets delay, the application of bypass routes primarily supposes balancing of load and efficient use of network resources to provide QoS characteristics.

That's why the solution of quality characteristics problem of QoS in the MPLS-TE network with the organization of bypass routes of traffic transmission is considered by authors as the question of present interest.

Quite an important issue of using bypass traffic transmission routes is the mechanism of their choosing, which is determined by the number of nodes connecting paths, may be the shortest of all and so on. In this work as a criterion of choosing bypass routes the packet delay time is used.

To solve this problem it is advisable to use tensor methods to take into account the nature of the traffic stream and within a single tensor method simultaneously investigate the structural characteristics and functional properties of the network to meet the needs for appropriate quality of service characteristics.

Earlier, the authors obtained solution of traffic management problems in MPLS-TE network by node tensor method.

Under conditions of known values of intensities of network traffic and paths and the length of the output packet queue, its application allows to solve a significant class of traffic routing problems for networks of different topologies and technologies, by choosing a certain sequence of network nodes on set criteria specifics of a structure and network operation.

The aim of this work is solving the problem of providing quality characteristics of QoS in MPLS-TE network with bypass routes of traffic transmission and without them and the comparison of the results. This will allow effectively to apply and efficiently to load network resources, to provide balancing traffic in a network and to prevent possible overloads and routes failures.

2 TRAFFIC BALANCING IN MPLS-TE NETWORK UNDER CONDITIONS OF BYPASS ROUTES OF TRAFFIC TRANSMISSION

Let's consider the solving of quality characteristics QoS problems in the network under conditions of only main routes of traffic transmission by nodal tensor method.

Let's consider the output structure scheme of MPLS-TE network with ten paths of transmission that is shown on Figure 1.

The fragment of output network (Figure 1) is given as a graph G(N,V), where N = {N_j, j=1,5} – the set of vertices which are network nodes – routers, and V = {v_i, i=1,10} – set of arcs modelling network branches that are presented by network paths. In this case for the set fragment of output network only the main routes of traffic transmission are used.

We consider that the traffic transmission is performed in the direction from the network router N_1 to the router N_3 (on the structural scheme, the direction is shown by dash-and-dot line).

Let us set the main routes of TE-tunnel traffic transmission in the network, shown on the Figure 1: $N_1 \to N_3$, $N_1 \to N_2 \to N_3$, $N_1 \to N_5 \to N_4 \to N_3$, $N_1 \to \to N_6 \to N_5 \to N_4 \to N_3$, $N_1 \to N_5 \to N_2 \to N_4 \to N_3$, $N_1 \to \to N_6 \to N_1 \to N_6 \to N_5 \to N_2 \to N_4 \to N_3$, $N_1 \to N_2 \to N_4 \to \to N_3$, $N_1 \to N_6 \to N_5 \to N_2 \to N_3$.

To solve the set problem let we find the packets delay in T_v paths and on T_η nodes of the network, when between the nodes there are only basic routes of TE-tunnel traffic transmission by nodal tensor method.

We write the basic matrix of the pairs B_η according to network structure (Figure 1):

$$B_\eta = \begin{pmatrix} 0 & 0 & 0 & 1 & 0 & 1 & 0 & -1 & -1 & 0 \\ 0 & 0 & 0 & 0 & 1 & 0 & 0 & 0 & 1 & 1 \\ 0 & 0 & 0 & 0 & 0 & 0 & 1 & 1 & 0 & -1 \\ 0 & 1 & 1 & 0 & 0 & -1 & -1 & 0 & 0 & 0 \\ 1 & 0 & -1 & 0 & 0 & 0 & 0 & 0 & 0 & 0 \end{pmatrix} \quad (1)$$

Let us define the length of the output packet queue, which is transmitted from router N_1 to router N_5 and is represented by tensor components of average length of packet queues H^+_v (th.pack):

$$H^+_v = (0 \quad 0 \quad 0 \quad 0 \quad 100 \quad 0 \quad 0 \quad 0 \quad 0 \quad 0)^t, \quad (2)$$

where t – is the sign of transportation.

The average traffic intensities L_v (th.pack/s) in the paths of network are known and given in Table 1.

Table 1: Average intensities values of traffic in the network paths without bypass routes of traffic transmission.

Number of path	1	2	3	4	5
L_v	700	500	300	850	0
Number of path	6	7	8	9	10
L_v	400	350	650	800	600

As a functional invariant equation, we use the formula of Little, which according to [3-4] in tensor presentation is:

$$h_i = l^{i\alpha}\, \tau_{i\alpha}, \quad i = 1,n, \quad (3)$$

where h_i – average length of packet queues in the i-th network path, l^i – average traffic intensity in the i-th network path, τ_i – average time of packets delay in i-th network path, n– number of paths, α – index of summarizing.

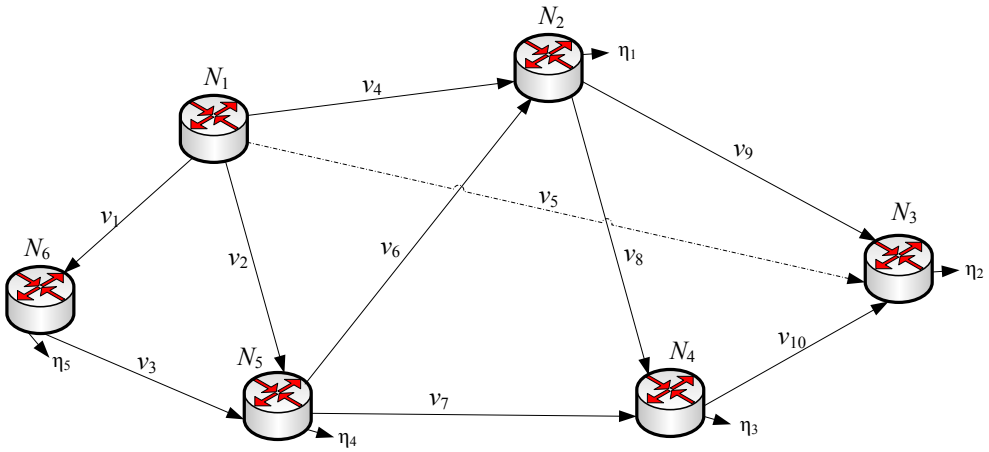

Figure 1: Block diagram of MPLS-TE network without bypass routes of traffic transmission.

Invariant equation (3) is presented in tensor form in the specified coordinate systems (SC) of branches and network node pairs:

$$H_v = L_v T_v, \quad H_\eta = L_\eta T_\eta, \qquad (4)$$

where H_v, H_η – covariant tensors of average length of packet queues in the SC branches and node pairs respectively, T_v, T_η – are covariant tensors of average packets delays in SC branches and node pairs, and L_v, L_η – are covariant tensors of average intensities of traffic in SC branches and network node pairs respectively.

Tensor of packets time delay T_η in network nodes is defined by the formula (4), as:

$$T_\eta = (L_\eta)^{-1} H_\eta. \qquad (5)$$

The transformation of the tensors projections by changing the SC is carried out:

$$T_v = B^t_\eta T_\eta, \; H_\eta = B_\eta H^+_v, \; L_\eta = B_\eta \; L_v \; B^t_\eta, \quad (6)$$

where B_η – matrix of basic node pairs, H^+_v – tensor of output packets queue in the SC network branches.

Let us define loading of network nodes while transmitting output packet queue, by calculation of tensor projections of packets queue length H_η in SC network node pairs.

According to equation (6) and given expression (1) of basic matrix of nodal pairs B_η and expression (2) of tensor of packets queues of average length H^+_v we get tensor of packets queue length in the network nodes:

$$H_\eta = (0 \quad 100 \quad 0 \quad 0 \quad 0)^t. \qquad (7)$$

Let we find L_η tensor which components in SC nodal pairs determine the intensities of traffic of each network node.

Using the equation (6) and known average traffic intensities L_v in network paths given in Table 1 and basic matrix of nodal pairs B_η given by the expression (1), we get:

$$L_\eta = \begin{pmatrix} 2700 & -800 & -650 & -400 & 0 \\ -800 & 1400 & -600 & 0 & 0 \\ -650 & -600 & 1600 & -350 & 0 \\ -400 & 0 & -350 & 1550 & -300 \\ 0 & 0 & 0 & -300 & 1000 \end{pmatrix}. \quad (8)$$

Using expressions (5), (7) and (8), we find the value of the average delay of packets in each router of MPLS-TE network, by calculating tensor projections T_η in SC network node pairs:

$$T_\eta \approx (0{,}079 \quad 0{,}160 \quad 0{,}102 \quad 0{,}046 \quad 0{,}014)^t \quad (9)$$

where t – is the sign of transportation.

Let we define the value T_v of packets delay for each path of the network according to the equation (6) in the SC network branches.

According to the obtained values of packets delay time for each network router given by tensor T_η (9) and known basic matrix of nodal pairs B_η, given by the expression (1) we obtain packets delay time T_v in network paths.

The results are presented in Table 2.

Table 2: Value of average packets delay in network paths without bypass routes of traffic transmission

Number of path	1	2	3	4	5
T_v, c	0,014	0,046	0,032	0,079	0,160
Number of path	6	7	8	9	10
T_v, c	0,033	0,056	0,023	0,081	0,058

Taking into account that the value of packets delay is additive along the appropriate route let we find packets delay time in the network in the TE-tunnel for all set routes of traffic transmission.

The results of values calculations of average packets time delay in network nodes and paths which connect them in the case of absence the bypass routes of traffic transmission are shown in Figure 2.

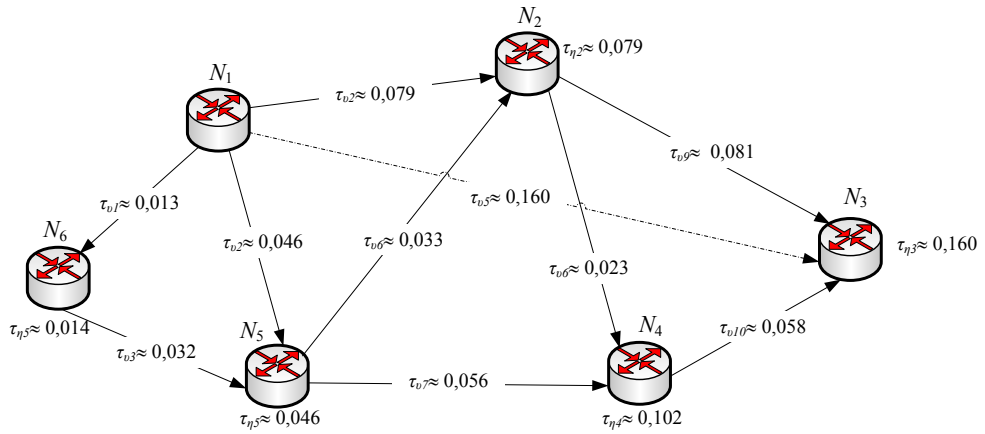

Figure 2: Results of packets delay calculations in the network without bypass routes of traffic transmission.

According to the conducted calculations (2-9) the values of packets delay time along different routes traffic transmission between set nodes pairs without bypass routes of routing are received. The results are given in Table 3.

Table 3: The values of average time of packets delay in the network routes without bypass routes of traffic transmission.

Route of traffic transmission	Number of branches ν (paths), that are included into the route	Value of average time τ of packets delay, s
$N_1 \rightarrow N_3$	ν_5	0,160
$N_1 \rightarrow N_2 \rightarrow N_3$	ν_4-ν_9	0,160
$N_1 \rightarrow N_5 \rightarrow N_4 \rightarrow N_3$	ν_2-ν_7-ν_{10}	0,160
$N_1 \rightarrow N_6 \rightarrow N_5 \rightarrow N_4 \rightarrow N_3$	ν_1-ν_3-ν_7-ν_{10}	0,160
$N_1 \rightarrow N_5 \rightarrow N_2 \rightarrow N_4 \rightarrow N_3$	ν_2-ν_6-ν_8-ν_{10}	0,160
$N_1 \rightarrow N_6 \rightarrow N_5 \rightarrow N_2 \rightarrow N_4 \rightarrow N_3$	ν_1-ν_3-ν_6-ν_8-ν_{10}	0,160
$N_1 \rightarrow N_2 \rightarrow N_4 \rightarrow N_3$	ν_4-ν_8-ν_{10}	0,160
$N_1 \rightarrow N_6 \rightarrow N_5 \rightarrow N_2 \rightarrow N_3$	ν_1-ν_3-ν_6-ν_9	0,160

3 TRAFFIC BALANCIING IN MPLS-TE NETWORK WITHOUT BYPASS ROUTESS OF TRAFFIC TRANSMISSION

Let we consider the solving of quality characteristic QoS providing problems in MPLS-TE network under condition when between the network nodes apart from basic routes there are additional routes of traffic transmission that allow to perform balancing the traffic and to prevent probable uploading routes failures.

Considering that the additional route has to be calculated simultaneously with basic one on the structural scheme of the network (Figure 3), let we set both basic and additional routes of traffic routing.

Let we consider the structural scheme of MPLS-TE network shown in Figure 3.

Let we set the network fragment in the form of multigraph G(N,V), where N = {N_j, j=1,5} – the set of vertices which are represented by the network

nodes – routers, and V = {v_i, i=1,15} – set of arcs that are modelling network branches presented by network paths, ten of which (v_1 –v_{10}) are basic and five (v_{10} –v_{15}) – bypass routes.

In the case when output network structure has not bypass routes of traffic transmission, the structure of network (Figure 1) is presented in the form of simple graph (graph without multiple edges).

But in the considered network there are bypass routes that's why it is reasonable to apply multigraph that allows describing network in which one and the same pair of vertices is connected by some arcs.

Then the basic matrix of node pairs B_η will have the form:

$$B_\eta = \begin{pmatrix} 0 & 0 & 0 & 1 & 0 & 1 & 0 & -1 & -1 & 0 & 1 & 1 & 0 & -1 & 0 \\ 0 & 0 & 0 & 0 & 1 & 0 & 0 & 0 & 1 & 1 & 0 & 0 & 0 & 1 & 1 \\ 0 & 0 & 0 & 0 & 0 & 0 & 1 & 1 & 0 & -1 & 0 & 0 & 1 & 0 & -1 \\ 0 & 1 & 1 & 0 & 0 & -1 & -1 & 0 & 0 & 0 & 0 & -1 & -1 & 0 & 0 \\ 1 & 0 & -1 & 0 & 0 & 0 & 0 & 0 & 0 & 0 & 0 & 0 & 0 & 0 & 0 \end{pmatrix}$$

Known average traffic intensities L_v (th. pack/s) in the bypass paths of the network that are given in Table 4.

The results of calculations of the average packets delay in the network nodes and paths, which connect for the network with bypass routes of traffic transmission, are shown in Figure 4.

Table 4: Values of average traffic intensities in the paths with bypass routes of traffic transmission.

Number of path	11	12	13	14	15
L_v	450	600	300	500	200

According to carried out calculations (2-9), we obtained that the value of packets delay time along different routes of traffic transmission between given pairs of nodes is $\tau \approx 0{,}108$ s in the case of additional routes of traffic transmission.

The results are given in Table 5.

Therefore, we obtain that the value of packets delay time in MPLS-TE network with bypass routes of traffic transmission between routers in TE-tunnels for different routes between set nodes pairs is the same and equals 0,108 s.

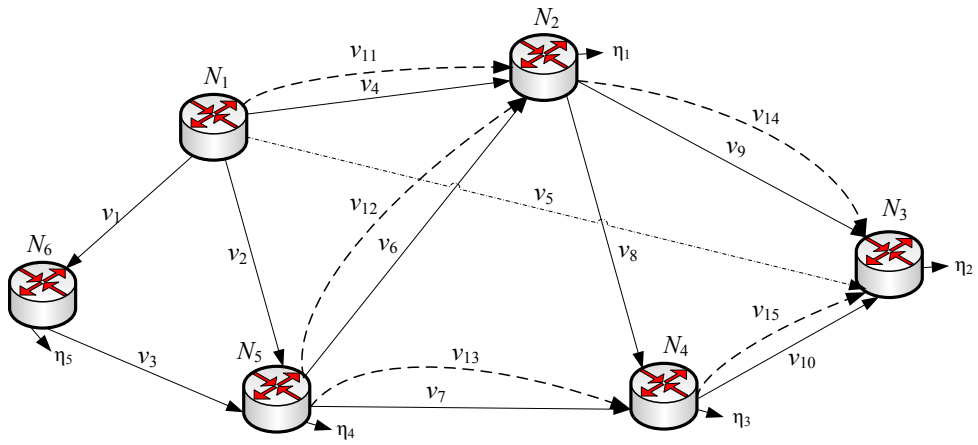

Figure 3: Structural scheme of MPLS-TE network with additional route of traffic transmission in the form of multigraph.

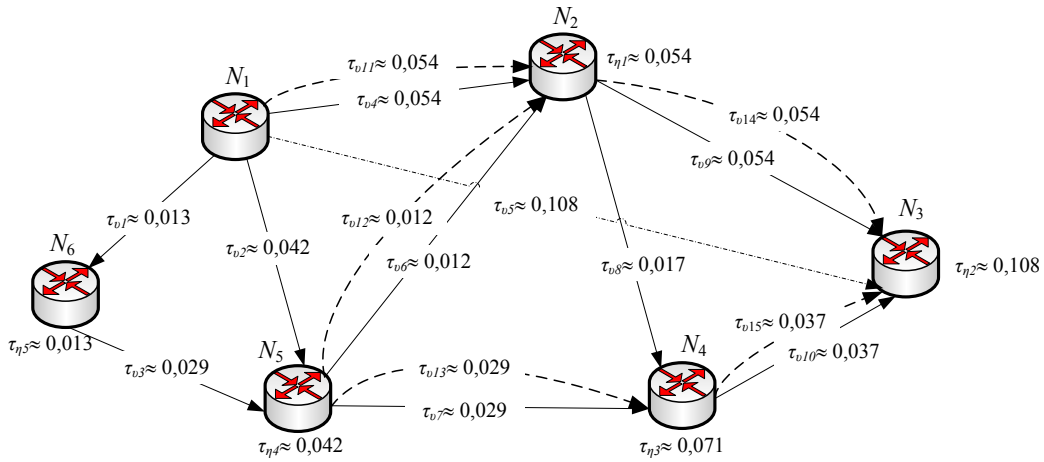

Figure 4: Results of calculations of packets delay time in the network with bypass routes of traffic transmission.

Table 5: Values of average packets delay time in the network with bypass routes of traffic transmission.

Routes of traffic transmission	Number of branches ν (paths), that are included into routes	Values of average time τ packets delay, sec
Basic routes		
$N_1 \rightarrow N_3$	ν_5	0,108
$N_1 \rightarrow N_2 \rightarrow N_3$	ν_4-ν_9	0,108
$N_1 \rightarrow N_5 \rightarrow N_4 \rightarrow N_3$	ν_2-ν_7-ν_{10}	0,108
$N_1 \rightarrow N_6 \rightarrow N_5 \rightarrow N_4 \rightarrow N_3$	ν_1-ν_3-ν_7-ν_{10}	0,108
$N_1 \rightarrow N_5 \rightarrow N_2 \rightarrow N_4 \rightarrow N_3$	ν_2-ν_6-ν_8-ν_{10}	0,108
$N_1 \rightarrow N_6 \rightarrow N_5 \rightarrow N_2 \rightarrow N_4 \rightarrow N_3$	ν_1-ν_3-ν_6-ν_8-ν_{10}	0,108
$N_1 \rightarrow N_2 \rightarrow N_4 \rightarrow N_3$	ν_4-ν_8-ν_{10}	0,108
Bypass routes		
$N_1 \rightarrow N_2 \rightarrow N_3$	ν_{11}-ν_{14}	0,108
$N_1 \rightarrow N_2 \rightarrow N_5 \rightarrow N_4 \rightarrow N_3$	ν_{11}-ν_{12}-ν_{13}-ν_{15}	0,108

4 COMPARISON OF TRAFFIC BALANCING RESULTS IN MPLS-TE NETWORK WITH AND WITHOUT BYPASS ROUTES OF TRAFFIC TRANSMISSION

Let we conduct the results comparison of characteristics performance in MPLS-TE network according to the criterion of the value of packets delay time for set routes in case of additional routes in the network of traffic transmission and case of its absence.

Received solution of set problem in the case of application of the same output data for the network structure, in which there are no bypass routes of traffic transmission, allow to get packets delay time τ≈0,160 s, the same along all routes of traffic transmission is received.

Accordingly, for the network structure with bypass routes of traffic transmission, packets delay time is τ≈0,108 s. and is also the same along all routes of traffic transmission.

It allows to state about reasonability of application of bypass routes of traffic transmission.

It is known, that when determining the packets delay along the traffic transmission route in MPLS-TE network, it is necessary also to consider not only packets delay in network paths, and also to take into account the value of packets time delay in network nodes.

Of course, the value of packets delay time in the nodes in MPLS-TE network depends on the functional features of equipment (volumes of buffer devices, mechanisms of organization and service of queue in the buffer devices), used protocols and other factors.

However, specifically packets delays in network nodes significantly affect the resulting value for quality of service QoS.

Therefore, we define the value of packets delay in the set traffic transmission routes in MPLS-TE network with additional directions and without them

taking into account the received values of packets delay T_η in the network nodes (expression (9)).

For the network with basic routes of traffic transmission (Figure 1) the average time of packets delay τ_{delay} in the route taking into account delays in network nodes, is given in Table 6.

Table 6: Values of average packets delay time in the networks routes without bypass routes of traffic transmission taking into account delays in network nodes.

Routes of traffic transmission	Number of branches ν that are included into the route	Number of nodes that are included into the route	Value of average time τ_{delay} packets delay, s
$N_1 \rightarrow N_3$	ν_5	N_1, N_3	0,320
$N_1 \rightarrow N_2 \rightarrow N_3$	ν_4-ν_9	N_1, N_2, N_3	0,399
$N_1 \rightarrow N_5 \rightarrow N_4 \rightarrow N_3$	ν_2-ν_7-ν_{10}	N_1, N_5, N_4, N_3	0,468
$N_1 \rightarrow N_6 \rightarrow N_5 \rightarrow N_4 \rightarrow N_3$	ν_1-ν_3-ν_7-ν_{10}	N_1, N_6, N_5, N_4, N_3	0,482
$N_1 \rightarrow N_5 \rightarrow N_2 \rightarrow N_4 \rightarrow N_3$	ν_2-ν_6-ν_8-ν_{10}	N_1, N_5, N_2, N_4, N_3	0,547
$N_1 \rightarrow N_6 \rightarrow N_5 \rightarrow N_2 \rightarrow N_4 \rightarrow N_3$	ν_1-ν_3-ν_6-ν_8-ν_{10}	N_1,N_6, N_5, N_2, N_4, N_3	0,561
$N_1 \rightarrow N_2 \rightarrow N_4 \rightarrow N_3$	ν_4-ν_8-ν_{10}	N_1,N_2, N_4, N_3	0,501
$N_1 \rightarrow N_6 \rightarrow N_5 \rightarrow N_2 \rightarrow N_3$	ν_1-ν_3-ν_6-ν_9	N_1, N_6, N_5, N_2, N_3	0,459

For the set basic routes of traffic transmission and the network structure with bypass routes of traffic transmission (Figure 3) the time of packets delay τ_{delay} taking into account delays in the network nodes, given in Table 7, is received.

Thus, the value of packets delay time in the set routes of traffic transmission taking into account the delays in the network nodes is the same as for the basic and as for the bypass routes.

For example, for the route $N_1 \rightarrow N_2 \rightarrow N_3$ with bypass routes and without them, the time of delay is the same and equals $\tau_{delay} \approx 0{,}270$ s.

For example, for the route $N_1 \rightarrow N_5 \rightarrow N_4 \rightarrow N_3$ with bypass routes the time of delay $\tau_{delay} \approx 0{,}329$ s and without them $\tau_{delay} \approx 0{,}468$ s.

For example, for the route $N_1 \rightarrow N_2 \rightarrow N_4 \rightarrow N_3$ with bypass routes the time of delay $\tau_{delay} \approx 0{,}501$ s and without them $\tau_{delay} \approx 0{,}341$ s.

Table 7: Values of average time of packets delay in the network routes with bypass routes of traffic transmission taking into account delays in the network nodes.

Routes of traffic transmission	Number of branches ν that are included into the route	Number of nodes that are included into the route	Value of average time τ_{delay} packets delay, s
Basic routes			
$N_1 \rightarrow N_3$	ν_5	N_1, N_3	0,216
$N_1 \rightarrow N_2 \rightarrow N_3$	ν_4-ν_9	N_1, N_2, N_3	0,270
$N_1 \rightarrow N_5 \rightarrow N_4 \rightarrow N_3$	ν_2-ν_7-ν_{10}	N_1, N_5, N_4, N_3	0,329
$N_1 \rightarrow N_6 \rightarrow N_5 \rightarrow N_4 \rightarrow N_3$	ν_1-ν_3-ν_7-ν_{10}	N_1, N_6, N_5, N_4, N_3	0,342
$N_1 \rightarrow N_5 \rightarrow N_2 \rightarrow N_4 \rightarrow N_3$	ν_2-ν_6-ν_8-ν_{10}	N_1, N_5, N_2, N_4, N_3	0,383
$N_1 \rightarrow N_6 \rightarrow N_5 \rightarrow N_2 \rightarrow N_4 \rightarrow N_3$	ν_1-ν_3-ν_6-ν_8-ν_{10}	N_1,N_6, N_5, N_2, N_4, N_3	0,396
$N_1 \rightarrow N_2 \rightarrow N_4 \rightarrow N_3$	ν_4-ν_8-ν_{10}	N_1,N_2, N_4, N_3	0,341
$N_1 \rightarrow N_6 \rightarrow N_5 \rightarrow N_2 \rightarrow \rightarrow N_3$	ν_1-ν_3-ν_6-ν_9	N_1, N_6, N_5, N_2, N_3	0,325
Bypass routes			
$N_1 \rightarrow N_2 \rightarrow N_3$	ν_{11}-ν_{14}	N_1, N_2, N_3	0,270
$N_1 \rightarrow N_2 \rightarrow N_5 \rightarrow N_4 \rightarrow N_3$	ν_{11}-ν_{12}-ν_{13}-ν_{15}	N_1, N_2, N_5, N_4, N_3	0,383

5 CONCLUSIONS

1. The solution of quality characteristics providing problems of QoS in MPLS-TE network with bypass routes of traffic transmission and without them is suggested.

2. The comparison of traffic balancing results in the network is conducted:

– for the network structure, without bypass routes of traffic transmission (Figure 1), the value of average time of packets delay for different routes of

traffic delivery (Table 3) between set nodes pairs that is $\tau \approx 0{,}160$ s and is the same for all routes of traffic transmission in the network, is received;

– for the network structure with bypass routes of traffic transmission (Figure 3), the value of average time of packets delay for different routes of traffic delivery (Table 3) between set nodes pairs that is $\tau \approx 0{,}108$ s and is the same for all routes of traffic transmission in the network, is received;

– the reduction of average time of packets delay for the network with bypass routes of traffic transmission allows to state about their application reasonability.

– thus in both cases, advantages of node tensor method, namely equality off average time of guaranteed packets delivery between given network nodes are preserved.

3. The values of packets delay time in the set routes of traffic transmission in MPLS-TE network with bypass routes of traffic transmission and without them taking into account the values of packets delay time in the network nodes are received:

– for the network with bypass routes of traffic transmission the value of packets delay for different routes of traffic delivery between set nodes pairs taking into account the values of packets delay in the network nodes (Table 7), where the time of packets delay is in the period of $\tau \in [0{,}270;0{,}407]$ s, is received;

– for the network without bypass routes of traffic transmission the values of packets delay time (Table 6) is $\tau \in [0{,}399;0{,}547]$ s;

– it is shown that in the network with bypass routes of traffic transmission the balanced loading of available network resources and its resiliency is provided.

REFERENCES

Vorobiyenko, P.P., Nikitiuk, L.A. and Reznichenko, P.V., 2010. *Telecommunications and Information Networks*. Kiev: Summit-Knyga.

Roslyakov, A.V., Vanyashyn, S.V. and Samsonov, M.Yu., 2008. *Networks of Next Generation NGN*. Moscow: Eco-Trends.

Zykov, A.A., 1987. *Principals of graph theory*. Moscow: Nauka.

Strelkovskaya, I.V., Solovskaya, I.N., 2010. Application of tensor method in TCN calculations, represented by node network. *Problems of Telecommunications*, 1(1), pp. 68-75.

Strelkovskaya, I.V., Solovskaya, I.N. and Smaglyuk, G.G., 2010. Problems solving of traffic management in MPLS-TE networks using tensor models. *Digital Technology*, 8, pp. 57-65.

Strelkovskaya, I.V., Solovskaya, I.N., 2015. Routing in MPLS-TE network with additional directions of traffic transmission. *Communication*, 1, pp. 25-30.

Strelkovskaya, I.V., Solovskaya, I.N., 2015. Solution to a problem of routing in MPLS-TE network with additional directions of traffic transmission. *Problems of Infocommunications Science and Technology*, 13-15 Oct., pp. 54-57.

Algorithm of Handling Out-of-Order Delivery for Multithreaded UDP-based Data Transport

Dmytro Syzov, Dmitry Kachan and Eduard Siemens
Department of Electrical, Mechanical and Industrial Engineering,
Anhalt University of Applied Sciences, Bernburger Str. 55, 06366 Köthen, Germany,
{dmytro.syzov, dmitry.kachan, eduard.siemens}@hs-anhalt.de

Keywords: High-Speed Data Transport, Mutli-threading, Out-Of-Order Delivery, Transport Protocols.

Abstract: As industry of information technologies evolves, demand for high speed data transmission steadily increases. The need in it can be found in variety of different industries – from entertainment withtrends for increasing of video to scientific research. One of the consequences is a demand for new improved transport protocols that would use the capacity of Long Fat Pipes by maximum, where common TCP performs much slower than it is expected. Such protocols are mostly based on UDP and work at the user space. To improve their network throughput, there is an option to implement sending data in a multi-threading way, but that can bring complications with it. One of the main obstacles is a possibility of out-of-order delivery due to race conditions. This problem is researched in current paper. Causes of reorder are studied regarding UDP-based transport protocols. Based on the results of the testing, a simple algorithm for compensating out-of-order delivery is proposed. It's effect then is analysed on the example of RMDT.

1 INTRODUCTION

The common limitation of operating systems – involving of significant resources on each system *send* and *receive* calls – leads to the performance limitation on sender side of such an application. Of particular interest is a problem of a high data rate traffic generation on a sender side. Especially in cases of point-to-multipoint communications, when the same data has to be transmitted to multiple destinations, as sender has to produce more traffic than each of the receivers has to process. This can be resolved by introducing of a multi-threaded send process into a transport protocol. The idea behind the use of multi-threading for performance improvement lies in fact that only part of system call actually concerns working with NIC. So, theoretically it could be possible to invoke *sendmsg()* or *recvmsg()* system calls, which can be used as "send" and "receive" operations on Linux from different cores and all processing, that is not concerned NIC, will be performed in parallel. Such approach can be applied as *sendmsg()* and *recvmsg()* are thread safe and re-entrant (Linux Programmer's Manual, 2017). Thus, these calls can be performed in parallel and so resulting data rate can be increased. Another important fact is that UDP preserves message boundaries (IEEE Standards Interpretations, 2017). Theoretically, there is no reason to assume that within this method there are some fundamental limitations of maximum data rate achievable.

Besides the speed boost, multi-threading in sending and receiving data can bring a number of problems on its own. One of them is a problem of efficient scalability regarding the system limitations. Another one is possible interleaving of packets due to asynchronous send operations, which is subject of investigations in current paper. For transport protocols this may present certain pitfalls as packets that are out of order could be considered lost by its ARQ algorithm. This work aims at provision of some insights into the packet reordering problem and proposes a simple algorithm to overcome it.

In general, there are mechanisms, such as signals, mutexes, conditional variables, that allow to avoid

such packet reordering problems. However, the downside of using these mechanisms is radically reduced performance as they usually include waiting for synchronization, and when the data rates are on the level of gigabits per second, even a block for a small amount of time can decrease output from NIC significantly. Thus, it is important to keep sender lightweight. Considering arguments, presented earlier, only lockless data exchange mechanisms are used in this work – precisely lockless queues.

For a simple application that consists of a lockless queue as IPC mechanism and *sendmsg()* system call which performs the interaction with network hardware, is considered as a test subject. In such an application – a few points of possible reorder are present:

- out-of-order timings of *dequeue()* operations
- out-of-order return of the object from a queue
- out-of-order send call

First and second points can be generally considered as one since they produce the same result – reordered read from the IPC queue.

There is a possibility to handle out-of-order packets without mechanisms that create additional load on sender. This work analyses the behaviour of a multithreaded data transmission application and analyses the proposed algorithm that handles the problem of reordering without locking and works on the receiver side, which is important, as its implementation does not create an additional load on the sender threads, thus does not decrease sender performance.

2 RELATED WORK

The lack of networking performance caused by CPU limitation is a problem that is of relevance in almost every multi-gigabit data transmission environment. This problem is clearly shown in research (Srivastava, 2014), which explores the problem of traffic generation for a 40 Gbps channel by comparison of several generators: D-ITG, packETH, Ostinato. As a result, S. Srivastava et al. state that no traffic generator was able to achieve the 40 Gbps rate. Authors suggest to use multithreaded generation of traffic. D-ITG - a generator from proposed research, which utilizes the channel using 16 threads. However, no additional research on impact of multithreading on packet-reordering was presented. To obtain more data on implementation of multi-threading the advantages of a multi-threaded approach for a network UDP-based application were investigated in a separate work (Syzov, 2016). Conclusion is, that multi-threading is beneficial for the fast traffic generation. It compares performance of cases with various amount of threads (from 2 to 20) on a 10 Gbps link. This work shows clear increase in performance with increasing number of threads as with 3 threads almost 10 Gbps rate has been achieved. With more than 12 threads, data rate starts decreasing. This number corresponds to exceed of the amount of CPUs and can be explained by overhead on threads management.

Another work (Nguyen D., 2007) shows the methodology for development of a multi-threaded network application, which correlates with this work. Research, among other subjects, considers two of the main pitfalls in a multithreaded network application - race conditions on data transport and inter-process communication. As explained by Nguyen D. et al., in an unsynchronized application, there is a possibility of data races and stresses the potential harm that it may cause due to reordering and data corruption. However, that work does not go into detail and does not propose a solution. In current research, the problem of possible reorders, caused by race conditions, is investigated further with tests made and a proposed algorithm for reordering avoidance.

3 TESTING ENVIRONMENT

All tests were performed in 10 GE Laboratory of Future Internet Lab Anhalt (FILA, 2017). The core element here is the WAN emulator Netropy 10G that can be used to create an emulation of WAN links.
During each test, 10 GB of data are transmitted. MSS is equal to 1472 bytes as it corresponds to common 1500 Ethernet v2 MTU (IETF, 2017). For sending and receiving, two Linux servers are used. Their specifications are presented in table 1.

Table 1: Servers' specifications.

Name	Server 1	Server 2
Kernel	4.4.0-38generic x86_64	4.4.0-45lowlatency x86_64
CPU	Intel Xeon X5690 (6-core) 3.5 GHz	AMD Opteron(tm) 4238 (6-core) 3.3 GHz
Memory	40 GB DDR3	32 GB DDR3
NIC	Chelsio Communications Inc. T420CR	Intel Corporation 82599ES

Since system call execution times can show significant spikes, all the figures with measurement results present filtered data – significant deviations are treated as outliers and are removed from data set. It is done in order to have a closer look on the behaviour of the tested configuration as original data often contains spikes that are rare and have different causes, which are not studied in this paper. The outlier filtering is performed by Tukey method (Frigge, 1989), it rejects outcomes, which are out of inter-quartile range (approximately 2.698σ).

For tests, apart from *C Library* and *C++ Standard Library*, following open source non-standard libraries were used:

- moodycamel::ConcurrentQueue (concurrent queue, 2017) for inter-process communication;
- HPTimer (Fedotova, 2013) for precise time measurements.

3.1 IPC Means

Since an intensive use of threads is present in this work, an appropriate IPC mechanism is required. Due to specific use case, there are some key requirements for a queue:

- Ability to work in a Single Producer, Multiple Consumers mode
- Low time of enqueue and dequeue operations.

Also a few additional requirements are given, that simplify usage of the queue and give more options to a developer:

- Ability to acquire approximate number of elements in the queue or avoiding overflow and gaining information on senders' performance without direct communicating with sender threads;
- Support of a dynamic allocation of additional memory for the option to increase queue size if senders significantly slows down for some period of time.

Following these requirements, *moodycamel::ConcurrentQueue* was chosen as it provides fast enough operations and also slow degradation of performance. It provides approximate amount of objects currently placed in the queue, which can be used to determine if threads work correctly without additional queue for the backward channel. Apart from this, the possibility to enqueue only if there is free allocated memory is present, which is useful if dynamic behaviour is not desired.

3.2 Time Acquisition

In order to retrieve data on timings of various operations a precise time acquiring mechanism is required. For this purpose the HPTimer library has been used, since it provides faster time acquisition than standard std::chrono library (Fedotova, 2013). It is worth to note that each measurement contains overhead of the timer itself which however is non-negligible.

4 TEST AND ANALYSIS OF REORDERS

For analysis and evaluation of reorder causes, some research should be made in order to analyze the behavior of a multi-threaded application in general. The stability of send call timings is of interest as inconsistency may lead to race conditions. In a real case, however, each send iteration includes additional operations that are not directly connected to a send call itself, the program as a whole is not executed constantly and, apart from all else, the system call may not take the same time on each iteration. To assess, how system handles *sendmsg()* call, some experiments have to be performed.

To acquire information on timings of main operations on sender threads' side, a test has to be performed with measurements of *sendmsg()* and *dequeue()* operations in sequence. The algorithm is minimalistic for precise measurements. It does not contain any operations apart from measured ones, time measurements and *std::vector::push_back()* operation to a reserved storage per loop. Results are presented on figures 1-3.

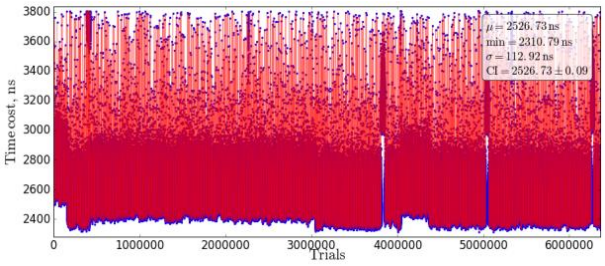

Figure 1: *sendmsg()* operation time measurements on Server 1 in a thread.

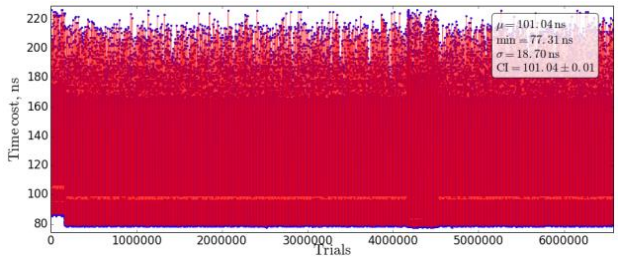

Figure 2: *enqueue()* operation time measurements on Server 1 in a thread.

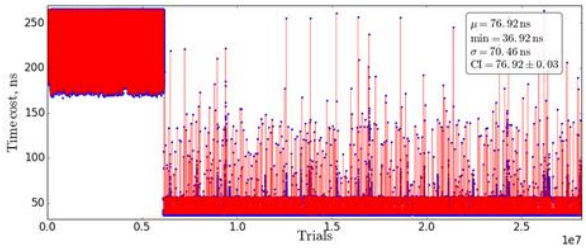

Figure 3: *dequeue()* operation time measurements on Server 1 in a thread.

On all figures, there is some inconsistency observed. The most prominent one is a significant drop on figure 3, that occurs when enqueue process on producer side (figure 2) is finished. However, it should be noted, that in tested case *dequeue()* takes much less time than *sendmsg()*. Also, in comparison to pure *sendmsg()* in a single thread, there are more inconsistencies in this case (deviation of 112ns vs. 63ns).

Next test aims to determine the volume of packet reorders in an application. As there are two main possible points of reorder causing operations, each of them is tested separately and then in combination. For this purpose, a set of test applications has been developed.

For tests, all data collection is placed at the receiver. In the test with no queue, the differentiation between sender threads is performed by setting predefined calculation of sequence numbers. The one, used in this test is defined by formula 1:

$$SN_i = ID * N_{threads} \quad (1)$$

where SN_i it the sequence number of message *i*; *ID* – thread identification number; $N_{threads}$ – amount of threads. In that way, each sending thread has its own sequence of numbers, that differs from others. With this approach, it would be incorrect to count out-of-order numbering inside one loop of each thread. More appropriate would be to count reorder cases, when order of numbers differs on each loop or if one of the threads sends messages faster than others. For the final test with queue, no additional functionality on the sender side is required. Receiver simply gets the message, then separates and stores a sequence number. The amount of threads, that are of interest, are 2, 3 and 11. Amounts of 2 and 3 are important as in this cases the maximum bandwidth of a 10 Gbps link is reached. The case with 11 threads represents the maximum quantity of sender threads for having one thread per CPU as one thread is a main application. However, for a better overview of the behavior, two additional numbers of threads between 3 and 11 are also considered. Such test can provide some information about significance of reorders as necessity of handling them depends on it.

For each case 40 trials were conducted. Collected data is analysed and the mean percentage of reorders is calculated. Each deviation from the expected next number is treated as reorder in case if factual number is bigger than expected. Results are presented in table 2.

Table 2: Percentage of reordered packets on Server 1.

Tested case, threads	2	3	5	8	11
sendmsg()	50%	33%	21%	16%	10%
Sendmsg() + dequeue()	0.02%	4.2%	6.2%	14%	31.3%

As can be seen, *sendmsg()* is not handled well by the kernel in regard to proper ordering. Another conclusion is that internal blocking of the send call in kernel space can decrease the reordering percentage, since the increase in the amount of threads decreases reorder percentage. As for combined *sendmsg()* and *dequeue(),* there is an expected increase in percentage of out-of-order delivery. However, it is not linear. And in case of 2 threads, the percentage is small enough to be neglected.

To check if this behaviour is the same for different hardware, an additional test for a *sendmsg()+dequeue()* was conducted on a different server. Results are presented in table 3

Table 3: Percentage of reordered packets on Server 2.

Tested case, threads	2	3	5	8	11
Sendmsg() + dequeue()	2%	3%	6%	18%	30%

As can be seen, while the percentage is different for some cases, the difference is generally not significant and the behavior remains the same.

Apart from percentage of reorders, the depth (in packets) between expected receive of a reordered packet and factual is of interest. It can show how long the application should wait before it can send NACK to get optimal performance. Results of processing collected data are presented in table 4 for cases with 2, 8 and 11 threads.

Table 4: Depth of reorders (in %).

Depth / Scenario	1	2	3	4	5	6 and more
Server 1, 2 threads	1	69	1	7	7	15
Server 1, 8 threads	4	33	21	13	3	25
Server 1, 11 threads	4	25	16	9	4	42
Server 2, 2 threads	0	97	0.3	0.3	0.3	2
Server 2, 8 threads	2	11	7	3	1	76
Server 2, 11 threads	2	6	3	1	2	86

From data, presented in table 3 it can be concluded that generally reorders tend to have depth of 2 or 3. Also, there is a significant difference between results on server 1 and 2. While on server 1 most of reorders have depth of 2 or 3 even if the amount of threads is increased, on server 2 with additional threads added percentage significantly shifts to more deep.

In a more close to a real use scenario with a serialized sequence of *dequeue()* and *sendmsg()*, the presence of a single data producer via the queue mostly compensates the timing reordering of packets by the kernel. Also, the percentage of reorders in the case of two threads is negligible. This is important as in some cases two threads can already reach 10 Gbps data rate, which might be enough for most applications. However, with addition of more threads there is a rapid increase in out-of-order delivery percentage. This fact means that there is a necessity in a mechanism that would handle such behavior to avoid decrease in utilization due to packet reorders.

5 PROPOSED REORDER HANDLING IN THE PROTOCOL

To compensate out-of-order delivery an algorithm is suggested for implementation on the receiver side which handles the packet reordering in a feasible way. Basic principle of the algorithm is that every thread sends packets with thread-specific sequence numbering in addition to the connection-specific numbering. In the described multi-threaded sending scenario, is safe to assume that all packets that have numbers lower than the least number from received last from each thread, are either lost or received. For purposes of this algorithm, some bytes at the header have to be reserved for a number of a thread, that sends the data packet. This has two main consequences:

- Maximum amount of sender-threads is restricted by the maximum thread number in the respective header field;
- Additional operations for processing data are to be placed on the receiver side.

A flow chart of the described approach is shown on figure 4 and visual representation of packet reordering on figure 5.

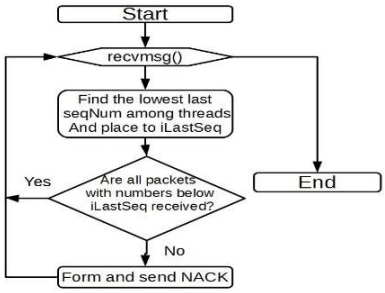

Figure 4: Flow chart of the reorder handling algorithm.

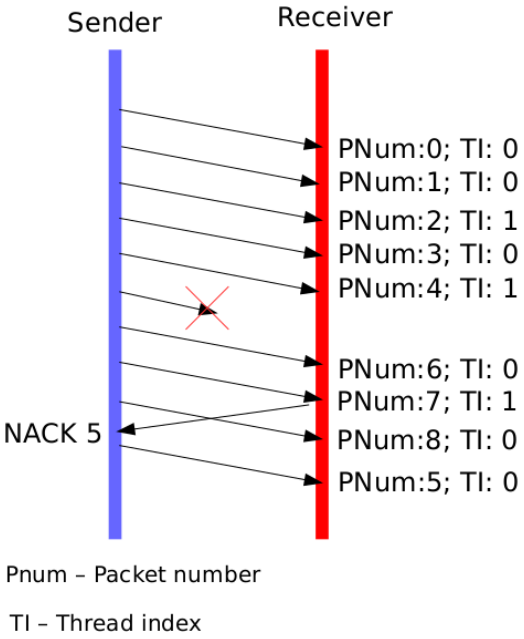

Figure 5: Visualization of the reorder handling algorithm.

Here TI is a unique thread ID and P_{num} is a connection-global sequence number of a packet. As can be seen, packet 5 was lost during transmission, but receiver does not send NACK immediately, but

rather waits until it can be sure that the packet is actually lost. NACK is sent after packet 6 from thread 0 and packet 7 from thread 1 are received.

When implemented on the receiver side, it can handle reorders caused by multithreading by such approach. However, it does not cover other causes for out-of-order delivery. Also, in real-world scenarios, apart from principles, described in the algorithm, some modifications have to be applied. The reason for that is the possibility of packet losses. As receiver has to notify sender about missing packets at some point, some functionality regarding this has to be implemented. Two generally used solutions are:

- Setting the timeout. If a missing packet was not received in a predefined period of time it is considered to be lost;
- Defining a number of packets, that can be received after a missing one. If missing data was not received after that number, a packet is considered to be lost.

TCP, for example, implements both approaches as it has a defined window, but also TCP has a timeout for each packet to be received. If timeout is exceeded or if last message of a window is received, missing packets are considered to be lost. In regard to algorithm explained in this chapter, the number of packets that are received after a missing one depends on the depth of reorders.

With example of RMDT, the use of 8 theads with server 1 as a sender, unhandled reorders will result in 14% loss on it's own. And if transmission is performed throug channel with losses, the total percentage of packets retransmitted can be even higher, thus, decreasing overall performance of a protocol. However, by implementation of reorder handling algorithm with waiting window of 4, most of reorders will be handled and difference in performance between these two cases is more than 10%. On the other hand, in a scenario of 2 threads, the percentage of reorders is low enough to be ignored.

The main difference between this algorithm and simple wait for a defined number of packets or a timeout is that it allows to differentiate between loss and reorder on the run. Thus, it does not significantly decrease the performance of the ARQ protoclol.

5 CONCLUSIONS

There is a demand in transport protocols, that can efficiently and reliably transmit data. To develop such a protocol, a number of problems have to be considered. One of them is a preservation of the ordering of data packets as for some types of ARQ, an out-of-order packet might be equal to a lost packet. In this work, basic reasons for out-of-order delivery caused by multithreading were considered. With measurements on timings of operations involved and reorders themselves, some insight was provided into behaviour of a multithreaded network application. In a case of 2 threads, depending on hardware, the percentage of reorders ranged from 0.02% to 02% with depth mostly equal to 2 (from 69% to 97% of reorders).

For the problem of reordering, to optimize data integrity preservation, an algorithm was suggested and it's benefits evaluated on the example of RMDT.

5 FUTURE WORK

Possible continuation of this work is developing and testing more complex algorithm that would include handling out-of-order delivery in general, not only that caused by multi-threading. More work can be done on evaluating the influence of reorders in a real transport protocol. In particular, the subject of reordering in wide area networks should be researched. Such research may provide information necessary for developing an appropriate out-of-order handling mechanism in protocols that operate on wide area network.

Additional tests should also be performed for different setups. Of special interest are tests with different types of hardware and its´ configuration. Also, tests with dynamically changing load on CPU and memory usage are of interest. Based on the results of such tests, the proposed algorithm can be improved to be able to handle variety of situations correctly.

For testing approach as a part of a real protocol, if all functionality will be proved to work correctly, this approach can be tested as a part of an UDP-based multi-threaded transport protocol for high speed data transmission.

ACKNOWLEDGMENTS

This work has been funded by Volkswagen Foundation for trilateral partnership between scholars and scientists from Ukraine, Russia and Germany within the project CloudBDT: Algorithms and Methods for Big Data Transport in Cloud Environments.

REFERENCES

Linux. socket. In *Linux Programmer's Manual*

IEEE. *IEEE Standards Interpretations for IEEE Std 1003.1c. Amendment 2: Threads Extension.* [Online]. Available from: http://standards.ieee.org/findstds/interps/1003-1c-95_int/pasc-1003.1c39.html. 2017.02.12

Srivastava S., Anmulwar, S., Sapkal, A. M., Batra, T., Gupta, A., and Kumar, V., 2014. Evaluation of traffic generators over a 40Gbps link, in *Computer Aided System Engineering (APCASE)*, Asia-Pacific Conference, pp. 43–47.

Syzov, D., Kachan, D., Siemens E., 2016. High-speed UDP Data Transmission with Multithreading and Automatic Resource Allocation in *Proceedings of the 4th International Conference on Applied Innovations in IT*, Koethen : Hochschule Anhalt, pp. 51-56

Duc Chinh, N., Kandasamy, E., Yoke Khei, L., 2007. Efficient Development Methodology for Multithreaded Network Application in *The 5th Student Conference on Research and Development-SCOReD* 2007 11-12 2007, Malaysia

FILA. *Future Internet Lab Anhalt* [Online]. Available from: https://fila-lab.de. 2017.02.12

Apposite. *Apposite Technologies :: Linktropy and Netropy Comparison.* [Online]. Available from: http://www.apposite-tech.com/products/index.html. 2017.02.12

Internet Engineering Task Force. *RFC 894 - A Standard for the Transmission of IP Datagrams over Ethernet Networks.* [Online]. Available from: https://tools.ietf.org/html/rfc894. 2017.02.12

Frigge M.,, Hoaglin D. C., Iglewicz, B., 1989. *Some Implementations of theBoxplot,* The American Statistician, vol. 43, no. 1, pp. 50–54.

Concurrent queue*. A fast multi-producer, multi-consumer lock-free concurrent queue for C++11*. [Online]. Available from: https://github.com/cameron314/concurrentqueue/ 2017.02.12

Fedotova, I., Siemens, E., Hu, H., 2013. *A high-precision time handling library,* J. Commun. Comput., vol. 10, pp. 1076–1086.

Providing of QoS-Enabled Flows in SDN
Exemplified by VoIP Traffic

Jannis Ohms[1], Olaf Gebauer[1], Nadiia Kotelnikova[1,2], Diederich Wermser[1] and Eduard Siemens[2]
[1]*Research Group IP-Based Communication Systems, Ostfalia University of Applied Sciences, Salzdahlumer Str. 46/48, D-38302, Wolfenbüttel, Germany*
[2]*Future Internet Lab Anhalt, Anhalt University of Applied Sciences, Bernburger Str. 55, D-06366 Köthen, Germany*
{jannis.ohms, ola.gebauer, n.kotelnikova, d.wermser}@ostfalia.de, eduard.siemens@hs-anhalt.de

Keywords: Software-Defined Networking, SIP, QoS, OpenFlow.

Abstract: This paper provides a proof of concept of an SDN Application to provide QoS for real-time services on SDN networks. Common real-time services are for example VoIP or M2M protocols like OPC UA and MQTT. We provide a proof of concept in the form of a specialized application for SIP traffic. The application lowers the latency and call-setup-time for VoIP calls. The application uses the metering and queueing features of OpenFlow 1.3 to assure high quality of service. The evaluation and optimization of the application is still in progress.

1 INTRODUCTION

Software-Defined Networking or (SDN) for short is a new approach for the implementation of computer networks. SDN will be an integral part of the new 5G mobile network (Tsagkrais, 2015). SDN Networks consist out of multiple SDN switches and at least one SDN controller. The controller has an overview of the whole topology and creates flow rules for the switches. The controlled switches forward packets according to the flow rules they received. The primary used protocol for SDN is OpenFlow (Open Flow Network Foundation, 2012) which is specified by the Open Networking Foundation (ONF). Reactive forwarding increses the overall latency (Keqiang, et al., 2015). This could be curcumvented through the use of proactive forwarding which creates the requierd flows in advance. Low latency is a requirement of real-time applications like M2M communication or VoIP. Through the use of specially designed SDN applications, it could be possible to reduce the latency even further if the required flows would be provided proactively before the traffic needs to be forwarded. The required SDN application is related to the required protocol. In this paper, we are using the SIP (Session Initiation Protocol) (Rosenberg, et al., 2002) protocol as an example.

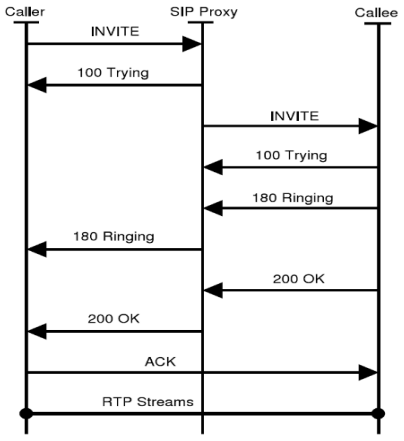

Figure 1: Sequence diagram of a SIP call setup with SIP proxy.

2 THE SIP PROTOCOL

SIP is a protocol used to implement the signaling in VoIP systems. The actual media data is transported by the RTP (Real Time Protocol) protocol (Schulzrinne, et al., 2003).

Figure 1 shows the call setup when a SIP proxy is used. The caller sends an invite message that is acknowledged with a trying response by the proxy. The proxy forwards the invite to the callee, which replies with a trying response. After that the call

sends a RINGING message to the proxy to indicate that the called phone is ringing. The proxy forwards the RINGING message to the caller. The callee sends an OK message which contains the used codecs and media endpoints of the callee's telephone besides other information. The caller receives the OK message of the proxy and acknowledges it with an ACK message. After the ack message is received, the RTP stream for the media data is set up. To terminate a call, one party can send a BYE message, which is passed through the proxy and afterwards is acknowledged by an ok message.

3 BASIC IDEA OF THE SDN APPLICATION

The proposed application receives a copy of any SIP traffic on the network. This opens the opportunity to proactively push flows to establish a path for the RTP stream. The application can use the media description of the callee's OK message to make a bandwidth estimation and reservation to ensure a feasible quality of service. This happens proactively before the switches forward the actual RTP streams.

4 RELATED WORK

Adami et al. (Adami, et al., 2015) propose a special load-aware routing application to guarantee QoS for VoIP calls in Software-Defined Networks. The application measures the link utilization and chooses a path with low utilization for VoIP data. In contrary to that Egilmez et al. (Egilmez, et al., 2013) developed a special SDN controller which monitors the states of the different links in the topology to detect congested links. Walner et al. (Wallner & Cannistra, 2013) propose the use of OpenFlow queues in combination with ToS (Types of Service) Header fields. The disadvantage of the ToS field is that it has to be set at the client devices. Our application will provide QoS without the manipulation of the clients. Jeong et al. (Jeong, et al., 2012) developed a new NOS (network operating system) which uses network slicing and virtualization to enable QoS. Our approach combines active traffic analysis with OpenFlow queues. Our approach does not need to monitor the network state since the bandwidth needed is reserved by the queues. There are also approaches from within the field of industrial automation to use SDN for industrial automation. Herlich et al. (Herlich, 2016) use an open real-time Ethernet standard on regular SDN switches. Through the use of SDN, they achieve a more robust and flexible topology. SDN enabled them to dynamically change routes in the case of errors like link failures or broken switches. They achieved low latency and the required QoS through the use of a master node which enforced a strictly organized media access. The use of master nodes is fairly common in industrial Ethernet standards (Dürkop, et al., 2015). This forms a contrast to our approach since we would not rely on a central master or specific Ethernet based protocol.

5 DEVELOPMENT AND TESTING ENVIRONMENT

The testing and development environment for the application as seen in Figure 2 consists of the following:

- Two Snom VoIP phones representing user equipment
- One System running an instance of the Camalio SIP Proxy
- One System running an Instance of the Floodlight SDN controller
- Three Edgecore AS4610-30T bare metal switches running PicOS as operating system.

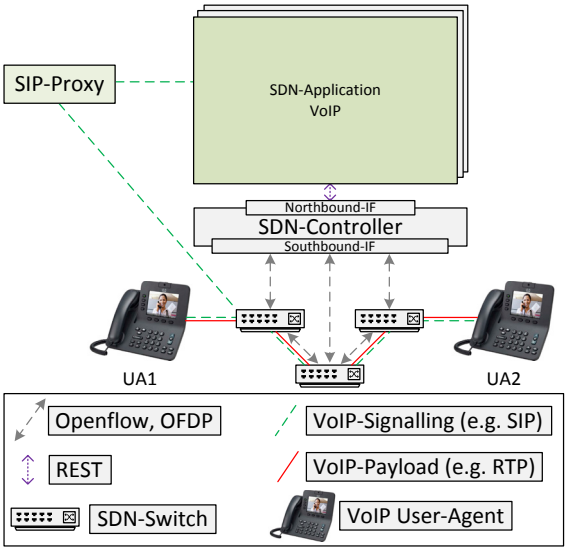

Figure 2: Testing a development environment for the VoIP-application.

6 LOGICAL ARCHITECTURE OF THE APPLICATION

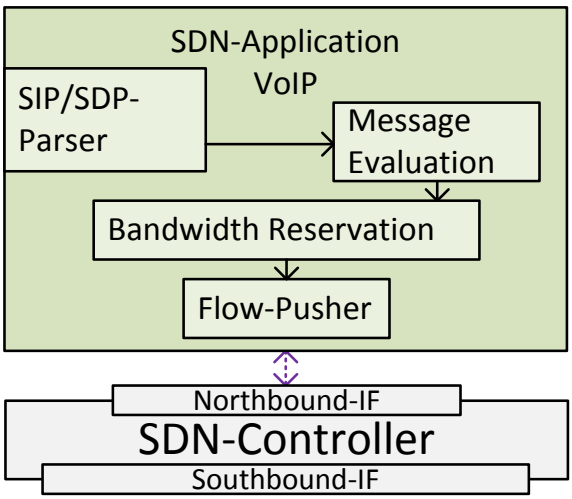

Figure 3: The internal components of the application on an abstract level.

The application consists of four components. The SIP/SDP (Handley, et al., 2006) parser is used to convert the received SIP packets into objects and to remove malformed packets. The Message Evaluation extracts the needed information for the bandwidth reservation and the routing. The information extracted from the Message Evaluation gets passed on to the bandwidth reservation which then estimates the bandwidth and assigns an OpenFlow queue for the call. The Flow-Pusher takes the callers and callees IP and calculates a path on the present topology. After the path is calculated all required flows get pushed. The Flow-Pusher also pushes a flow to every new switch which copies any SIP traffic and sends it to the controller.

This architecture provides the following main benefit: A clear separation between traffic processing analysis and path selection, which makes the components highly reusable and adaptable. This makes it possible to adapt the application for other protocols by providing a new analysis module and making minor changes like adjusting port numbers for the traffic processing. This architecture is visualized in Figure 3.

7 DEVELOPMENT OF THE SDN APPLICATION

Figure 4 shows the internal architecture of the Floodlight SDN controller (Project Floodlight, 2017). The controller consists of multiple independent and logical modules to provide a Java API as a northbound interface for user defined applications to use. Furthermore, the controller provides a REST and a Java API (Thomas, 2000) for external applications. The Java API provides huge performance benefits since the module can use all advantages of the controller like the module loading system and thread pools for concurrent execution. The proposed application will process any incoming SIP packets, so the usage of the Java API is advantageous for the performance. Floodlight provides a well gathered documentation and an easy understandable architecture which makes Floodlight a good project for prototyping and easy development. Our SDN-application consists of three modules. The first module is the SIPFlowPusher which receives incoming SIP traffic and sets up newly added switches to forward incoming SIP traffic to the controller. The second module is the SIPMsgAnalyzer which takes the SIP traffic from the SIPFlowPusher to extract the information. This is necessary to setup the required RTP streams. The RTPFlowPusher takes the extracted information to set up a path through the network and to choose the appropriate queue for a good quality of service.

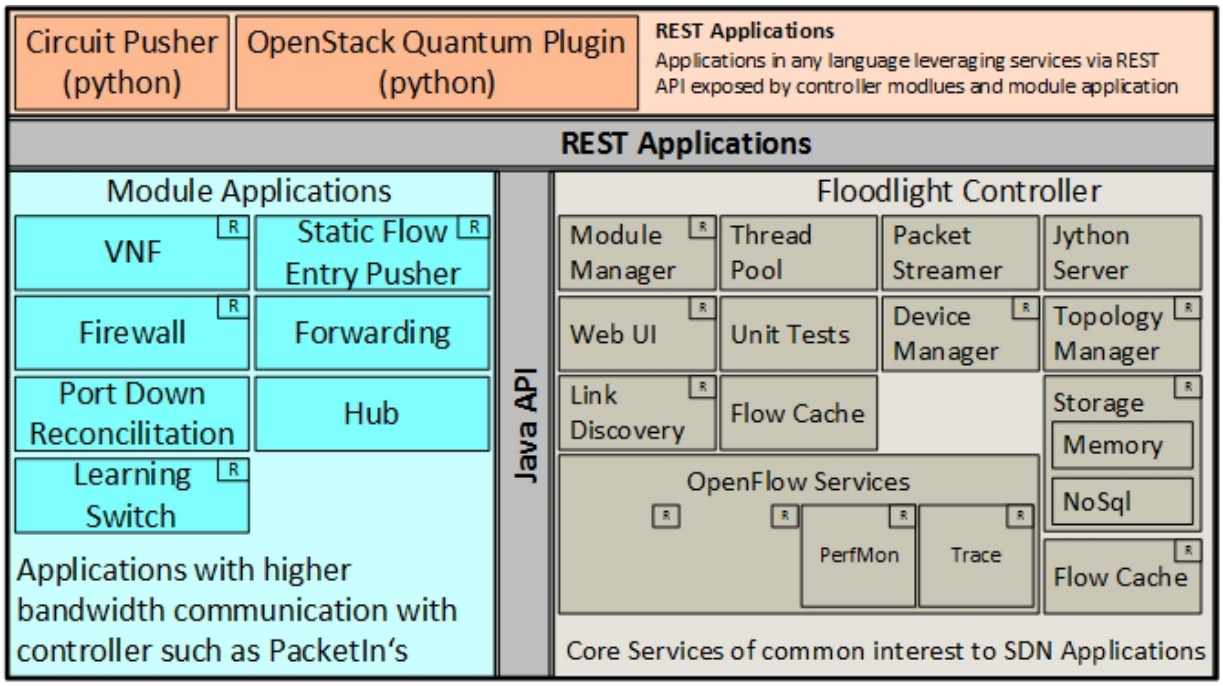

Figure 4: Architecture of the Floodlight SDN-controller (mod (Project Floodlight, 2017)).

The application uses the following services and interfaces of the controller

- **IFloodlightModule:** This interfaces is implemented by any of the three modules to indicate their status as a module to the rest of the system.
- **IOFMessageListener:** This interface enables the SIPFlowPusher module to receive incoming SIP traffic for further processing.
- **IOFSwitchListener:** This interface notifies the SIPFlowPusher when a new switch is connected to the network.
- **OFSwitchService:** This service enables a module to send OpenFlow messages to the switch to manipulate the content of the switches flow table.
- **RoutingService:** The RoutingService is used by the SIPMsgAnalyzer to determine a route for the RTP streams.
- **DeviceService:** The DeviceService is used to determine the physical port and MAC addresses of connected terminal devices.

The application also uses a third party library which is not part of the controller. The jain-sip library (O´Doherty & Ranganathan, 2017) provides a SIP parser for the application. The use of this library reduces the implementation time for the SIPMsgAnalyzer drastically since we don't have to write our own parser.

8 MEASUREMENTS

We performed the following measurements to examine if a bandwidth reservation can be provided by OpenFlow queues. Our measurement setup is shown in Figure 5. We connected two load generators to the switch; we also use a receiver to measure the amount of data received. The load generator LG1 generated one high priority stream of 700 Mbit/s. LG2 generated a low priority stream of 1 Gbit/s. The high priority stream has a duration of 10 seconds; the low priority stream has a length of 30 seconds. The high priority stream started roughly 10 seconds after the low priority stream. We compared the throughput of the different streams using different transport protocols (TCP and UDP) with different OpenFlow queue configurations. Figure 6 shows the use of TCP without queues. The bandwidth of the outgoing interface is shared equally between the two streams which implies the usage of a round robin algorithm. Figure 7 shows the use of TCP with queues in place. The queue is configured to reserve 700Mbit/s for the high priority stream. The graph indicates that the reserved bandwidth is provided. The Figure 8 and Figure 9

show the same results regarding UDP. The bandwidth could not be provided. One explanation for this could be the absence of flow control for UDP, this could create an overflow in the switches packet buffer which results in a drop of incoming packets. To further analyze the results regarding UDP we repeated our experiment with an overestimated queue size. We reserved 700 Mbit/s for a 100 Mbit/s stream. The results are shown in Figure 10. The results seem to imply that the size of the queue needs to be overestimated in order to work for UDP. This could also be an indicator that the throughput of the load generator and the throughput of the queue are measured on different OSI Layers.

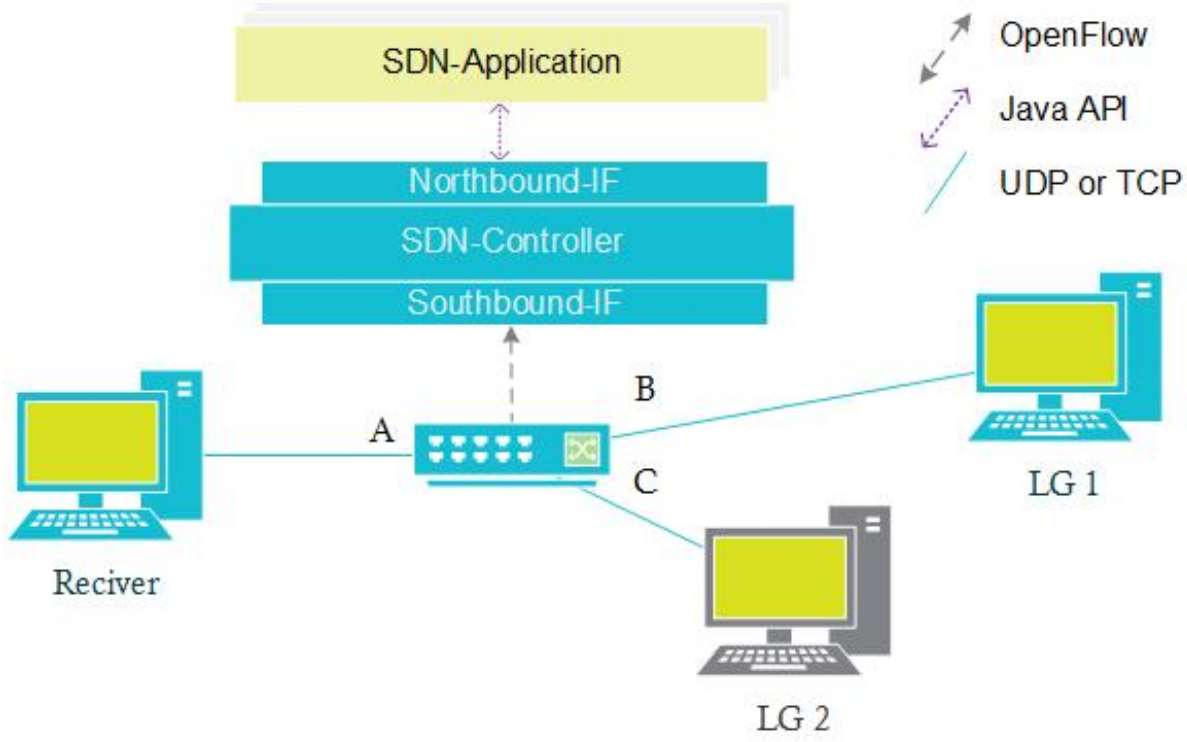

Figure 5: Measurement setup.

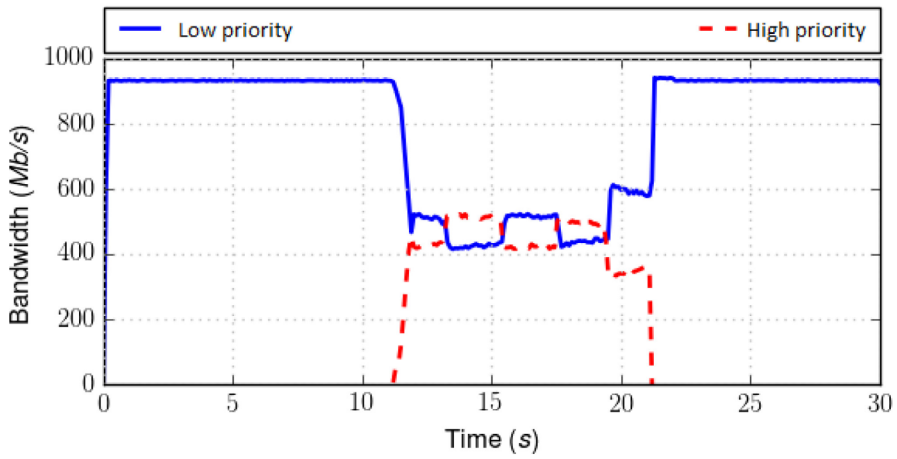

Figure 6: No bandwidth reservation, TCP.

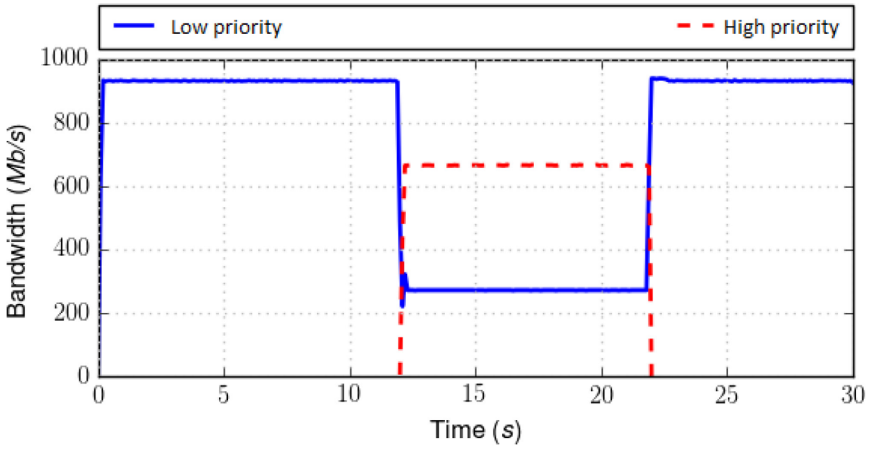

Figure 7: 700 Mbit/s bandwidth reservation, TCP.

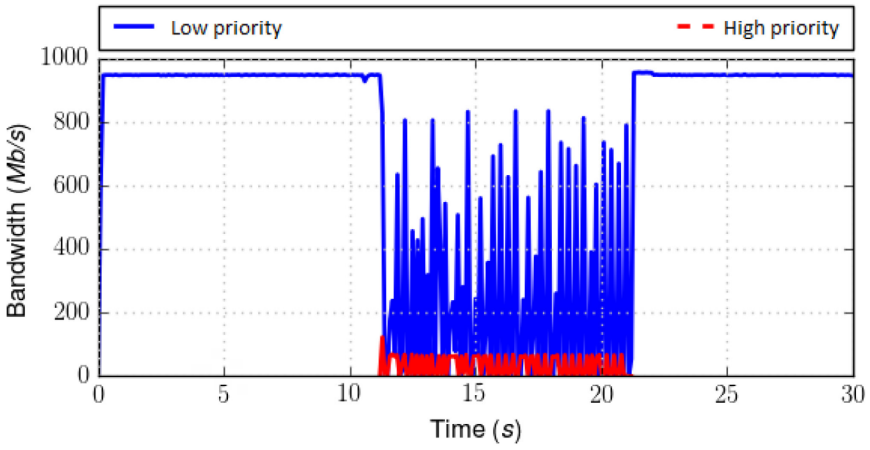

Figure 8: No bandwidth reservation, UDP.

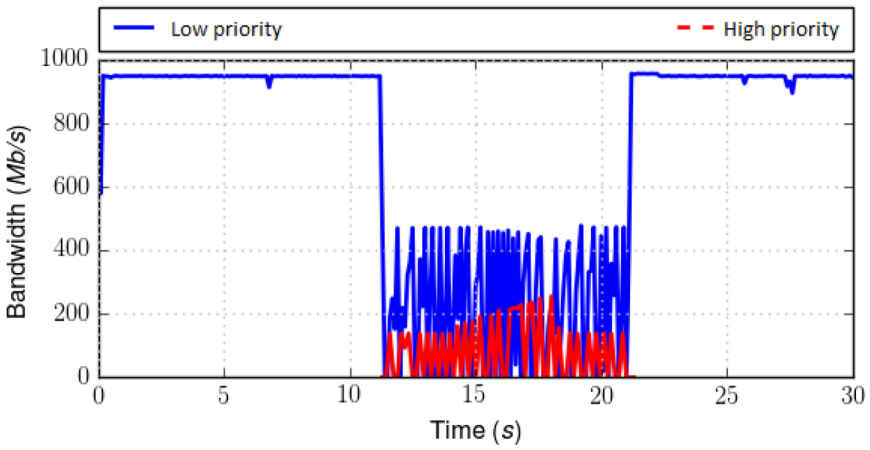

Figure 9: 700 Mbit/s bandwidth reservation, UDP.

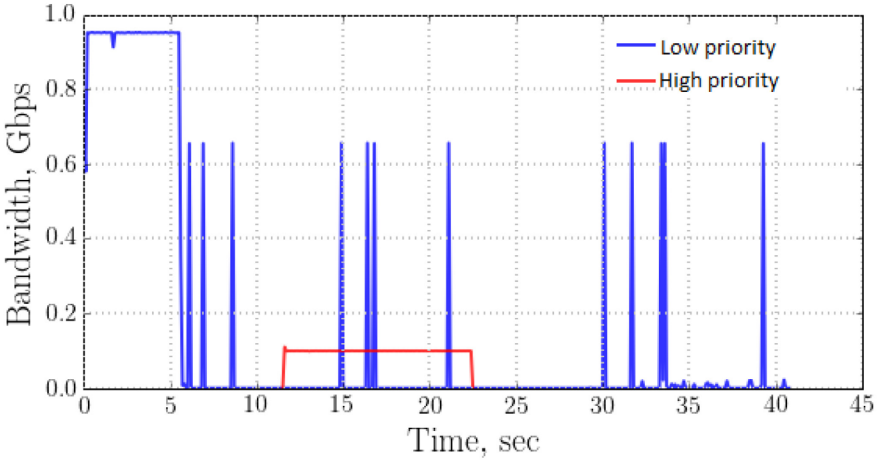

Figure 10: 100 Mbit/s high priority stream with a 700 Mbit/s bandwidth reservation, UDP.

9 CONCLUSIONS

The results show that a bandwidth for TCP streams can be guaranteed with OpenFlow queues. The results for UDP show that further research in the area of queue planning and capacity estimation needs to be done. Also, additional aspects such as jitter and delay of the streams need to be analysed.

ACKNOWLEDGEMENTS

The research presented in this paper is partly funded by the BMWi (Bundesministerium für Wirtschaft und Energie) within the ZIM-Programm (Zentrales Innovationsprogramm Mittelstand). This work is part of the INAASCA project (Integrated Network as a Service Solution as Part of Cloud IT Application Portfolio) (Gebauer, et al., 2016). Additionally, this work is funded by Volkswagen Foundation for trilateral partnership between scholars and scientists from Ukraine, Russia and Germany within the project CloudBDT: Algorithms and Methods for Big Data Transport in Cloud Environments.

REFERENCES

Adami, D., 2015. *Towards an SDN Network Control Application for Differentiated Traffic Routing - IEEE 978-1-4673-6432-4.* [Online] Available from: http://ieeexplore.ieee.org/stamp/stamp.jsp?arnumber=7249251 2017.01.02.

Dürkop, L., Jasperneite, J. & Fay, A., 2015. *An analysis of real-time ethernets with regard to their automatic configuration. In: Factory Communication Systems (WFCS).* IEEE World Conference , IEEE.

Egilmez, H. E., Dane, S. T. & Bagci, K. T., 2013. *OpenQoS: An OpenFlow controller design for multimedia delivery with end-to-end Quality of Service over Software-Defined Networks - IEEE. Signal & Information Processing Association Annual Summit and Conference (APSIPA ASC).*

Gebauer, O., Ohms, J., Wermser, D. & Wähling, S.-O., 2016. *Mechanisms for the Automated Setup of Software-Defined Networks - ITG-Fachbericht 263 ISBN 978-38007-4220-2.* Osnabrück: VDE Verlag.

Handley, M., Jacobson, V. & Perkins, C., 2006. *RFC 4566 - SDP: Session Description Protocol.* [Online] Available from: https://tools.ietf.org/html/rfc4566 2017.01.05.

Herlich, M., 2016. Proof-of-concept for a software-defined real-time Ethernet. In: Emerging Technologies and Factory Automation (ETFA). *IEEE 21st International Conference* , pp. 1-4.

Jeong, K., Kim, J. & Kim, Y.-T., 2012. QoS-aware network operating system for software defined networking with generalized OpenFlows. *IEEE Network Operations and Management Symposium,* pp. 1167-1174.

Keqiang, H., 2015. *Latency in Software Defined Networks: Measurements and Mitigation Techniques - ACM 978-1-4503-3486-0/15/06.* [Online] Available from: https://aaron.gember-jacobson.com/docs/he2015sigmetrics.pdf 2017.01.08.

O´Doherty, P. & Ranganathan, M., 2017. *JSIP: Java SIP specification Reference Implementation.* [Online] Available from: https://github.com/usnistgov/jsip 2017.01.06

Open Networking Foundation, 2012. *OpenFlow Switch Specification.* [Online] Available from: https://www.opennetworking.org/images/stories/downloads/sdn-resources/onf-specifications/openflow/openflow-spec-v1.3.1.pdf 2017.01.09.

Project Floodlight, 2017. *Floodlight OpenFlow Controller - Project Floodlight.* [Online] Available from: http://www.projectfloodlight.org/floodlight/ 2017.01.11.

Rosenberg, J., 2002. *RFC 2543 - SIP: Session Initiation Protocol.* [Online] Available from: https://www.ietf.org/rfc/rfc3261.txt 2017.01.04

Schulzrinne, H., Casner, S., Frederick, R. & Jacobson, V., 2003. *RFC 3550 - RTP: A Transport Protocol for Real-Time Applications.* [Online] Available from: https://tools.ietf.org/html/rfc3550 2016.12.15.

Thomas, R., 2000. *Architectural styles and the design of network-based software architectures - Doctoral Thesis.* University of California,: s.n.

Tsagkrais, K., 2015. Customizable autonomic network management: integrating autonomic network management and software-defined networking. *IEEE Vehicular Technology Magazine,* 10(1), pp. 61-68.

Wallner, R. & Cannistra, R., 2013. An SDN approach: quality of service using big switch's floodlight open-source controller. Proceedings of the Asia-Pacific Advanced Network. *Proceedings of the Asia-Pacific Advanced Network,* Issue 35, pp. 14-19.

FPGA Implementation of IP Packet Header Parsing Hardware

Danijela Efnusheva, Aristotel Tentov, Ana Cholakoska and Marija Kalendar
Computer Science and Engineering Department, Faculty of Electrical Engineering and Information Technologies, Ss. Cyril and Methodius University, Skopje, Macedonia
{danijela, toto, acholak, marijaka}@feit.ukim.edu.mk

Keywords: FPGA, Header Parser, IP Packet Processing, Multi-gigabit Networks, Network Processor.

Abstract: The rapid expansion of Internet has caused enormous increase in number of users, servers, connections and demands for new applications, services, and protocols in the modern multi-gigabit computer networks. The technology advances have resulted with significant increase of network connection links capacities, especially with the support for fiber-optic communications, while on the other hand the networking router's hardware and software have experienced many difficulties to timely satisfy the novel imposed requirements for high throughput, bandwidth and speed, and low delays. Considering that most network processors spend a significant part of processor cycles to provide IP packet header field access by means of general-purpose processing, in this paper we propose a specialized IP header parsing hardware that is intended to provide much faster IP packet processing, by allowing direct access to non byte- or word-aligned fields found in IPv4/IPv6 packet headers. The proposed IP packet header parser is designed as a specialized hardware logic that is added to the memory where the IP packet headers are placed; and is described in VHDL and then implemented in Virtex7 VC709 Field Programmable Gate Array (FPGA) board. The simulation timing diagrams and FPGA synthesis (implementation) reports are discussed and analyzed in this paper.

1 INTRODUCTION

Internet as the most popular and most widely used network is constantly growing with an extremely large pace, (Ahmadi, 2006). This is due to the ever increasing number of users, servers, connections and new applications. In parallel, the speed of the networking links grows constantly, especially with the great expansion of the fiber-optic technology. As a result of the increased network traffic, the networking hardware remains as the bottleneck for constructing high speed networks. Network processors (NPs) have become the most popular solution to this problem, (Wheeler, 2013). In general they are defined as chip-programmable devices, which are specially tailored to perform several network processing operations, including: header parsing, bit-field manipulation, pattern matching, table look-ups, and data movement, (Lekkas, 2013).

NPs are usually implemented as application specific instruction processors (ASIPs) that mainly include many processing engines (PE), dedicated hardware accelerators, network interfaces, adjusted memory architectures, interconnection mechanisms and provide support for various parallelization techniques, (Shorfuzzaman, Eskicioglu, Graham, 2004). NPs might be used in different types of network equipment such as routers, switches, IDS or firewalls, (Giladi, 2008). Over the last few years many vendors have developed their own NPs, which resuled with many NP architectures existing on the market. Moreover, many novel approaches, such as the NetFPGA architecture, (Naous, Gibb, Bolouki, McKeown, 2008), or software routers, (Petracca, Birkea, Bianco, 2008), are constantly emerging.

The most popular NPs, which are used today, include one or many parallel homo- or heterogeneous processing cores. For instance, Intel's IXP2800 processor, (Intel, 2005), includes 16 identical multi-threaded general-purpose RISC processors organized as a pool of parallel homogenous processing cores that can be easily programmed with great flexibility towards ever-changing services and protocols. Furthermore, EZChip has introduced the first NP with 100 ARM cache-coherent programmable processor cores, (Doud, 2015), that is by far the largest 64-bit ARM processor yet announced.

The discussed NPs confirm that most of the operations in NPs are performed by general-purpose RISC-based processing cores as a cheaper but slower solution, combined with custom-tailored hardware that is more expensive but also more energy-efficient and faster. If network packet processing is analyzed on general-purpose processing cores then it can be easily concluded that a significant part of processor cycles will be spent on packet header parsing, especially when the packet header fields are non byte- or word-aligned. In such case, some bit-wise logical and arithmetical operations are needed in order to extract the value of the appropriate field from the packet header.

Network processing usually begins by copying the packets into a shared memory buffer that is available for further processing by the processor. This buffer may be upgraded with specialized hardware to perform the field extraction operations directly on its output, before forwarding them to the processor. The basic idea of this approach is to replace the bit-wise logical and arithmetic operations by a special parsing logic that will extract the header fields from the on-chip memory and provide them to the processor. The result of using this header parsing logic should be a single-cycle memory access to these non byte- or word- aligned header fields.

The header parsing logic is simple to design, provided that it will be specially adapted to work with IPv4/IPv6 header formats. Actually, the proposed header parsing hardware will be used for reading a single IPv4/IPv6 header field from the memory, or writing to a single IPv4/IPv6 header field into the memory. If this logic is manufactured as an ASIC it cannot be reused for other header formats, so in this paper we investigate the possibilities to utilize a reconfigurable hardware platform like Virtex7 VC709 FPGA, (Xilinx, 2016). In fact, FPGA technology is very suitable for use, providing a compromise between performance, price and re-progrmability, (Cardoso, Hubner, 2011).

The rest of this paper is organized as follows: Section II gives an overview of different networking hardware and software solutions intended to speed up network processing and also discusses several aproaches used for simplifing packet header parsing. Sections III describes the proposed IP header parsing logic and explains its ability to allow single-cycle memory access to non byte- or word- aligned packet header fields. Section IV presents simulations and synthesis results from the FPGA implementation of the IP header parsing hardware model in VHDL. Section V concludes the paper, outlining the benefits of the proposed IP header parsing module.

2 STATE OF THE ART

Each network device that exists in the computer networks examines fields in the packet headers in order to decide what to do with each packet. As a result, the process of identifying and extracting fields in a packet header is subject to a vast amount of research, (Gibb, Varghese, Horowitz, McKeown, 2013). With the ever increasing speed of network links, the research is mostly focused on hardware acceleration for achieving suitable processing speeds, (Kořenek, 2013). This is mainly done by combining application-specific coprocessors with general-purpose multiprocessor systems, or reconfigurable FPGA platforms.

The basic function of each network device is to process the ingress data flow accepted by the physical interface, and then forward the packets to an outbound port, after the processing is finished. In order to achieve this, network devices are usually designed as a composition of four functional blocks: physical interface, data plane, control plane and switching interface, (Lekkas, 2013). Generally NPs are used to perform fast packet processing in the data plane. On the other hand, the slow packet processing in the control plane (configuration and management, execution of routing protocols) is mostly handed by general purpose processor.

NP operation begins with the receipt of an input stream of data packets. After that, usually the IP header of the received packets is being processed, by analyzing, parsing and modifying its content, (Giladi, 2008). NPs might include some specialized hardware units to perform classification of packets, lookup and pattern matching, queue management and traffic control. After the completion of all the required operations, the network processing is finished and the packet is sent out through the switching fabric to the appropriate outbound port.

According to (Hauger, Wild, Mutter, 2009) simpler packet processing and higher speeds can be achieved if the most time–consuming network processing operations are simplified, and some appropriate choices of the routing protocol functionalities are made. As a result, many different approaches have been proposed, including label concept and several other algorithms for faster table lookup given by (Gupta, Lin, McKeown, 1998) and (Eatherton, Varghese, Dittia, 2004).

In general, NP software is getting closer to the NP hardware, such as in (Kekely, Puš, Kořenek, 2014) where part of the packet processing tasks such as classification or security are offloaded to application-specific coprocessors that are used and

controlled by the software. In this way, the coprocessor hardware handles the heavy part of the packet processing, at the same time leaving more specific network traffic analyses to the general-purpose processor. As follows, a flexible network processing system with high throughput is built. Some researchers also try to unify the view on the various network hardware systems, as well as their offloading coprocessors, by developing a common abstraction layer for network software development, (Bolla, Bruschi, Lombardo, Podda, 2014).

Other proposals make big use of FPGA technology for packet parsing, as it is very suitable for implementation of pipeline architectures and thus ideal for achieving high-speed network stream processing, (Puš, Kekely, Kořenek, 2014). Actually, the reconfigurable FPGA boards can be used to design flexible multiprocessing systems that adjust themselves to the current packet traffic protocols and characteristics. This approach is given by (Attig, Brebner, 2011), who propose use of PP as a simple high-level language for describing packet parsing algorithms in an implementation-independent manner. Similarly, in (Brebner, Jiang, 2014), a special descriptive language PX is used to describe the kind of network processing that is needed in a system, and then a special tool generates the whole multiprocessor system as an RTL description.

3 DESIGN OF IP PACKET HEADER PARSING UNIT

The general idea of this paper is to propose an IP packet header parsing hardware module that will allow single cycle access (read or write) to various IP header fields. As a result, the proposed IP header parsing unit would speed up packet processing, allowing same access time for a packet header field as the access to any random memory word, even when it is not byte- or word- aligned. This approach would have huge impact on network processing hardware and would provide increased overall network throughput in computer networks at all.

In order to achieve single-cycle access, the proposed IP packet header parsing unit will use part of the memory address space to directly address various IP packet header fields. This technique is known as memory aliasing, and allows each IP header field to be accessed with a separate memory address value. When such address is input in the IP header parsing module it selects the corresponding word from memory, and afterwards depending on the field, the word is processed in order to extract it. This may include shifting the word and/or modification of its bits. A scheme of the proposed logic, used to read out a single IP header filed, is presented in Fig.1.

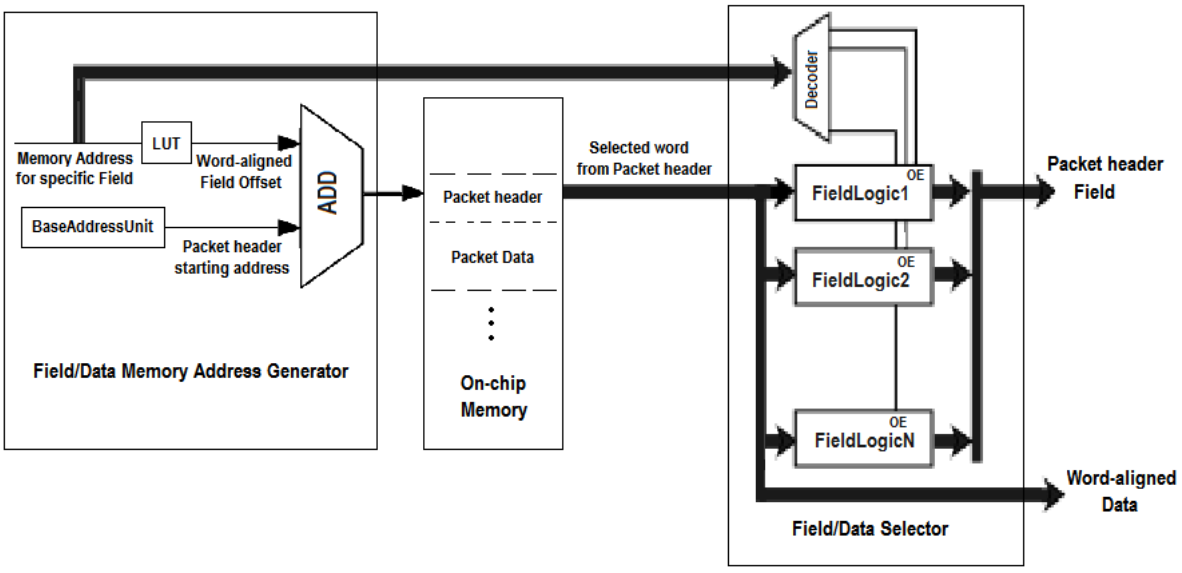

Figure 1: Reading a single IPv4/IPv6 header field with the IP header parsing hardware unit.

IPv4 Header

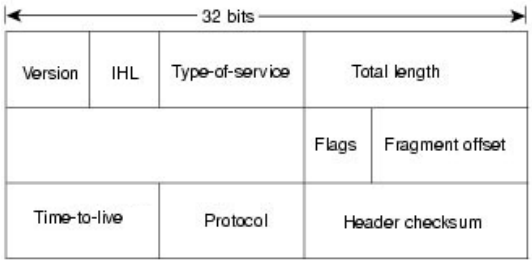

IPv4 Header @0000100000001000
version 4
headerLength 4
typeofService 8
firstwordfirstHalf 16 //used for IP checksum
totalLength 16
identifier 16
flags 3
fragmentOffset 13
secondwordsecondHalf 16 // used for IP checksum
timetoLive 8
protocol 8
thirdwordfirstHalf 16 //used for IP checksum
headerChecksum 16

IPv6 Header

IPv6 Header @0000110000000000
version 4
trafficClass 8
flowLabel 20
payloadLength 16
nextHeader 8
hopLimit 8

Figure 2: Description of IPv4 and IPv6 headers.

The IP header parsing logic is designed so that it assumes that a packet with IPv4 or IPv6 header format is located in a fixed area of the memory. The description of the format of IPv4 or IPv6 packet headers is shown in Fig. 2. In the given IP header descriptions the first line defines the name of the IP header and its location in memory, while each following line contains the definition of a single field. For each IP header field, the name and its size in bits are specified. The IP header fields are defined in the order that they appear in the IP header.

Table 1: Look up table in IP header parsing logic.

MemoryAddress for IP header field	**Word-aligned IP header Field Offset**
0000h (IPv4 version)	0000h (first word)
0001h (IPv4 headerLength)	0000h (first word)
0002h (IPv4 typeofService)	0000h (first word)
0003h (IPv4 firstwordfirstHalf)	0000h (first word)
0004h (IPv4 totalLength)	0000h (first word)
0005h (IPv4 identifier)	0001h (second word)
0006h (IPv4 flags)	0001h (second word)
0007h (IPv4 fragmentOffset)	0001h (second word)
0008h (IPv4 secondwordsecondHalf)	0001h (second word)
0009h (IPv4 timetoLive)	0002h (third word)
000Ah (IPv4 protocol)	0002h (third word)
000Bh (IPv4 thirdwordfirstHalf)	0002h (third word)
000Ch (IPv4 headerChecksum)	0002h (third word)
000Dh (IPv6 version)	0000h (first word)
000Eh (IPv6 trafficClass)	0000h (first word)
000Fh (IPv6 flowLabel)	0000h (first word)
0010h (IPv6 payloadLength)	0001h (second word)
0011h (IPv6 nextHeader)	0001h (second word)
0012h (IPv6 hopLimit)	0001h (second word)

The IP packet header starting address, which is specified in the IP header description, is placed in a specific base address unit that is part of the IP header parsing logic. Besides that, the input memory address for the specific IP header field is translated into a field offset by the lookup table (LUT), as given in Table 1. The field offset represents a word-aligned offset to the starting IP header packet address, which points to the location where the given IP packet header field is placed. This means that if the length of a specific field is smaller than the memory word length, then the closest word-aligned offset is selected and put in the LUT table.

The address of the memory word that holds the required IP packet header field is calculated by adding the field offset to the IP packet header starting address. Once the word is selected, it is read

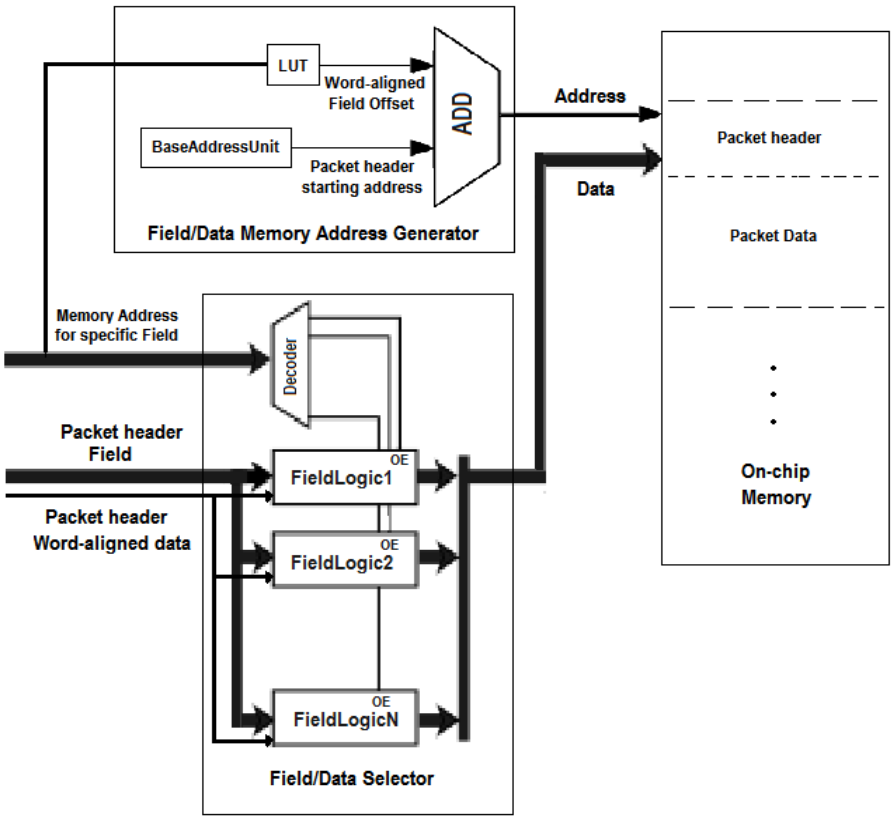

Figure 3: Writing to a single IPv4/IPv6 header field with the IP header parsing hardware unit.

from the memory and then forwarded to the field processing units. Each field processing is separated into a field logic (FL) block that is activated by the output enable (OE) signal connected to a decoder output. The decoder is also driven by part of the input memory address, causing only one of the FL units to be selected at a given moment. Each FL block is responsible to perform some bit-wise and/or shifting operations in order to extract and then zero-extend the appropriate IP header field. In the case when an IP header field is word-aligned, then its FL block is empty and the word is directly forwarded from memory to the module output.

The presented IP header parsing module form Fig. 1 shows the hardware that is needed to read out a single IP header field from memory. The same concept is used for writing directly to the IP header field in memory, as can be seen in Fig. 3. The both modules select the address of the memory word that holds the required IP packet header field in the same way. The only difference between them is that the packet header word-aligned data read from memory and the IP packet header field that should be written to the memory are applied to each field logic block, when writing is performed. In this way, the decoder that is driven by part of the input memory address activates only one of the FL units and then the selected FL block sets the input IP packet header field to the appropriate position in the input packet header word-aligned data. After that the whole word, including the appropriate IP header field is written to the generated address into the memory.

The given approach of direct access to IP header fields obviously brings much faster packet processing in comparison with the bare general-purpose processing, used by nearly all network processors. For example, a comparison between RISC-based general-purpose MIPS processor, (Patterson, Hennessy, 2014) with and without IP header parsing logic has shown that the number of instructions needed to load all fields from IPv4/IPv6 header is decreased by 40%/45% when IP header parsing unit is used.

4 FPGA IMPLEMENTATION OF IP PACKET HEADER PARSING UNIT

The proposed IP header parsing logic was described in VHDL, by means of Xilinx VIVADO Design Suite tool. This software environment includes a simulator for performing functional analysis of VHDL models, and several other tools for hardware synthesis and FPGA implementation. The FPGA technology is utterly suitable for research purposes, due to its advantage in terms of speed, cost, flexibility and ease of re-programmability, (Cardoso, Hubner, 2011). Therefore, for the FPGA implementation of the proposed IP header parsing logic, we make use of Virtex7 VC709 evaluation platform, (Xilinx, 2016).

The VHDL model of the proposed IP header parsing logic used for reading IP header fields is a module that includes three sub blocks: Field/Data address memory generator, on-chip memory and Field/Data Selector. This top module receives a memory address for specific IP header field and an IP packet header starting address as an input, and produces an IP packet header field or a word-aligned data as an output. This unit is optimized only to extract fields from IPv4 and IPv6 headers, but it can be easily extended and reconfigured to work with other packet header formats. This extension would introduce some modifications into the look up table and would require definition of novel field logic blocks in the IP header parsing logic.

The schematic of the IP header parsing logic used for direct access to IP header fields that has been generated in Xilinx VIVADO Design Suite is shown in Fig. 4. In addition to that, Fig. 5 presents the schematic of IP header parsing logic that is used for writing to IP header fields. This schematic has been generated in Xilinx VIVADO Design Suite and as shown in Fig. 5 is composed of RAM memory and a ShiftBackComputeDataAndAddress module that consists of memory address generator and data field selector, which are used to generate the write address and the data that should be written into the RAM memory.

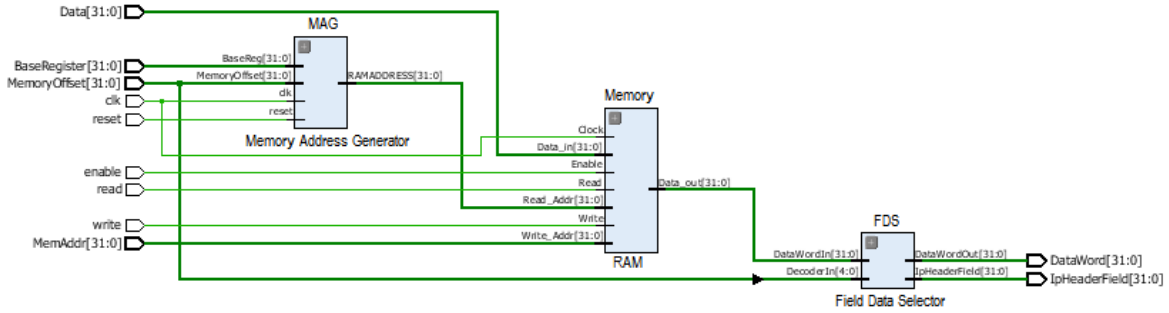

Figure 4: Schematic of IP header parsing logic used for direct access to IP header fields. The module is described in VHDL and then generated in Xilinx VIVADO Design Suite.

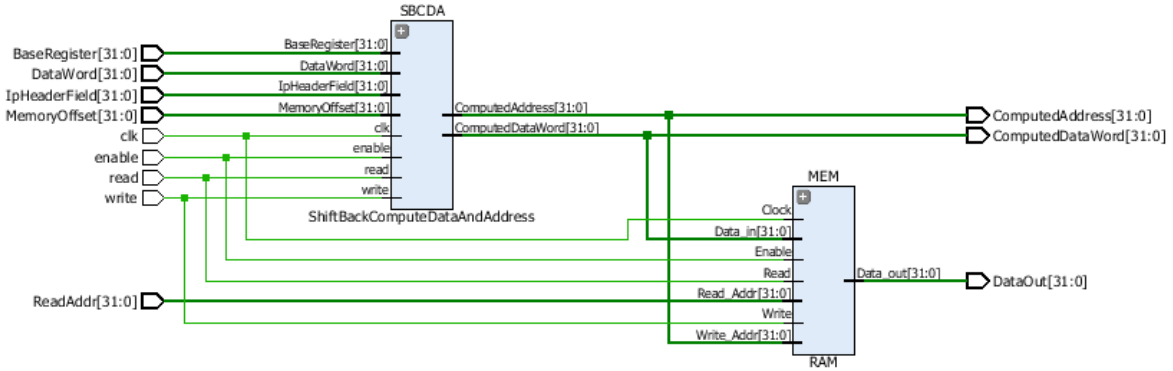

Figure 5: Schematic of IP header parsing logic used for writing to IP header fields. The module is described in VHDL and then generated in Xilinx VIVADO Design Suite.

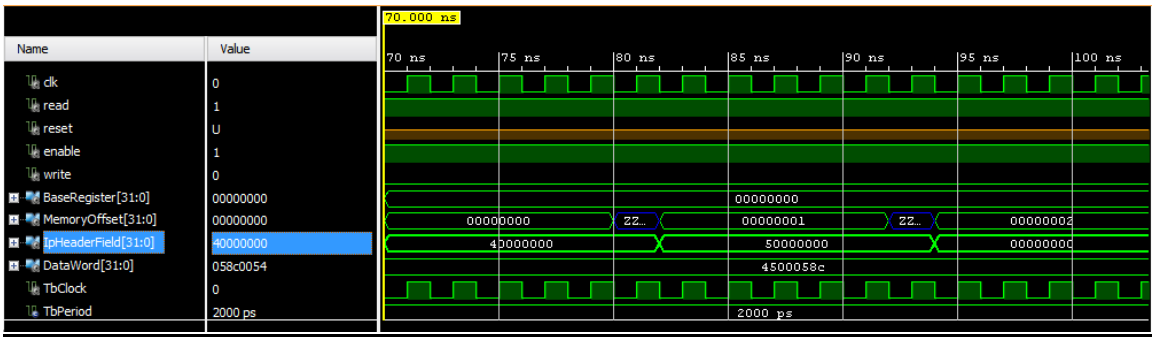

Figure 6: Simulation of direct access to IP header fields in VIVADO simulator.

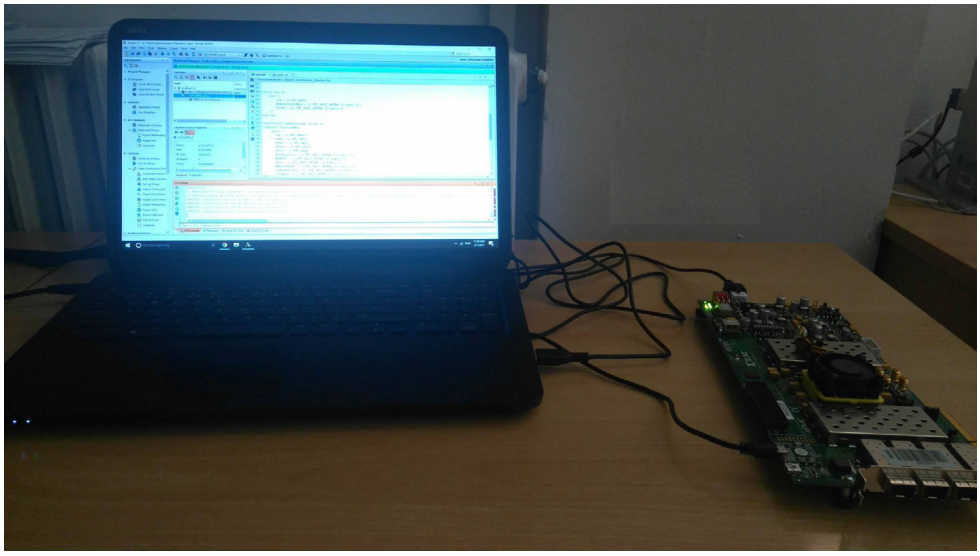

a)

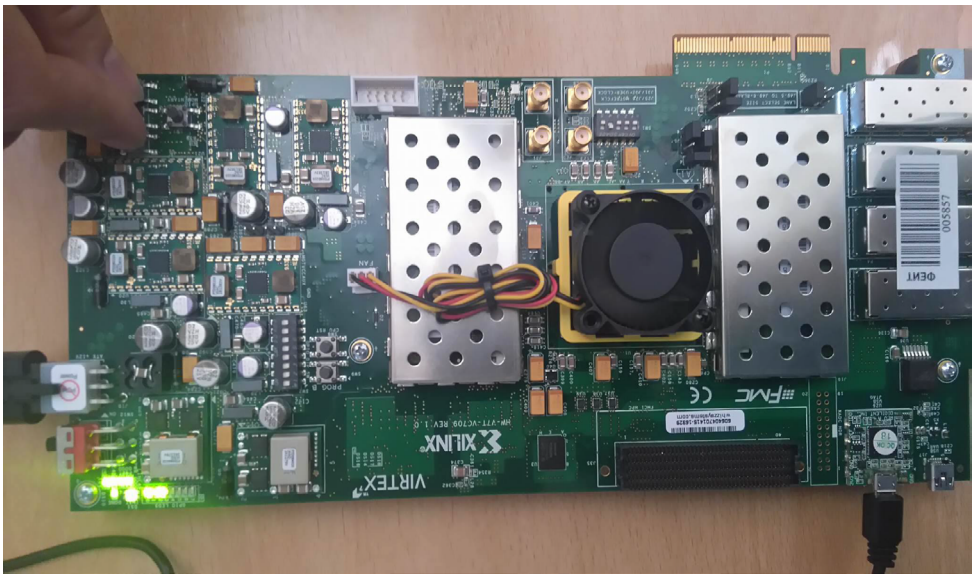

b)

Figure 7(a and b): Implementation of IP header parsing logic in Virtex 7 VC709 FPGA board.

Fig. 6 presents simulation results of the IP header parsing top module (which includes modules for read or write to IP header fields), while performing extraction of several fields (version, header length and type of service) from an IPv4 packet header. For the given simulation scenario, it is considered that the memory is already filled with several IP packets, whose IP headers are later parsed and inspected. The waveform signal given in Fig. 6 verifies that the proposed IP header parsing logic works properly.

Once the functional simulation is finished, FPGA synthesis and implementation of the proposed IP header parsing module are performed. The synthesis results show that the IP header parsing logic can be implemented in Virtex7 VC709 evaluation platform, by utilizing 0.01% of the slice registers and 0.35% of the slice LUT resources, which is less than 1% of the occupied FPGA slice resources. As a result of the low FPGA resource's utilization, the initial IP header parsing logic design can be further extended (for other packet header formats) and then implemented in the same Virtex 7 VC 709 FPGA board. According to that, the use of FPGA technology makes the proposed IP header parsing hardware very flexible and also cheap for implementation.

Fig. 7 presents the FPGA implementation of the proposed IP header parsing logic. For that purpose we have created a constraint file which makes use of the input Switch Pins and output LEDs of the Virtex 7 VC 709 FPGA board. Therefore, we have used the Switch Pins to set the specific memory address of the IP header field that should be parsed. Once the IP header field has been selected, the output LEDs light were showing which FL block was activated, during the appropriate IP header field extraction. In this way we were able to test the proposed IP header parsing module in real hardware (FPGA prototype).

5 CONCLUSIONS

This paper proposes an IP header parsing hardware module that allows single- cycle memory access to non byte- or word- aligned fields in IPv4 and IPv6 packet header formats. This approach accelerates the packet processing in both general-purpose and application-specific processor architectures, as IP header field access is a very frequent operation in network processing. Actually, it was shown that a MIPS processor that is extended with IP header parsing logic achieves 40/45% faster header parsing of IPv4/IPv6 packets, in comparison with a bare MIPS processor.

The main focus of this paper is the FPGA implementation of the proposed IP header parsing logic. Considering that the implemented IP header parsing logic utilizes less than 1% of the occupied FPGA slice resources, future work would include comparison of hardware complexities for various header formats and justification of the additional hardware over the performance improvement. It is obvious that these modifications would require extensions of the look up table and definition of novel field logic blocks in the existing IP header parsing logic. Having this possibility to generate parsing modules for specific packet headers, and reconfigure the system to start using them, whenever there is a need for a new networking protocol, is very attractive. This approach makes use of FPGA re-configurability, which has proven to be an ideal solution for achieving reasonable speed at low price.

REFERENCES

Ahmadi, M., Wong, S., 2006. Network processors: challenges and trends. In *17th Annual Workshop on Circuits, Systems and Signal Processing.*

Wheeler, B., 2013. *A new era of network processing*. LinleyGroup Bob Wheeler's White paper.

Lekkas, P. C., 2013. *Network Processors: Architectures, Protocols and Platforms*, McGraw-Hill Professional.

Shorfuzzaman, M., Eskicioglu, R., Graham, P., 2004. *Architectures for network processors: key features, evaluation, and trends,* Communications in Computing, pp.141-146.

Giladi, R., 2008. *Network Processors - Architecture, Programming and Implementation*, Ben-Gurion University of the Negev and EZchip Technologies Ltd.

Naous, J., Gibb, G., Bolouki, S., McKeown, N., 2008. NetFPGA: reusable router architecture for experimental research, in *Sigcomm Presto Workshop*.

Petracca, M., Birkea, R., Bianco, A., 2008. HERO: High speed enhanced routing operation in software routers NICs. in *IEEE Telecommunication Networking Workshop on QoS in Multiservice IP Networks*.

Intel, 2005. *Intel® IXP2800 and IXP2850 network processors*, Product Brief.

Doud, B., 2015. Accelerating the data plane with the Tile-mx manycore processor, in *Linley Data Center Conference*.

Xilinx, 2016. *VC709 Evaluation Board for the Virtex-7 FPGA*. User guide.

Cardoso, J. M. P., Hubner, M., 2011. *Reconfigurable Computing: From FPGAs to Hardware/Software Codesign*, Springer-Verlag.

Gibb, G., Varghese, G., Horowitz, M., McKeown, N., 2013. Design principles for packet parsers. In

ACM/IEEE Symposium on Architectures for Networking and Communications Systems, pp. 13–24.

Kořenek, J., 2013. Hardware acceleration in computer networks. In *16th International Symposium on Design and Diagnostics of Electronic Circuits Systems*.

Hauger, S., Wild, T., Mutter, A., 2009. Packet processing at 100 Gbps and beyond—challenges and perspectives. In *15th International Conference on High Performance Switching and Routing*.

Gupta, P., Lin, S., McKeown, N., 1998. Routing lookups in hardware at memory access speeds. In *IEEE Infocom'98*, pp. 1240–1247.

Eatherton, W., Varghese, G., Dittia, Z., 2004. Tree bitmap: hardware/software IP lookups with incremental updates. In *Sigcomm Computer Communication Review*, vol. 34, no. 2.

Kekely, L., Puš, V., Kořenek, J., 2014. Software Defined Monitoring of application protocols. In *IEEE Conference on Computer Communications*, pp. 1725–1733.

Bolla, R., Bruschi, R., Lombardo, C., Podda, F., 2014. OpenFlow in the Small: A Flexible and Efficient Network Acceleration Framework for Multi-Core System. In *IEEE Transactions on Network and Service Management*, pp. 390-404.

Puš, V., Kekely, L., Kořenek, J., 2014. Design methodology of configurable high performance packet parser for FPGA. In *17th International Symposium on Design and Diagnostics of Electronic Circuits Systems*, pp. 189–194.

Attig, M., Brebner, G., 2011. 400 Gb/s Programmable Packet Parsing on a Single FPGA. In *Seventh ACM/IEEE Symposium on Architectures for Networking and Communications Systems*, pp. 12-23.

Brebner, G., Jiang, W., 2014. High-Speed Packet Processing using Reconfigurable Computing. In *IEEE Micro*, vol. 34, no. 1, pp. 8– 18.

Patterson, D., A., Hennessy, J., L., 2014. *Computer organization and design: the hardware/software interface*, Elsevier. 5th ed.

Specificity of Undivided Time Series Forecasting Described with Innovation Curves

Mikhail Sadiakhmatov, Leonid Mylnikov
Perm National Research Polytechnic University
Komsomolsky Prospekt 29, 614990, Perm, Perm Krai, Russia
fortis3000@gmail.com, leonid.mylnikov@pstu.ru

Keywords: Time Series, Innovation Curve, Forecasting, Production and Economic System, Function Description, Dynamic Time Warping.

Abstract: In this paper, we consider characteristics of remote time period forecasting in the case when particular time periods could be described with innovation curves. Also, time series, whose periods determined by the curve types known, are not clearly seen. However, the fact that the time series describe projects with the same product evolution is known, and the time when new generations appear is determined.

1 INTRODUCTION

It is well known that many production and economic systems parameters are described with special curves. The type of curve, which describes the parameter, depends on that parameter. Innovation curves describe economic indexes, e.g. profits, sales volume, market share, which is held by company or product, a number of rival firms or products, how many people are recruited in the project work, product quality, etc. Engineering and process-dependent parameters are described with S-Curves, e.g. developing and the introduction of the new technology, performance index, the degree of maturity of the technology or process, etc. The S-Curves show the degree of the technology development and prospects of its modernization. Each parameter of the innovation project could be at its developmental stage and described its own functional dependence.

Issues, concerned with conceptual modeling (Mylnikov, 2015) and prognostic model development for management tasks solving in production and economic systems to remote time periods, are becoming more and more relevant in view of business conducting under market conditions. There is no way to develop these models without employing parameters predictions. And in this case, when considering the long-term statistics, as a rule, attention is not paid to revision and product modification peculiarities as it is considered as insignificant. However in terms of market modifications are individual products with its own life cycle properties concerned with modernization level, different from the main products one and which are in functional dependence on main parameters.

In order to forecast undivided time series, approaches based on the fitting criteria and fractal methods of forecasting are traditionally used. The fractal approach requires a lot of statistics. This characteristic makes it impossible to analyze financial reporting (Crownover, 1995). Moreover, the fractal methods are best suited to describe the parameters, which are characterized by chaotic changing (Feder, 1988). Modeling based on fitting criteria has the low precision of describing in the case when the product has several generations (Bjorck, 1996). For mathematical formulation, in this case, could be applied dynamic time warping.

2 DATA PREPARATION FOR SOLVING FORECAST TASKS

To test the hypothesis we construct the model using Ford concern's historical data of various car generations and models for various periods. For that, we take sales volume and pricing data from official concern [corporate.ford.com/investors/reports-and-filings/monthly-reports.html] (monthly reports from 2012 to 2016) and supplement them with data from

computational knowledge engine WolframAlpha [www.wolframalpha.com].

Table 1: The statistics of Ford Expedition price and sales volume changing.

Year	Expedition			
	Sales volume	Price $ (min)	Price $ (med)	Price $ (max)
1997	45974	27620	30914	34225
1998	214524	28225	31449	34690
1999	225703	29355	33989	39095
2000	233125	29845	34645	39885
2001	213483	30195	35204	40850
2002	178045	30555	35501	41085
2003	163454	31820	36763	41560
2004	181547	32500	36870	41995
2005	159846	33455	39703	46340
2006	114137	32660	38815	45240
2007	87203	29245	35445	39995
2008	90287	31345	38294	43590
2009	55123	34845	42196	47850
2010	31655	35585	42906	48590
2011	37336	36205	43265	49655
2012	40499	36530	43380	49680
2013	38062	40605	46763	51355
2014	38350	41975	49558	56205
2015	44632	43845	55257	62410
2016	41443	45435	56563	63375

Production and economic system's parameters could be defined with output goods' parameters. Two parameters: sales volume and the current price could be used for simplified estimation of competitiveness. Sales volume reflects customers' preferences and could be a criterion of competitiveness. The product price allows estimating proceeds and profit of the system. The ratio of profit and sales volume also characterize business and economic activity efficiency of the system. It is possible to make initial forecast of the system's parameter behavior with the help of received data. Production and economic system's parameters describing might be more accurate when more parameters adding. Consequently, their forecasting also improves.

For conducting research we collected data about models Ford Expedition, C-Max (01.01.2013 – 01.10.2016), Edge (01.01.2007 – 01.10.2016), Escape (01.01.2001 – 01.10.2016), Expedition (01.01.1997 – 01.10.2016), Explorer (01.01.1991 – 01.10.2016), Fiesta (01.01.2013 – 01.10.2016), Focus (01.01.2000 – 01.10.2016), Fusion (01.01.2006 – 01.10.2016), Mustang (01.01.1991 – 01.10.2016), Transit (01.01.2015 – 01.10.2016). To work with the model we represent Ford Expedition data in table 1.

Distinctive feature of the data is that there are several model generations in considered time periods. Besides, we know periods of simultaneous production of old and new model generations. Sales volume and price changing of each model could be described with the innovation curve (Mylnikov, 2013). However, the whole time series cannot be described with the curve. Therefore we make innovation and S-Curve for each generation each model.

3 PIECEWISE FUNCTION DESCRIPTION OF CONTINUOUS TIME SERIES USING INNOVATION CURVE

Innovation curve is a piecewise function and consists of exponential growth, linear growth, and parabolic maternity piece. Set of equations describing the curve:

$$\begin{cases} f_1(t) = e^{c_0 t}, & 0 < t < t_1 \\ f_2(t) = c_1 + c_2 t, & t_1 < t < t_2 \\ f_3(t) = c_3 + c_4 t + c_5 t^2, & t_2 < t < t_3 \end{cases}$$

Factors c define the function's position, shape and increasing (decreasing) and depend on innovation project specifics. Values t_1, t_2, t_3 correspond to time values of transition points between innovation project stages.

The problem of determining the transition points could be solved with expert method based on innovation curve characteristics, such as (Wolberg, 2006): the area bounding with exponential growth piece (market entry piece) is 3% of the total figure area; the area bounding with linear growth piece is 13% of the total figure area; the area bounding with parabolic maternity piece is 34% of the total figure area; the area bounding with decline piece is 16% of the total figure area.

When calculating the data collected, we neglect the first growth stages of some models because of short entry market period or its absence and also the inadequate amount of date during the life cycle of the models under consideration.

To fulfill the conditions of the curve smoothness it is necessary to provide coincidence of value of functions and their first-order derivative. For that, we could use known function transition point's values. As the result of initial data analysis we could make a set of equitation describing Ford Expedition model:

For period corresponding to 1st generation:

$$\begin{cases} f_1(t) = e^{10.736t}, & -1 < t < 0 \\ f_2(t) = 45974 + 168550t, & 0 < t < 1 \\ f_3(t) = 10221 + 240056t - 35753t^2 & 1 < t < 7 \end{cases}$$

For period corresponding to 2nd generation:

$$\{f_3(t) = -211007 + 111294t - 8147.29t^2, 6 < t < 11$$

For period corresponding to 3rd generation:

$$\{f_3(t) = -590577 + 134158t - 6638t^2, \ 10 < t < 14$$

We chose negative transition point value of exponential growth of the first generation as the first Expedition generation was put on sale about one year previously. Figure 1 shows various functions of maternity piece describing. Transition points are chosen also expertly.

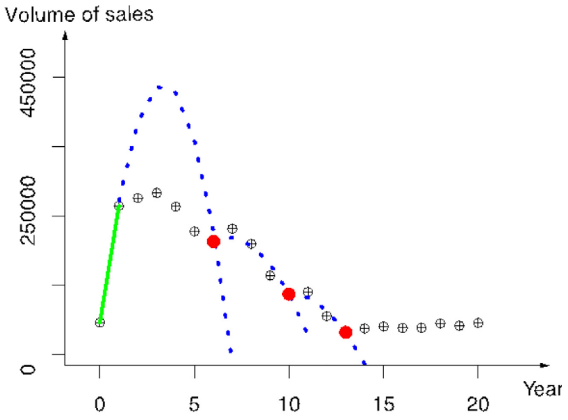

Figure 1: Sales volume modeling with innovation curve.

Another example of undivided interval described time series is car sales volume changing. Collected data include Ford Expedition's minimal, average and maximal prices values. When describing average prices with innovation curve we receive (Figure 2):

For the Ford Expedition 1st generation period:

Minimal price:

$$\begin{cases} f_1(t) = 27620 + 867.5t, & 0 < t < 2 \\ f_2(t) = 27368.8 + 1118.8t - 62.8t^2, & 2 < t < 6 \end{cases}$$

Average price:

$$\begin{cases} f_1(t) = 30914 + 1537.5t, & 0 < t < 2 \\ f_2(t) = 30070 + 2381.5t - 211t^2, & 2 < t < 6 \end{cases}$$

Maximal price:

$$\begin{cases} f_1(t) = 34225 + 2435t, & 0 < t < 2 \\ f_2(t) = 32406 + 4254t - 455t^2, & 2 < t < 6 \end{cases}$$

For the Ford Expedition 2nd generation period:

Minimal price:

$$\begin{cases} f_1(t) = 26915 + 817.5t, & 6 < t < 8 \\ f_2(t) = -66605 + 24198t - 1461.3t^2, & 8 < t < 10 \end{cases}$$

Average price:

$$\begin{cases} f_1(t) = 27943 + 1470t, & 6 < t < 8 \\ f_2(t) = -87225 + 30262t - 1799.5t^2, & 8 < t < 10 \end{cases}$$

Maximal price:

$$\begin{cases} f_1(t) = 27200 + 2390t, & 6 < t < 8 \\ f_2(t) = -150780 + 46890t - 2781.3t^2, & 8 < t < 10 \end{cases}$$

For the Ford Expedition 3rd generation period:

Minimal price:

$$\begin{cases} f_1(t) = 1245 + 2800t, & 10 < t < 12 \\ f_2(t) = -25233 + 7213t - 183.9t^2, & 12 < t < 19 \end{cases}$$

Average price:

$$\begin{cases} f_1(t) = 1690 + 3375.9t, & 10 < t < 12 \\ f_2(t) = -25528 + 7912t - 189t^2, & 12 < t < 19 \end{cases}$$

Maximal price:

$$\begin{cases} f_1(t) = 720 + 3927.5t, & 10 < t < 12 \\ f_2(t) = -34450 + 9789t - 244t^2, & 12 < t < 19 \end{cases}$$

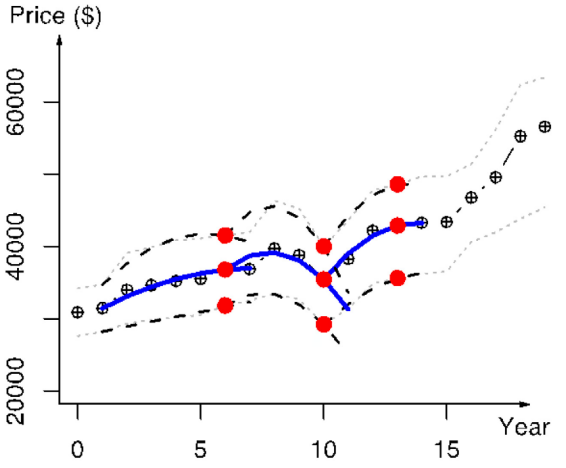

Figure 2: Price changing model described with innovation curve.

Knowledge of regularities in value changes makes it possible to describe them functionally and thereby forecast values necessary to plan economic activity and management decision making on the goods which they describe.

As a case in point, we compare the proposed describing method with functional describing with the method of least squares. Least-squares method applied to sales of Ford Expedition volume describing gives a function $y = 242800 - 5847x - 107x^2$, for the sales changing $y = 13707 - 1040x - 15x^2$, $y = 36487 - 909x - 62x^2$, $y = 38674 - 609x + 57x^2$ (for minimal, average and maximal prices accordingly).

Model verification with chi-square criterion for time series describing sales volume shows that LSM model does not pass inspection $\left(Y_i^3 - \sigma \le Y_T \le Y_i^3 + \sigma\right)$. Thus the model is not adequate. Increasing of polynomial order does not make any different basically. As is well known, considerable increasing of polynomial order decreases forecast precision in following periods. Model based on innovation curve passes inspection of chi-square criterion.

Both approaches give sales volume models that pass the chi-square criterion, but when the innovative curve is used we get a more accurate description.

As a result of conducted analysis, we could draw a conclusion that methods based on fitting criterion give the best fit to describe undivided time series when a large amount of statistic data are available. However in the case when a small amount of the data is available the knowledge of values changing regularities gives us better results. A short time period, which data could be forecasted, is a limitation of the method. It is related to the fact that we could forecast values of the unfinished time period, which is functionally describing.

To forecast long-term parameters knowledge of regularities of innovation curve time changing is necessary.

4 SPECIFICITY OF UNDIVIDED TIME SERIES FORECASTING HAVING INITIAL PART DESCRIBED WITH INNOVATION CURVE

The approach mentioned above could be applied when historical data are used. Due to the lack of data and resulting difficulty in practical forecasting, it is necessary to determine new parameters of the innovation curve on the basis of previous stages. The time series described with one of the innovation curve types could describe the life cycle of each product variety by means of the similar functions.

We could see confirmation of the hypothesis when dynamic time warping algorithm (Luzianin, 2016) is applied to maternity periods of car models (Figures 1 and 2). As a result, we could see that values' changing obeys the same tendencies, which could be represented as both displacement time and value axis and spread of the parabola's branches. The parabola branches behavior depends on parabola's factors. Unknown values could be found with axis displacement and parabola's branches spread estimation on basis of statistics. It allows extrapolating the tendencies to the future.

Quoted Ford Expedition statistics displays the tendency of sales volume decreasing and price increasing. This tendency could be evaluated through the axis displacement and parabola's branches spread. From previous computations, we got table 2. Formulas to complete the table are (Aufmann, 2008): $X_a = -\frac{b}{2a}$, $Y_a = -\frac{D}{4a}$, $D = b^2 - 4ac$ from the equation $y = ax^2 + bx + c$.

Table 2: Factors of parabola's displacement when functional sales volume and price changing describing of various Ford Expedition generations.

	Vertex coordinates		Focus coordinates ($Y_f = Y_a - 1/4a$)	Vertex displacement		Focus displacement
	X_a	Y_a		ΔX	ΔY	
Fig. 1 gen. 1	3,357	413172,4	422110,6	—	—	—
Fig. 1 gen. 2	6,830	169068,9	171105,7	3,473	-244103,5	-251004,9
Fig. 1 gen. 3	10,105	87276,6	88936,1	3,275	-81792,3	-82169,6
Fig. 2 gen. 1	7,303	37000,7	37035,7	—	—	—
Fig. 2 gen. 2	7,784	39193,5	39384,1	0,481	2192,7	2348,4
Fig. 2 gen. 3	13,825	43267,3	43401,0	6,041	4073,9	4016,9

Table 2 shows that vertex and focus displacement could be described functionally (Figures 3 and 4). The Figure 3 shows that the parabola could be plotted with the derived points. It agrees with the assumption that sales volume decrease when price increasing.

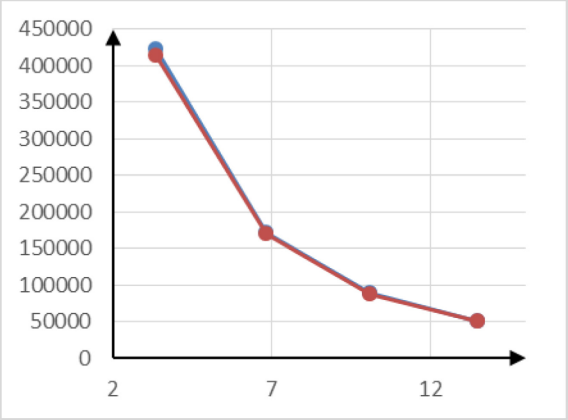

Figure 3: Value of the functions $Y_a(X_a)$ (the blue curve) and $Y_f(X_a)$ (the red curve) for sales volume changing.

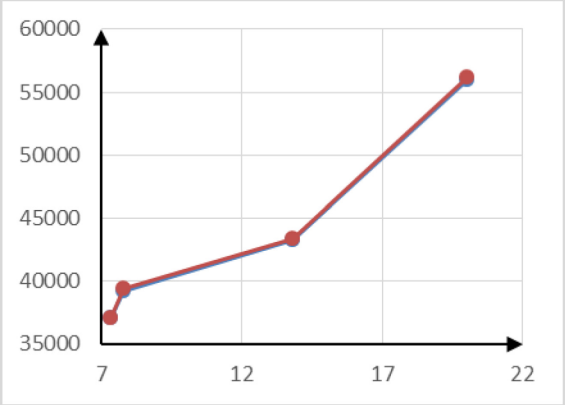

Figure 4: Value of the functions $Y_a(X_a)$ (the blue curve) and $Y_f(X_a)$ (the red curve) for price changing.

The fourth points were received for the forecasting curve.

We applied the received values to forecasting parabolic curves construction after the inverse factors determining. The results are shown in Figures 5 and 6. The received curves satisfy the model χ^2 method verification.

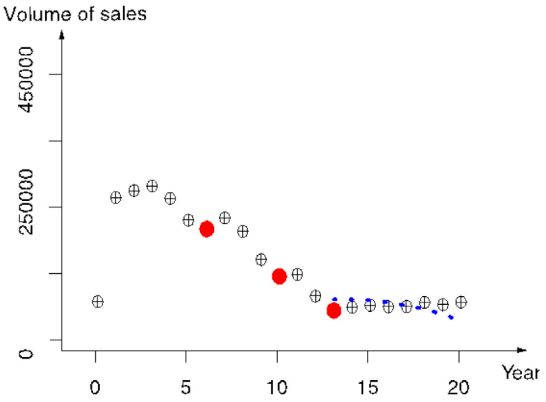

Figure 5: The fourth generation of Ford Expedition sales volume changing forecasting and its comparison to retrospective data.

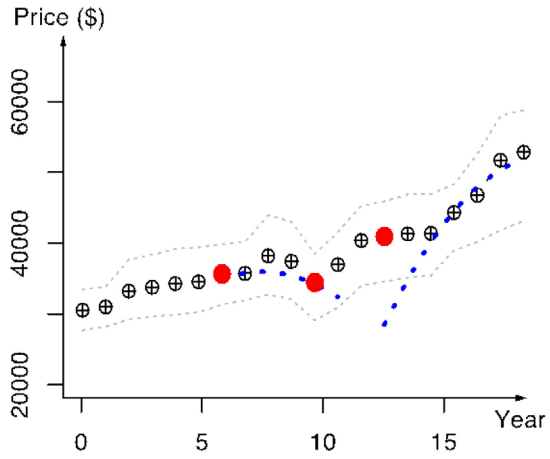

Figure 6: The fourth generation of Ford Expedition price changing forecasting and its comparison to retrospective data.

Another result is that selection of any value pairs doesn't change significantly type of the curves. And findings are also adequate. It allows making initial forecasts and updating when new data appearing. It could be made with both parabola vertex and focus coordinates specifying and e.g. factors determination with the least-square method. Moreover, received vertex coordinates of the parabola, which describes price changing of the Ford expedition the second generation, don't be on the curve (Figure 4). Vertex moving to the parabola gives us describing accuracy enhancement (Figure 6). It could be accounted in the case that the stated hypothesis about curves construction character is correct. The method of least squares allows only finding the optimum factors for available data.

To exclude random factor we made the same computation of the Ford Explorer model, which has also data on the several generations.

5 CONCLUSION

As a result of this investigation, the values describing sale volume and price changing on the periods next to the first one could be described with a parabolic function provided for enough statistics. Besides vertex and focus displacement also could be described mathematically. Thus, characteristics of new model output could be estimated before its production and specified with functional-analytic approach when the first statistics appearing.

Another result is that demand for any product without considerable modification which puts a new innovation curve will decrease when price increasing.

Dynamic time warping allows defining tendency and describing regularity of product parameters changing. However, the algorithm ignores model individuality. In particular, sales volume jumping distorts the forecasting displacement function.

REFERENCES

Aufmann R.N., Barker V.C., Nation R., 2008. *College algebra*, Houghton Mifflin. Boston.

Wolberg J., 2006. *Data analysis using the method of least squares extracting the most information from experiments*, Springer. Berlin.

Amberg M., Mylnikov, L., 2009. *Innovation project lifecycle prolongation method.* Innovation and knowledge management in twin track economies: challenges & solutions № 1-3.

Knuth D. E., 1997. T*he art of computer programming*. Reading, Mass. Addison-Wesley, 3rd ed-e.

Luzianin I., Krause B., 2016. *Modeling of Self-similar Traffic*. Proceedings of International Conference on Applied Innovation in IT, № 4.

Mylnikov L., 2015. *Conceptual Foundations of Modelling of Innovative Production Projects.* Proceedings of International Conference on Applied Innovation in IT, № 3.

Mylnikov, L., Amberg M., 2013. *The Forecasting of Innovation Projects Parameters*. 21st International-Business-Information-Management-Association Conference on Vision

2020: Innovation, Development Sustainability, and Economic Growth.

Crownover, Richard M., 1995. *Introduction to fractals and chaos*, Jones and Bartlett. Berlin.

Feder, Jens. *Fractals.*, 1988. *Physics of Solids and Liquids*, Plenum Press. New York.

Bjorck A., 1996. *Numerical Methods for Least Squares Problems*, SIAM, Philadelphia.

Innovating Information System Development Methodologies with Design Thinking

Gerhard H. Steinke, Meshal Shams Al-Deen and Ryan C. LaBrie
School of Business, Government, & Economics, Seattle Pacific University, 3307 Third Avenue West, Seattle, WA, USA
gsteinke@spu.edu, shamsaldeenm@spu.edu, ryanl@spu.edu

Keywords: Design Thinking, Waterfall System Development Methodology, Agile Development.

Abstract: Design thinking has emerged as a means of solving problems by focusing on the perspective of the customer to better determine the user's application requirements. A major complaint with the Waterfall System Development Methodology is the difficulty gathering all requirements up front prior to development, making it hard to implement customer change requests later in the development cycle. Alternatively, the Agile Development Methodology allows for constant system revisions and improvements, potentially making it hard to budget and plan for the completion of a system. This paper looks at integrating Design Thinking into the traditional Waterfall and Agile system development methodologies. Using the Design Thinking components of empathize, define, ideate, prototype, and test leads to improvement of both the developer and customer experience.

1 INTRODUCTION

Design thinking has emerged as a means of solving problems from the perspective of the customer or user in order to better determine the user and application requirements (Shapira et al., 2017; Geissdoerfer et al., 2016). Design thinking principles have been utilized by some of the world's most influential technology corporations such as SAP, IBM, Apple, Uber, Airbnb, and Capital One as a means of developing better products and services (Vetterli et al., 2016; Sutton & Hoyt, 2016; Waloszek, 2012). The concepts of innovation and empathy are a reoccurring pattern in design thinking as a development methodology. In the traditional project management and system development methodologies, whether waterfall or agile, customer interaction and participation is mostly limited to a specific time set aside to determine user requirements.

Design thinking builds on the process of empathizing and interacting with the customer from the start of the project until one has a solution that meets the customer's needs and environment (Plattner, 2016). As the name implies, design thinking is a problem-solving framework and not an exclusive project execution framework such as waterfall and agile. This paper seeks to integrate the innovative concept of design thinking into the traditional waterfall and agile system development methodologies.

2 THE DESIGN THINKING CONCEPT

Design Thinking starts by defining the problem and then developing a solution—with a focus on the customer or user of the final product (Plattner, 2016). As you focus on understanding the customer's problem, you can then create a prototype solution. This prototype is then tested – allowing you to continue to learn and improve upon your solution.

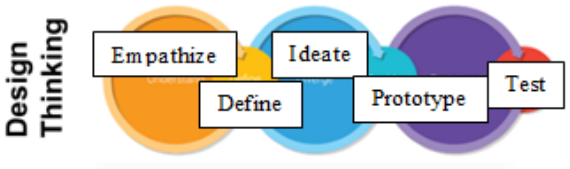

Figure 1: Design Thinking Components.

The design thinking process as a solution-based framework consists of five components including: empathize, define, ideate, prototype, and test (Dam

& Siang, 2016; Waloszek, 2012). Unlike traditional project management processes such as waterfall, design thinking is not a linear methodology. For instance, while in the empathize phase, people could also be working on a prototype to learn more about the subject, gain a deeper understanding, and create a better solution.

Empathize: A major component of design thinking is empathy. During the empathize phase the researcher or group works to understand the customer or the user who is going to be using the final product or service. When a researcher truly understands the user, he or she will be able to more clearly understand the issues they are facing. Requirements gathering processes such as observing, engaging through conversation, and interviewing are used – but with a deeper goal of empathizing with the user, to more thoroughly understand the problem and the related issues. Researchers should be able to develop and gain similar insights of the experiences as the users have. The goal of this phase is to gather requirements by better understanding the experiences of the users.

Define: Based on what is learned during the empathize phase, the define stage is where researchers bring focus and clarity to the parameters of the issue. The researcher, with the deeper understanding of the requirements gained from the empathize phase, along with their knowledge and view of the whole environment, should be able to document the requirements in a clear manner. Those working on this design thinking approach use tools to focus and understand the problems experienced by the users. The researcher should be able to step back and see the problem from a higher level or a more comprehensive perspective. By learning more about the user and the situation and environment, the researcher will see the problem more clearly. Once the requirements are defined, a research team is able to move to the next phase to generate ideas to address the problems. The define phase should conclude with a statement about the requirements that clearly sets out the scope and parameters of the problems.

Ideate: The ideate phase consists of generating multiple ideas that could be possible solutions to the problems previously defined, or at least part of the solution to the proposed challenge. This is done by creating the widest possible range of ideas. Generating a wide range of ideas allows researchers to use their imagination and look beyond obvious solutions potentially leading to more innovative ideas. The ideating phase includes various innovation techniques include building prototypes, body storming, mind mapping, and sketching. Prototyping is especially important during the ideating phase since it provides new views of the problems as well as of possible solutions.

Prototype: A prototype could range anywhere from post-it notes on a board to a tangible product. The more realistic the prototype is to what an actual user is going to use, the better the feedback and insights for improvement. Prototypes allow teams to recognize flaws in their design thinking progress while having the freedom to iterate their product.

Test: Testing is a way to solicit feedback from the prototypes and ideas created in the previous phase. Testing allows for repeating the process of applying empathy to how users experience the prototype and comparing the feedback to their initial notes. Feedback from the testing phase will help refine prototypes, and ultimately indicate whether the defined problems are addressed appropriately.

Although design thinking has been introduced as phases in a framework, often these five stages are not sequential. The team may return to a phase or even start again at the first phase of empathizing, as they try to determine if an idea or prototype actually meets the requirement, or exposes other related issues. These stages could also be viewed as components that contribute to a project, rather than a step-by-step guide.

3 DESIGN THINKING AND THE WATERFALL METHODOLOGY

The waterfall system development methodology consists of major sequential steps or phases, including: analyze, design, build, test, and deploy (Royce, 1970; Bell & Thayer, 1976). With the waterfall method, approval committees and project sponsors are required to sign-off at the conclusion of each phase in order for the project to proceed to the next sequential phase. While the waterfall methodology is beneficial in identifying requirements before a system is developed, it is not meant to be iterated upon once the design phase is complete. This leads to projects missing requirements or including feature and requirements that are not needed or wanted by users. This poses challenges in dynamic environments where potential new technology and new requirements are desired by users. Another downfall to the waterfall methodology is that researchers and teams often become overwhelmed with satisfying project approvals and meeting deadlines that they lose focus on the primary goal of the project; which is to develop a better product for the users and sponsoring organizations.

Although the waterfall methodology does share similar steps to design thinking, the latter is distinguished by its extremely heavy emphasis on empathy and human-centered design. Thus, for those companies looking to improve their products while retaining their waterfall system development practices, it is possible to incorporate both methodologies, as shown in figure 2 below. Design thinking can be combined into the waterfall method during the analysis and design phases.

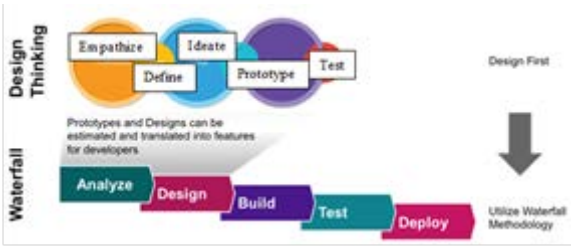

Figure 2: Design Thinking and Waterfall Methodology (adapted from Kramer, 2016).

In traditional project management methodologies, a project is determined successful if it is completed on time and within budget, assuming that the project goals and methods of achieving them are defined at the beginning of a project (Turner & Cochrane, 1993). Organizations continue to base project success on defined goals, budgets, and timelines which has proven successful if the goals and constraints are clear from the start. In the case where goals and constraints are ill-defined or unknown, organizations suffer adequate guidance and base project success on irrelevant benchmarks. According to Turner and Cochrane (1993), projects where the desired value and goals are not clearly known are most likely to fail.

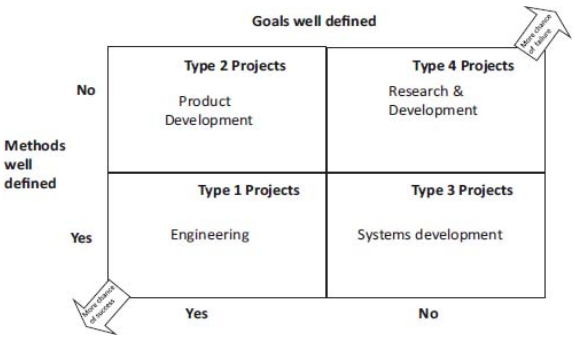

Figure 3: Goals-and-Methods Matrix (adapted from Turner & Cochrane, 1993).

For instance, in the analysis phase of waterfall, a well-defined goal and a quick interpretation of a situation are essential in order to move forward. This could be in the form of a team receiving an assignment from a client to complete a project. Design Thinking approaches problem formulation as the start of a dialogue with decision makers and users. Goals and parameters are uncovered through intensive observation, challenging stereotypical perception, and postponing problem definition. (Dijksterhuis & Silvius, 2016) In other words, the Design Thinking process is best utilized for an ill-defined problem in an organizational and/or social context.

While more research and case studies are needed for the integration of design thinking into system development, a couple of use case success stories are worth mentioning. For example, Netflix's 2011 User Experience (Web interface) redesign was design thinking inspired. The lesson learned there was that though initially there seemed to be a loud, vocal resistance, that the minority voice was overruled by the sheer number of new users delighted with the simplified interface. Similarly, Japan's largest airline, All Nippon Airways (ANA) used design thinking principles to create a customer loyalty (WonderFLY) platform offering customers products never offered before.

4 THE AGILE DEVELOPMENT METHODOLOGY

Although examples of iterative development came up time after time in software development history, agile methods did not gain popularity until the 1990s (Houston, 2014). During this time, software engineers began to question traditional waterfall methods and looked for methods that they felt better supported an engineer's requirements to develop good working software in an efficient manner.

The Agile manifesto, published in February 2001, is based on four values of agile methodologies, as paraphrased by Houston (2014):

- Individuals and interactions over processes and tools;
- Working software over comprehensive documentation;
- Customer collaboration over contract negotiation;
- Responding to change over following a plan.

Agile methodologies do not follow sequential development practices that traditional methodologies like waterfall follow. Agile focuses on an incremental approach for developing an application. Agile is often used where there is ambiguity of the requirements and the organization does not know what they want up front. With agile, organizations provide a general idea, and then the system is developed in sprints, each time working on another aspect of the system or changing those parts that do not meet the user requirements.

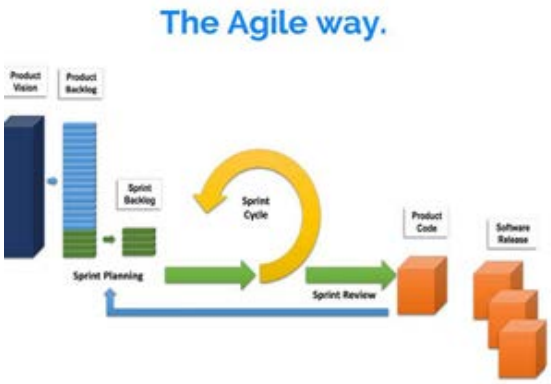

Figure 4: The Agile Development Methodology.

5 DESIGN THINKING AND THE AGILE METHODOLOGY

Integrating Design Thinking into the Agile system development methodology means that not only is the customer a part of every sprint, but that much more focus is put in the beginning to determine the customer needs, requirements, and environment (Roach, 2015). Design Thinking would enable clearer focus of the customer requirements – affecting the product vision and product backlog. There would be less rework during the sprints, since there is a more clear vision of requirements and customer expectations at the start.

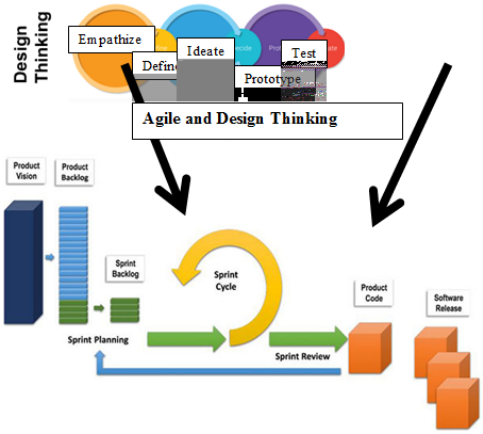

Figure 5: Design Thinking and Agile Development Methodology.

Cicoria et al. (2013) document a number of IDEO's integration of design thinking with the agile methodology in which IDEO's work helped some of the largest corporations in the world. This includes Apple & Microsoft's computer mouse design and development as well as the Ford Motor Company and Wayne Helix manufacturing divisions.

6 CONCLUSION AND FUTURE RESEARCH

The essence of design thinking as a problem-solving methodology is meant to bring the user's experience with a product to the system designers, engineers, and developers – who will then be able to understand and solve user issues more accurately. The premise of design thinking is that products need designing from the user's perspective in order to be most effective. By concentrating on the user, the development teams will be able to build products and services better suited to customer needs. Furthermore, design thinking can and should be combined with waterfall and agile system development methodologies to more clearly understand system requirements. Design thinking will require the different system development

methodologies to spend more time and focus on analyzing user requirements.

While clearer requirements will provide significant advantages in system development, further research is needed to determine how the extra time spent up front will affect the total project timeline and cost. Even though design thinking enables customer requirements to be better understood and a more innovative solution may be offered, customers will potentially still have change requests. It is not clear to what degree there will be fewer change requests due to the implementation of design thinking into the system development methodologies.

REFERENCES

Bell, T., Thayer, T., 1976. Software requirements: Are they really a problem? In *Proceedings of the 2nd international conference on Software engineering.* IEEE Computer Society Press.

Cicoria, S., Sherlock, J., Clarke, L., Muniswamaiah, M., 2013. IDEO and Design Thinking as an Agile Innovation Practice. [Online]. Available from: http://csis.pace.edu/ctappert/dps/d891b-14/Agile4.pdf 2017.01.24.

Dam, R., Siang, T., 2016. 5 Stages in the Design Thinking Process. [Online]. Available from: https://www.interaction-design.org/literature/article/5-stages-in-the-design-thinking-process/ 2016.12.09.

Daniel, K., 2015. How to Run an Agile Project in Government. [Online]. Available from: https://www.digitalgov.gov/2015/01/16/how-to-run-an-agile-project-in-government/ 2016.12.09.

Dijksterhuis, E., Silvius, G., 2016. The Design Thinking Approach to Projects, *PM World Journal*, 5(6), 1-15.

Geissdoerfer, M., Bocken, N., Hultink, E., 2016. Design thinking to enhance the sustainable business modelling process – A workshop based on a value mapping process. *Journal of Cleaner Production*, 135, 1218-1232.

Houston, D., 2014. Agility beyond Software Development, In *Proceedings of the 2014 International Conference on Software and System Process*, ACM Digital Library, 65-69.

Kolko, J., 2015. Design Thinking Comes of Age. *Harvard Business Review,* 93(9), 66-69.

Kramer, J., 2016. The Role of Design Thinking in Waterfall Methodology. [Online]. Available from: http://joshkramer.ca/the-role-of-design-thinking-in-waterfall-methodology/ 2016.12.09.

Plattner, H., 2016. An Introduction to Design Thinking Process Guide. [Online]. Available from: https://dschool.stanford.edu/sandbox/groups/designresources/wiki/36873/attachments/8a846/ModeGuideBOOTCAMP2010.pdf/ 2016.12.09.

Roach, T., 2015. How to Combine Design Thinking and Agile in Practice. [Online]. Available from: https://medium.com/startup-study-group/how-to-combine-design-thinking-and-agile-in-practice-36c9fc75c6e6#.z0eexdn5v/ 2016.12.09.

Royce, W., 1970. Managing the Development of Large Software Systems. In *Proceedings of IEEE WESCON* August 1970, 26, 1–9.

Shapira, H., Ketchie, A., Nehe, M., 2017. The integration of Design Thinking and Strategic Sustainable Development. *Journal of Cleaner Production*, 140, 277-287.

Sutton, R., Hoyt, D., 2016. Better Service, Faster: A Design Thinking Case Study. *Harvard Business Review*, Digital Articles, 2-6.

Turner, J., Cochrane, R., 1993. Goals-and-methods matrix: Coping with projects with ill defined goals and/or methods of achieving them. *International Journal of Project Management,* 11(2), 93-102.

Vetterli, C., Uebernickel, F., Brenner, W., Petrie, C., Stermann, D., 2016. How Deutsche Bank's IT Division Used Design Thinking to Achieve Customer Proximity. *MIS Quarterly Executive,* 15(1), 37-53.

Waloszek, G., 2012. Introduction to Design Thinking. [Online]. Available from: https://experience.sap.com/skillup/introduction-to-design-thinking/ 2016.12.09.

Automated Intellectual Analysis of Consumers' Opinions in the Scope of Internet Marketing and Management of the International Activity in Educational Institution

Daniil Gorbushin, Dmitriy Grinchenkov, Anastasia Kolomiets and Nguyen Phuc Hau
Platov South-Russian State Polytechnic University (NPI)
Prosveshchenie Str. 132, 346400, Novocherkassk, Russia
gorinwww@gmail.com, grindv@yandex.ru, anastasia.srstu@gmail.com, phuchauptit@gmail.com

Keywords: International Activities, Internet Marketing, Social Media Marketing, SMM, Sentiment Analysis, Computational Linguistic, Opinion Mining, Information Extraction, Social Networks Analysis.

Abstract: The issue of internet marketing in the international cooperation in institutions of higher education is studied in the article. Social media marketing technologies are offered to solve the task, paying special attention to the analysis stage. It is offered to consider social networks users' messages as analytical material. Intellectual sentiment analysis is offered as a method for such analyses. Approaches to the solution of a sentiment analysis problem are considered. The perspective application methods of collecting and the intellectual analysis of information necessary for the feedback organization and ensuring high-quality educational services are described.

1 INTRODUCTION

International relations and international academic exchange are compound integral part of modern higher educational institutions functioning. International orientation plays a key role almost in all Higher Education Institutions, as well as in the common context of the higher education policy. The international research cooperation gains more and more value. Besides, graduates are often looking for the place on the world market to find themselves. Besides, increase in global budgets and target use of resources also brings need for evaluation methods of the international level.

Now this area is presented by means of the considerable set of parameters, the majority of which has gaged character, as it is realized in the existing ratings of carrying out comparisons at the international level, for example, the Shanghai rating, Times Higher Education rating, etc. Besides gaged parameters, there are also other factors which exert the considerable impact on quality of the international activity which cannot be measured quantitatively, but which can be revealed on the basis of the analysis of the opinion of consumers expressed by them, for example, on social networks.

The international experience of activity of departments of institutional researches in the leading foreign centers and universities of the USA, the Netherlands, Germany, Great Britain and other countries confirms need of an evidence-based decision making for questions of strategic scheduling and assessment of the international activity of higher education institutions (Green, 2008), (Branderburg, 2007).

Nowadays many educational organizations are interested in efficient international cooperation, at the same time a task of establishment and support of partner contacts between employees and students of universities is rather actual. A possible way to draw attention to the educational organization is to create a marketing strategy, especially on social networks and blogs, as it is one of the main important channels for modern marketing. First of all, it is due to fast-growing percentage of social networks traffic on the internet, possibility to use targeted marketing and by great number of active users.

Scientific literature review makes it possible to allocate one of the perspective directions in the field of internet marketing - Social media marketing (SMM). SMM is a process of drawing attention to a brand through social platforms. It appeared in the marketing less than ten years ago and managed to prove the high performance, with increasing number of companies of different scale resorting to its help. SMM allows acquainting target audience with a brand, drawing attention to the activity, announcing

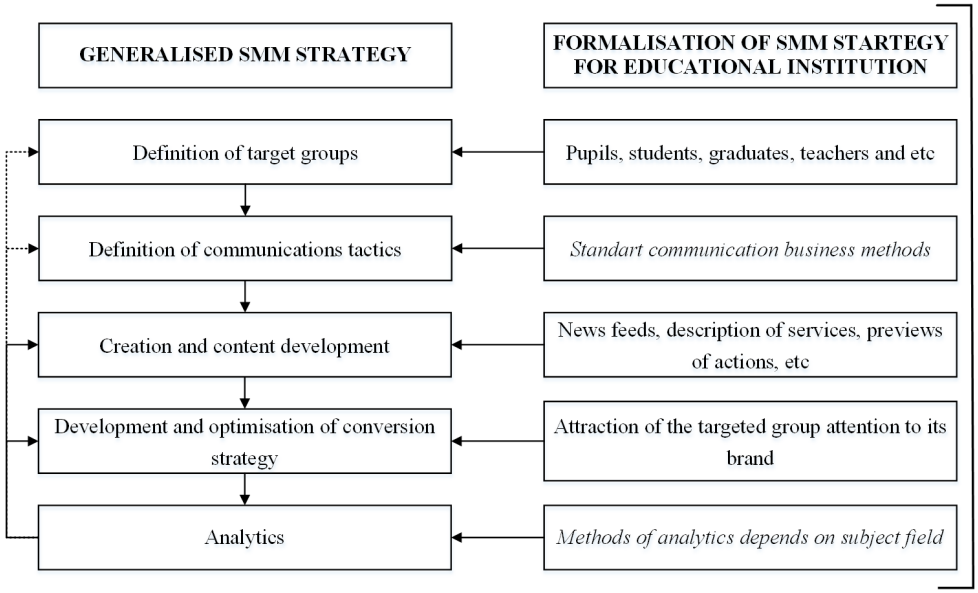

Figure 1: SMM strategy of an educational institution.

and advertising goods and services, making the website more frequently attended.

2 METHODOLOGY

There is a universal concept of SMM strategy. It fully meets the needs of the educational organizations, and some of its stages can be formalized in advance. The SMM strategy of educational institution is presented in Figure 1 (dashed lines show optional links).

Analytics stage is worth noting in particular as it is one of the most important and influencing stages. Monitoring of social networks and blogs, carrying out analytics of brand reference tonality, searching of negative sources on social networks and blogs, carrying out researches on social networks and defining the nature of negative information, analysis of advertising campaign effectiveness, etc. are among primal challenges of social networks analytics.

To have the above tasks solved qualified specialists, efficient tools for monitoring, collecting and analyzing the information obtained from social networks, and also tools for the intellectual analysis of opinions are required.

3 INVESTIGATION

The special place in the field of SMM analytics is allocated to identification of sentiment messages of social networks (positive / negative / neutral). By means of this information it is possible to estimate qualitatively effectiveness of the international activity of educational institution, to reveal a number of the factors influencing the brand image. Up-to-date criteria of sentiment information analysis in the international activity of educational institutions:

- identifications of brand attributes forming negative or positive customer response;
- evaluation of quality and effectiveness of advertising actions;
- effective detection of negative response in social networks;
- evaluation of target audience attitudes to study process of HEI, actions and events carried out by HEI;
- evaluation of target audience attitudes to international activities of HEI.

3.1 Sentiment Analysis

Nowadays the analysis of a tonality is made manually, however, as the information provided in social networks and expressing opinion of authors is in text format, the task of the tonality analysis from the mathematical point of view can be reduced to sentiment analysis task (Gorbushin, 2016). Sentiment analysis is a class of text processing mathematical methods in natural language for identification and analysis of text emotional component. The task of sentiment analysis is a special problem of texts classification and information extraction which lies in the field of the computational (mathematical) linguistics on the edge

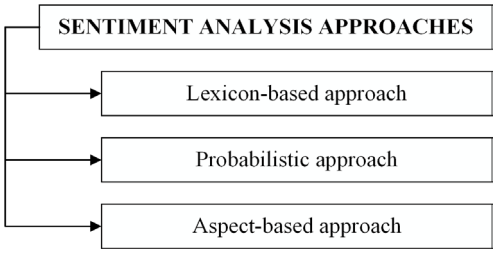

Figure 2: Sentiment analysis approaches.

of linguistics, mathematics, computer science and artificial intelligence (Gorbushin, 2014).

The text processing tool created at the sentiment analysis can be called as linguistic processor. The linguistic processor uses the formal model of language and is language dependent. Approaches to the sentiment analysis task are presented in Figure 2. Let's consider presented approaches to the solution of the sentiment analysis task:

1. Lexicon-based approach (dictionary approach) is based on search of emotive lexicon in text by using the sentiment dictionary (database of polarity words) and application of the boolean rules modeling grammars. It is worth mention that sentiment dictionaries is often used in other approaches. But the main distinctive feature of this approach is that tonality weights or valency of words are considered, on its base total value of text or sentence tonality are calculated.

2. Probabilistic approach is based on the assumption that sequence of words forming tonal unit in one text will have the same tonality in other one. Methods of supervised machine learning, training of qualifiers on the collections which are in advance marked by experts are the cornerstone of this approach (Pototskiy, 2008). Currently, training datasets for Russian language is not available in free access.

3. Aspect-based approach is based on opinion mining methods. It is the process of extraction and analysis of named entity or aspects of tonality object, which express opinion and can characterize its tonality. Supervised machine learning methods are very popular for solving the problem of aspect extraction. Such methods do not demand large training dataset. However, in a research (Collomb, 2014) aspect approach is considered as a way of overall assessment of text tonality.

Main problems of design and realization of the linguistic processor significantly influencing results of sentiment analysis are presented in Figure 3.

Statistical approach is seen as a most interesting one from the scientific point of view, while aspect-based approach is seen as better option from the qualitative estimation point of view. Linguistic approach does not have any intellectual features due to formalize already accumulated linguistic knowledge. However, rules used in this method can be successfully applied to other approaches to increase classification accuracy. For the analysis of short texts (one sentence) linguistic and aspect approaches are the most efficient methods, as well as some statistical methods. In work (Awadallah, 2012) the authors emphasize that short texts are difficult to be classified due to diverse and rarefying tonality of the linguistic features. At the moment statistical methods are seen as the most effective ones for the large texts analysis (Grinchenkov, 2015).

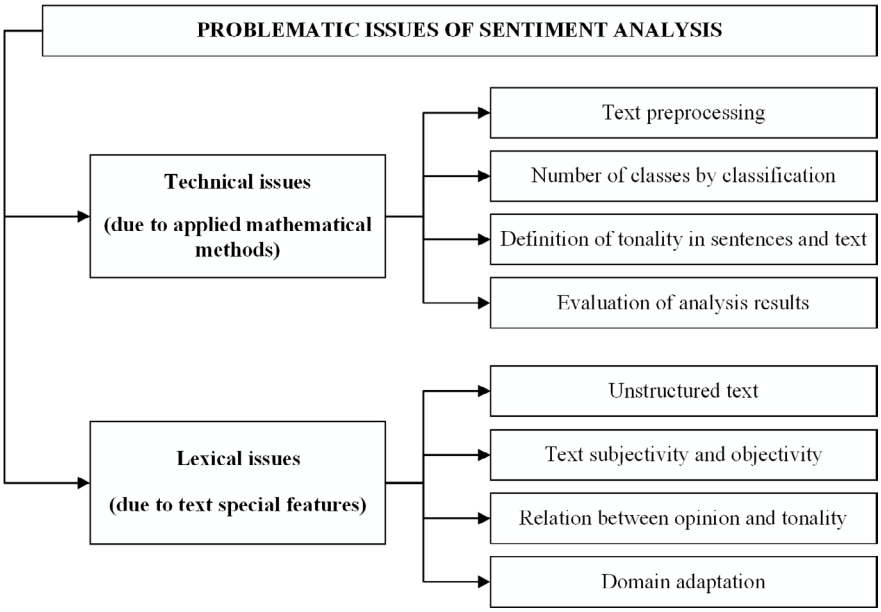

Figure 3: Problematic issues of sentiment analysis.

Problem of statistical methods is development of training dataset with examples from the domain in which the classifier is used. However, methods of linguistic approach have similar problems: sentiment dictionary, compiled for one domain that may not be appropriate for another. The preparatory phase of the statistical approach is the least labor-intensive methods. The main problem of the aspect-based approach is the complexity of drawing up of features extraction algorithms and preparation of ontologies, creating the necessary knowledge about the aspects of objects, which also depends on the subject area.

As for the problem of online marketing of international activities of educational organization it necessary to identify and analyze the opinions of social networks' users. To solve this task, the methods of the aspect approach are seen as the most appropriate.

3.2 Information Model

Taking into account the information above, one can build a model of the analysis of the university international activity management using SMM technology, social network analysis and sentiment analysis. The model is presented in Figure 4.

This model is divided into three main processes: monitoring of public opinion, expressed by the users of social networks; systematic analysis of the opinions and the development and application based on feedback SMM-strategy implemented by previous processes.

3.3 Algorithm

Using the received information, it is possible to develop an algorithm of the software part which is carrying out searching, collecting and the analysis of data from social networks. The algorithm is presented in Figure 5 and contains the following main steps:

- definition of subject domain in social network, keywords;
- search and monitoring of social network publications, including the accompanying data, saving data in the database;
- filtration of the taken data;
- sentiment analysis of the messages stored in the database:
- output the results to the user.

Messages of Vkontakte social network are supposed to be used as an initial data for analysis. To make it possible the keyword database is created for each targeted social network. Afterward the search of users messages are carried out in profile groups using VK API and keywords. As an extra search filters tonal dictionaries could be used. All found messages and extra information ("likes", "reposts") are stored in database.

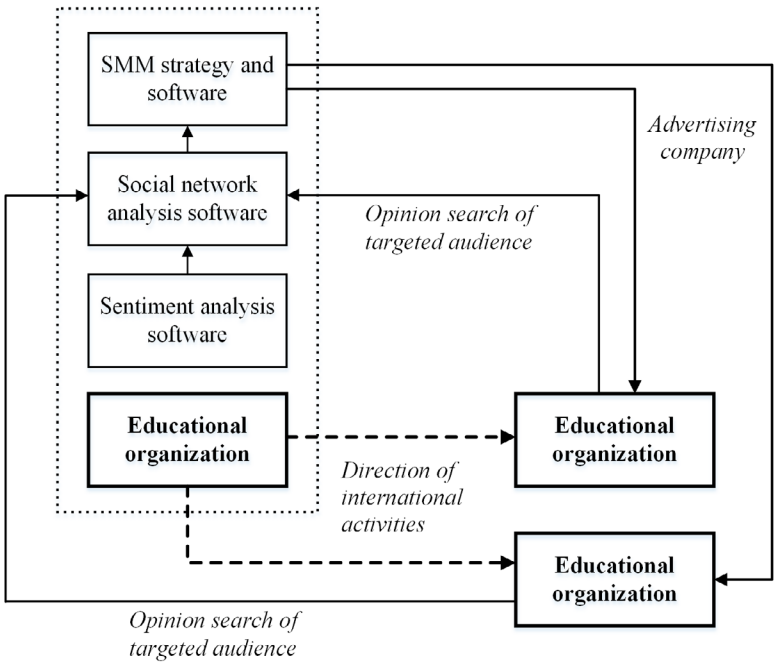

Figure 4: Information model of university international activity management using SMM technology and social network analysis.

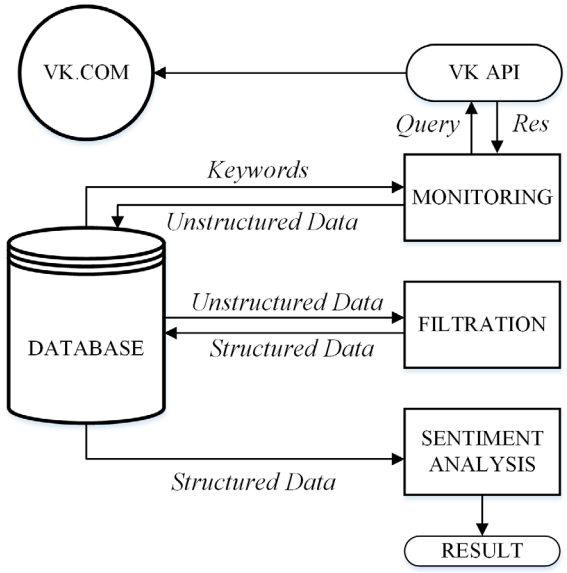

Figure 5: Algorithm.

The findings represent an unstructured text and for the further computer analysis is necessary to make a text preprocessing. At this stage, it could also use tonal dictionaries for filtration of neutral messages.

Next stage is the sentiment analysis of the obtained structured data. The main methods of analyzing of big data are supervised machine learning. They provide a high level of quality and accuracy, simply adapted to the subject area, but require the training dataset.

For the purpose of machine learning algorithms are often used standard vector representations of the text as part of the models «bag of words» or «bag of features». This model can be mathematically described as follows: given multiplicity $\{f_1, \dots, f_m\}$ of predefined features m, which may appear in a document, $n_i(d)$ – the number of iteration of feature f_i in a document d. In this case, each document can be represented as a vector:

$$\vec{d} := (n_1(d), n_2(d), \dots, n_m(d)) \quad (1)$$

Consider the basic mathematical methods that use this model.

3.3.1 Support Vector Machines

Support vector machines (support vector networks) is one of the most popular methods of supervised machine learning. The main idea of the method is to convert the original vectors into the space of the higher dimension and to search the separating hyperplane with the maximum interspace in this space. The separating hyperplane is based on two parallel hyperplanes that separate classes.

3.3.2 Naive Bayes Classifier

This classifier is based on the application of Bayes' Theorem with strict (naive) assumptions about independence. For the object of classification are calculated the likelihood function per each of classes, on which are calculated a posteriori class probability. The object is relating to the class where the posteriori probability is maximum (the principle of maximum a posteriori probability).

3.3.3 k-Nearest Neighbors Algorithm

k-Nearest Neighbors algorithm (k-NN) is the simplest metric classifier based on estimation of objects similarity. Classified object belongs to the class, which appertains to the nearest objects of learning sample. k-NN is one of the simplest classification algorithms, therefore, for the real problems it is often ineffective. Beside the accuracy of the classification, the problem of this classifier is the speed of classification: if in the learning sample is N objects, in the test sample is M objects and the dimension of the space is K, then the number of operations O for the classification of the test sample can be evaluated as

$$O = K * M * N \quad (2)$$

Except to considered methods, there are many other machine learning methods, however, they won't described in detail due to their low popularity.

3.3.4 Comparative Assessment of Methods

In the capacity of the assessment of quality of sentiment analysis is used the standard metrics for the assessment of quality text classification – precision, recall, F-measure (F1). In the research (Vasilyev, 2012) was carried out an experiment to assessment of quality of machine learning methods: SVM – the classifier of support vector machines, GMM – a Bayesian classifier based on mixtures of multivariate normal distributions, ROC – Riccios' classifier, KNN – the classifier k-Nearest Neighbours, VMF – von Mises-Fishers' classifier, TREE – the classifier based on decision trees. Metrics of Recall and Precision were considered separately for positive and negative results. The results of the analysis are presented in Table 1.

Table 1: Comparative assessment of methods of supervised machine learning.

Method	P_p	R_p	P_n	R_n
SVM	0.86	0.99	0.41	0.44
GMM	0.88	0.73	0.27	0.42
ROC	0.92	0.18	0.27	0.8
KNN	0.87	0.78	0.23	0.30
VMF	0.94	0.47	0.31	0.57
TREE	0.90	0.70	0.27	0.30

As you can see from the table above, the quality indicators for negative texts with the use of learning algorithms is noticeably worse than for positive texts. At that, the highest figures demonstrated algorithms: SVM, KNN, TREE.

For the number of classes more than two the results of the support vector method significantly reduced and it turns around mid-table 1. In general, SVM has usually high Precision, but low Recall and it can provide not a very good metric F1. In turn, low Recall is obtained due to the poor recognition of negative lexicon. The above-mentioned researches show that for to improve the quality of the tonal classification by this method it is necessary to apply additional algorithms for searching and processing of negative lexicon.

4 CONCLUSIONS

Application of the presented algorithm allows to obtain the following statistical and analytical information:

- the number of "like", "repost", followers and other quantitative characteristics of social networks and their publications;
- the number of mentions of key words and following word grouping;
- the content analysis of user messages: classification by macro-topics and by emotional tone;
- the clustering of publications according the themes.

The developed model fits into the market model b2c (Business-to-consumer - educational services market) and b2b (Business-to-business - job market). The above information model allows seeing the relationship between these markets and target audience for SMM-strategy, solves the problem of lack of feedback concerning the needs in specialists of a profile, thus solving the acute problem of b2c and b2b markets mismatch, leading to decrease in the efficiency of human resources and reduction in socio-economic development at the regional level. Information obtained in the analysis can be used not only for the purpose of advertising campaign, but also in the process of optimization and management of educational organization activities (Grinchenkov, 2014).

It is worth noting that the technology of social networks analyses and semantic analysis are the different fast developing fields of research. Current social media monitoring tools are poorly automated and require a lot of human participation, with the analysis being carried out manually. Full-scale intelligent monitoring and views analyzing tools are in the initial stage of development, presenting therefore great scientific and commercial interest.

REFERENCES

Awadallah, R. et al, 2012. PolariCQ: Polarity Classification of Political Quotations. In *Proceedings of the 21st ACM international conference on Information and knowledge management.* ACM, pp. 1945-1949.

Branderburg, A., Federkeli, G., 2007. How to measure the international activities and internationalization of educational institutions. Indicators and key indicators. Release No. 92, Berlin: Center for development of the higher education, 42 p.

Collomb, A., 2014. A Study and Comparison of Sentiment Analysis Methods for Reputation Evaluation. [Online], Available: http://liris.cnrs.fr/Documents/Liris-6508.pdf [05 Dec 2016].

Gorbushin, D.A., Grinchenkov, D.V., Mokhov, V.A., Nguyen, P.H., 2016. System analysis of approaches to solving the problem of identification of the text tonality. In *Proceedings of higher educational institutions. North-Caucasian region. Series: Engineering,* Novocherkassk, no. 2 (196), pp. 36-41.

Gorbushin, D.A., 2014. Analysis of methods of automatic classification of text tonality. In *Proceedings of Scientific-technical conference and exhibition of innovative project*, Novocherkassk, pp. 123-125.

Green, M., 2008. Measurement of internationalization at research universities, New York: American Council of training. 76 p.

Grinchenkov, D.V., Kushchiy, D.N., 2014. The formation of fuzzy collocation on the basis of semantic analysis of the framework curriculum of academic disciplines. In *Proceedings of Problems of modernization of engineering education in Russia: collection of scientific articles on problems of higher school*, Novocherkassk, pp. 298-300.

Grinchenkov, D.V., Kushchiy, D.N., 2015. On selection of keywords in the contents of the framework curriculum of academic disciplines. In *Proceedings of Traditions of the Russian engineering school: yesterday, today, tomorrow: collection of scientific articles on problems of higher school*, Novocherkassk, pp. 114-117.

Pototskiy, S.I., Grinchenkov, D.V., 2008. *Mathematical logic and theory of algorithms for programmers*, URGTU(NPI), Novocherkassk.

Vasilyev V. et. al, 2012. Sentiment classification by fragment rules. In *Kompjuternaja Lingvistika i Intellektual'nye Tehnologii*. Moscow, vol. 11(18), pp. 66–76.

Practical Aspects of Software Developing for the System of Structural and Functional Analysis of Power Supply Systems in Oil Companies

Ivan Luzyanin, Anton Petrochenkov
Electrotechnical Department, Perm National Research Polytechnic University,
Komsomolsky Ave. 29, 614990, Perm, Russia
{lis, pab}@msa.pstu.ru

Keywords: Structural and Functional Analysis, Oil-Producing Company, Power Supply System, Software, Electric Grid, Energy Efficiency, Decision Support System

Abstract: The article presents practical questions of software developing for system of structural and functional analysis of electric power supply systems (ESS) in oil companies. Software structure is described and internal structure and functions of each software element are considered. Software package includes four modules. Energy object data storage includes all data connected with ESS. Energy efficiency estimation module calculates current electric grid parameters an estimates energy efficiency of existing ESS structure. Energy efficiency control module is used for making recommendations on improving structure and functionality of existing ESS to achieve high energy efficiency under given constraints. User interface provides interaction between all modules of software package and end user. The approaches for energy efficiency analysis and control are discussed. The approach for planning arrangements on energy efficiency increasing is suggested.

1 INTRODUCTION

Under present-day conditions, oil companies face complicated task. Annual growth of oil output is needed for providing steady income. At the same time companies must fulfil government requirements on decrease of power consumption in oil fields. One way of achieving high energy efficiency is implementing intelligent control systems such as SMART GRID or Intelligent Well (Cochrane, 2013). Implementing these technologies requires upgrading of existing equipment and control technologies. The concepts also require logistical and structural changes in power supply system of a company as a whole.

Today automation level of different oil fields is not the same. System reengineering and applying new technologies are performing non-systematically. Reengineering often means installation of additional control system without replacing existing ones. It causes increase of amount of hardware and software systems. Each of them is used for solving a single task. Software and hardware systems often have proprietary interfaces that not allow interconnection between them. In addition, data stored in different systems are duplicated due to problems with data interchange.

Despite large variety of methods for ESS design and analysis (Brand, 1989, Chunmin, 2012), the method for structural and functional analysis of system as a whole and making concrete decisions on structural and functional optimization is not exists. One way of solving this task is developing of software and hardware package for modelling structural and functional schemes of PSS and testing them in a various operational modes (Kavalerov, 2013).

2 OIL FIELD AS AN ENERGY OBJECT

Structural scheme of oil field is presented on figure 1.

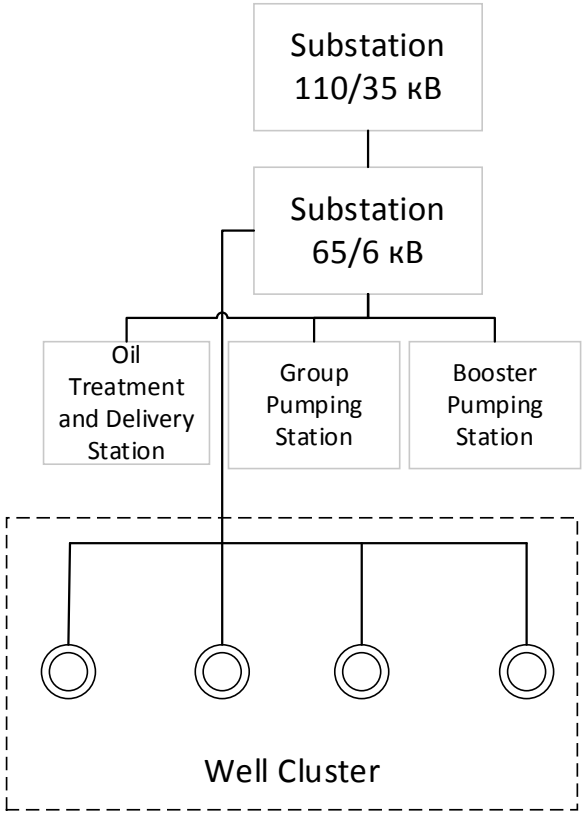

Figure 1: Structural scheme of oil field.

Oil fields ESS has large amount of consumers and complex topology. The main consumers are electric motors, heater cables and electric furnaces.

Because of connecting different types of load in different parts of grid, the unbalanced conditions appear. Long power lines cause additional power loses and make necessary to consider reactive components of their loads (Petrochenkov, 2012). Load changes depend on operational conditions of oil field and a season.

ESS is functioning in stationary and transient regimes. Transient regimes correspond to dynamic changes in electric grid (e.g. load connection and disconnection). They can be represented as a sequence of stationary regimes with a small time lapse. Therefore, modelling of stationary (quasi stationary) regimes is very important task of the study.

The aim of structural and functional analysis is finding problems in functioning of the ESS to make decisions on structure and functions changes and finally improve energy efficiency. To do this, existed system must be studied in different regimes. This task requires using of large variety of data describing ESS.

Besides the data, mathematical models and elements connection scheme need to be used in analysis procedure. Collection and storage of this information is a complicated task.

3 CONCEPTUAL MODEL OF SOFTWARE PACKAGE

Existing software systems for structural and functional analysis of ESS are usually developed for concrete system. They solve only single tasks and are not able to provide user with a complex tool of analysis the system as a whole. Software package (SP), proposed in the article, provides universality, portability and scalability within certain limits. General scheme of SP is presented on figure 2.

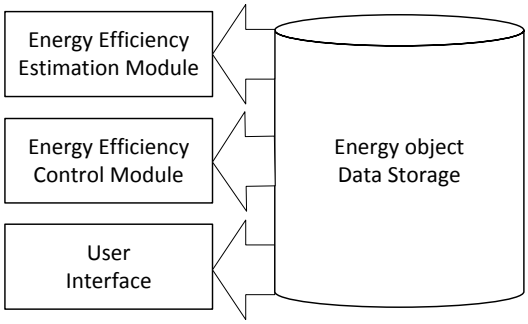

Figure 2: Structural and functional scheme of software package.

Energy object data storage (ODS) includes all data connected with ESS. Energy efficiency estimation module (EEM) allows calculating current electric grid parameters and estimating energy efficiency of existing ESS structure. It has two subsystems: calculation subsystem and estimation one. Energy efficiency control module (ECM) is a decision support system (DSS). It is used for making advices on improving structure and functionality of existing ESS to achieve high energy efficiency under given constraints. User interface (UI) includes graphical elements library and user interconnection system.

Next sections describe structure and functions of each SP module in detail.

4 ENERGY OBJECT DATA STORAGE

Data required for EES structural and functional analysis is presented on figure 3.

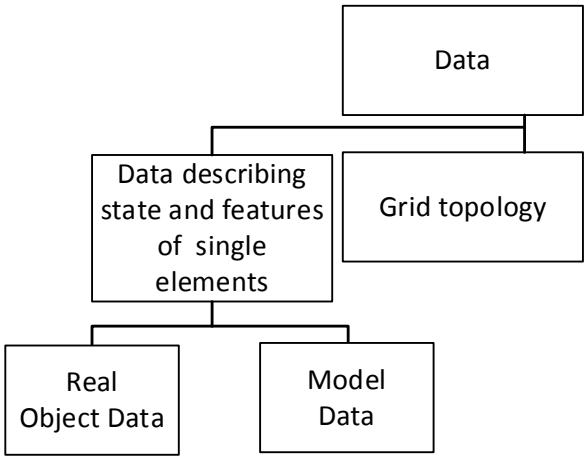

Figure 3. Data required for ESS structural and functional analysis.

These data can be divided into two groups: data describing state and features of single elements of the grid and data representing grid topology and interconnection between elements.

The first group is also divided into real objects data and model data. Real object data is presented in the form of single values and numerical series. Elements Models is describing by their equations (1-5)

Synchronous motor model

$$\begin{pmatrix} U_d \\ U_q \end{pmatrix} = \begin{pmatrix} r & X_d \\ -X_q & r \end{pmatrix} \begin{pmatrix} i_d \\ i_q \end{pmatrix} + \begin{pmatrix} 0 \\ E_q \end{pmatrix}. \quad (1)$$

Power line model

$$\begin{pmatrix} r_L & x_L \\ -x_L & r_L \end{pmatrix} \begin{pmatrix} I_d \\ I_q \end{pmatrix} = \begin{pmatrix} U_{d1} \\ U_{q1} \end{pmatrix} - \begin{pmatrix} U_{d2} \\ U_{q2} \end{pmatrix}. \quad (2)$$

Double-wound transformer model

$$\begin{pmatrix} r_T & x_T \\ -x_T & r_T \end{pmatrix} \begin{pmatrix} I_d \\ I_q \end{pmatrix} = \begin{pmatrix} U_{d1} \\ U_{q1} \end{pmatrix} - \begin{pmatrix} U_{d2} \\ U_{q2} \end{pmatrix} \quad (3)$$

Reactor model

$$\begin{pmatrix} 0 & x_r \\ -x_r & 0 \end{pmatrix} \begin{pmatrix} I_d \\ I_q \end{pmatrix} = \begin{pmatrix} U_{d1} \\ U_{q1} \end{pmatrix} - \begin{pmatrix} U_{d2} \\ U_{q2} \end{pmatrix}. \quad (4)$$

Complex static load model

$$\begin{pmatrix} r_{RLC} & x_{RLC} \\ -x_{RLC} & r_{RLC} \end{pmatrix} \cdot \begin{pmatrix} I_d \\ I_q \end{pmatrix} = \begin{pmatrix} U_d \\ U_q \end{pmatrix}. \quad (5)$$

Models are considered as branches of the equivalent circuit of electric grid i.e. they have two external terminals. Models equations determine currents and voltages of these terminals based on internal parameters of elements (complex resistances). Therefore, current values of voltages and currents as well as internal parameters of elements need to be stored in the ODS for describing the models. Since measuring of real changes of internal parameters in elements is difficult, reference parameters of elements are used in the models. These data can vary during the analysis. Data described above can also be presented as numerical series. Interaction between elements is carried out using currents and voltages in boundaries of the elements.

Second group of data includes information about grid topology. It is determined with the help of incidence matrix (nodes and branches matrix). The matrix defines the order of elements connections. For building it, electrical grid is represented as a graph. Each branch of the graph has its beginning and ending at the certain node and each element is placed in the branch. In this way, information about relative positions of nodes and branches can be stored in a table containing branch numbers with their beginning and ending nodes. Connection between branches and elements is also organized by the branch number.

In the SP a single relational database is used for data storing.

5 ENERGY EFFICIENCY ESTIMATION MODULE

Structurally EEM can be divided into calculation and estimation subsystems. The task of calculation subsystem is calculation parameters of electrical grid in the given regime.

The matrix topology approach is used for calculation. This method is very simple and provides

highest calculation performance in comparison with other ones. As an input data an incidence matrix and conductivity matrix is used. Formula (6) is used for calculation of voltages and currents (Petrochenkov, 2014).

$$\mathbf{\Pi A \Pi}^{\mathrm{T}}\mathbf{U} = \mathbf{\Pi W} - \mathbf{\Pi' I}, \quad (6)$$

where **I** is the extended current vector,

U is the extended vector of the voltages applied between the element's external terminals,

$\mathbf{W} = -\mathbf{BI} - \mathbf{H}$, **B** is a matrix, which dimensions depend on the coordinate system in which the structural component is simulated; **H** is a vector that determines the effect on the element of the means of controlling the electric parameters,

Π is a cellular incidence matrix. The cells of this matrix are zero matrices or transform matrices,

Π′ is a cellular matrix whose elements are zero cells or cells derived elements of the transform matrices,

A is a block quasi-diagonal conductance matrix of the branches (elements) that form the ESS.

Active and reactive power in nodes of electric grid is used as input data. Necessary parameters of elements are given by their models and equivalent scheme of their interconnection. As a result of calculation, nodal currents and voltages are obtained.

Estimation subsystem is used for analyzing current energy efficiency of ESS in the given regime. The main factor of energy efficiency is energy loses in electric grid and their distribution between elements. Loses are caused in two cases: distribution along power lines and consumers operation. Estimation subsystem must calculate the amount of loses. Subsystem calculates nodal loses in electric grid. Elements parameters allow estimating the distribution of loses between elements and causes of loses in each element. By this way one can estimate the energy efficiency of single elements. Overall efficiency is calculated as a sum of elements efficiencies.

6 ENERGY EFFICIENCY CONTROL MODULE

ECM must provide energy efficiency increasing arrangements of existing energy objects in oil fields. Input data for the module are electric grid calculation results and energy efficiency estimation. There are two approaches of energy efficiency improving: equipment upgrading and changing the ESS control methods. This requires significant financial and technological costs. Moreover, when doing these arrangements a number of constraints appear. They need to be taken into account both when planning and implementing arrangements.

One of the ECM functions is finding an optimal structural and functional scheme of ESS that provides given energy efficiency level based on optimization methods. Energy consumption parameters are used as optimization criteria. Gradient methods are used for optimization. Predominantly it seems to use designed classification models to estimate specific energy parameters (Ahmed, 1995, Utkin, 2014).

Optimization methods allow finding an optimal structural and functional scheme of ESS. However, in several cases costs of implementing this model are higher than achieved power saving. For solving this problem, the use of constraint satisfaction method is suggested (Lasota, 2017). The method allows finding a certain set of parameters that satisfies all given constraints at the same time. All constraints can be divided into initial (existing at the beginning of planning) and current (appearing when implementing the plan) ones. Initial constraints can be budget size, technological requirements, time limitations and so on. Current constraints are structural changes in the company budget reduction, increasing requirements on oil producing and so on.

When using the method, an optimal plan of achieving an optimal structural and functional scheme is producing. To allow for current constraints, the method is to be used iteratively when implementing the plan to change it with respect on new constraints. This approach allows fully implementing the plan with high probability.

Planning task is implemented in decision support system based on expert estimation methods. The structure of it is presented on figure 4.

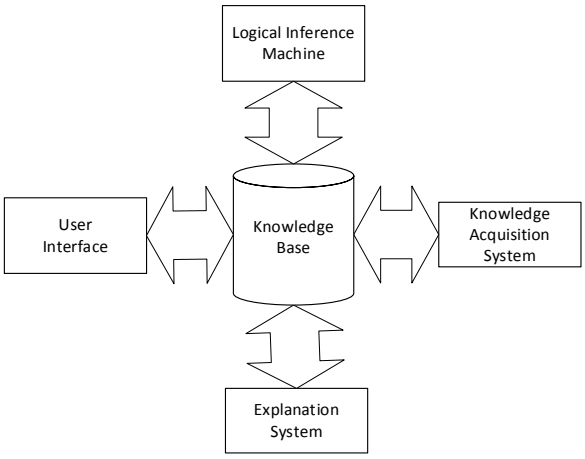

Figure 4. Decision support system structure of ECM.

This system has explanation module that allows expert to understand the way of decision making.

7 USER INTERFACE

UI provides user access for all SP functions. Data visualization is implemented using graphical objects library. User interaction system provides two operational modes of SP: observing and changing one.

In the observing mode user can see all changes in ESS parameters in current regime and get reports about current energy efficiency and ways of its increasing. Developing of energy efficiency increase plan is also allowed in this mode.

In the changing mode user can make changes in grid topology, replace elements of the grid, choose current regime and define its parameters.

8 CONCLUSION

The key aspects of software developing for the system of structural and functional analysis of PSS in oil companies are considered in the article. Requirements to the software functioning described here are the most common. Structural schemes of a whole software package and its parts are only conceptual models now. Despite that, the basic principles of software design that allow decrease programming complicity and increase flexibility of software components are presented. In the following, different tests and experiments will be carried out to find optimal mathematical methods of analysis and optimal data processing scheme. Software package prototype needs to be created. Testing of this prototype is a priority work at the next step of the research.

REFERENCES

Cochrane, L. Smart Energy Reference Architecture. [Online]. Available from https://msenterprise.global.ssl.fastly.net/wordpress/Reference_Architecture_pdf_whitepaper_2.pdf 2015.11.23

Brand, T.D., 1989. A new era in fault data acquisition and analysis. *Power Technology International*. pp. 97–100.

Chunmin, J., Li, Y., 2012. Analysis on automation of electric power systems based on GIS. *Proceedings of the 2012 International Conference of MCSA. AISC 191*. pp. 507–510.

Kavalerov, B.V., Petrochenkov, A.B., Odin, K.A., Tarasov, V.A., 2013. Modeling of the Interaction of Structural Elements. *Russian Electrical Engineering*, vol. 84, no. 1. pp. 9–13. doi: 10.3103/S1068371213010033.

Petrochenkov, A.B., 2012. Regarding Life-Cycle Management of Electrotechnical Complexes in Oil Production. *Russian Electrical Engineering*, vol. 83, no. 11. pp. 621-627. doi: 10.3103/S1068371212110090.

Petrochenkov, A.B., 2014. An Energy-Information Model of Industrial Electrotechnical Complexes. *Russian Electrical Engineering*, vol. 85, no. 11. pp. 692–696. doi: 10.3103/ S1068371214110108.

Ahmed, A., Bee, J.M., 1995. Computer simulation of electric power system. *Frontiers in Education Conference*. pp. 329–332.

Utkin, L.V., Zhuk, Y.A., 2014. Robust boosting classification models with local sets of probability distributions. *Knowledge-Based Systems.* vol. 61. pp. 59-75. doi: 10.1016/j.knosys.2014.02.007.

Lasota, S., 2017. Equivariant algorithms for constraint satisfaction problems over coset templates. *Information Processing Letters*. vol. 118, no. 11. pp. 44-52. doi: 10.1016/j.ipl.2016.09.009

Applicability of Extreme Value Theory to the Execution Time Prediction of Programs on SoCs

Irina Fedotova, Bernd Krause and Eduard Siemens
Department of Electrical, Mechanical and Industrial Engineering,
Anhalt University of Applied Sciences, Bernburger Str. 55, 06366, Köthen,
Germany {irina.fedotova, bernd.krause, eduard.siemens}@hs-anahlt.de

Keywords: Extreme Value Theory, Worst-Case Execution Time, Probabilistic Timing Analysis, Timing Verification.

Abstract: This paper describes in detail the estimation algorithm of upper bound prediction of the time acquisition task. We use the specific hardware from ARM Cortex-A series and empirical approach of time values retrieval from the timer counter. The robust Measurement-Based Probabilistic Timing Analysis (MBPTA) method based on the Extreme Value Theory (EVT) has been used for experimental verification of the algorithm. The MBPTA method allows deriving a reliable and safe worst-case execution time (WCET) estimation based on the limited number of measurements on the target platform. However, it requires an appropriate complete set of statistical tests for verifying EVT applicability. In ongoing work, we intend to outline challenges behind EVT assumptions and parameter tuning for timing analysis, and provide more coherent approach for safe probabilistic WCET estimations in order to increase the confidence that timing constraints will be met.

1 INTRODUCTION

The timing validation process for real-time systems requires guarantees that the probability of the system failing to meet its timing constraints is below an acceptable threshold. Here the metric, which is used to prove that a task will complete its function in time, called the Worst Case Execution Times (WCET). However, due to diverse features of modern CPU, usually cycle-true simulation becomes infeasible and consequently imposes correspondent limitations to the aimed timing analysis. One possibility to get around this problem is the development of statistical methods, which could allow predicting the probability distribution of the circuit delay.

In general, the goal of all timing analysis is providing a safe upper bound of execution time for a particular task (Wilhelm, 2007). Nowadays, a number of different approaches pursued that goal, primary such as deterministic (DTA) and probabilistic approaches (PTA). The difference is mainly that the deterministic method produces a unique WCET estimate, while probabilistic - multiple WCET estimates with their respective probabilities. Each approach has its static (SDTA, SPTA) and measurement-based (MBDTA, MBPTA) variants. Classical static timing analysis (STA) operates on deterministic processor architectures and provide safe WCET estimates as they are proven to be the worst ones (Abella, 2014). STA uses the exact modeling of the system or a simulator, which is in practice for modern complex real-time systems a quite challenging task. In contrary to that, the measurement-based method provides an estimation based on the derived maximal and minimal observed execution times or their distributions. Therefore, WCET estimates retrieved by static methods adds a possible extra margin, whereas WCET estimates retrieved by measurement-based methods is simply the maximum value observed or assumed during measurements: $WCET_{measured} <= WCET_{exact} <= WCET_{static}$. Moreover, with a probabilistic hardware architecture and measurement-based approaches, it is possible to guarantee an accurate predicted WCET (probabilistic WCET or pWCET), what is taken upon itself by MBPTA approach.

For characterizing the worst-case, the MBPTA (Measurement-Based Timing Analyses) approach aims at modeling extreme execution times values, relying on measurements and the application of the Extreme Value Theory (EVT). The EVT in its turn deals with the extreme deviations from the median of probability distributions. It estimates the tails of distributions, where the worst case should lie. However, hardware systemic effects in real-time systems make EVT applicability difficult with regard

to its required theoretical hypotheses. Initially, in this paper, we focus on a particular hardware presented on the Atmel SAMA5D4 board, which is based on ARM Cortex-A series processors. It employs a cache of random-replacement policy, where the failure probability of 10^{-9} is facilitated (Altmeyer, 2015).

In our resent work (Fedotova, 2016), we have already outlined the main consequences of EVT assumptions and their correct interpretation. In the ongoing paper, we expand this research, in order to overcome rest difficulties with EVT checking all hypotheses for generalizing its applicability. Therefore, based on the previous related work (Abella, 2014), (Radojković, 2016), (Guet, 2016) and as well as on our empirical experiments, we suggest a consequent and systematic step-by-step method, in order to remove the existing ambiguities in applying EVT for providing probabilistic WCET estimations. Furthermore, we consider only the certain task of time acquisition on SoCs, unlike other works, where mostly known benchmark tools have been applied.

The rest of the paper is organized as follows: In Section 2 the related work on solving the WCET calculation problem is described. Section 3 introduces the problem of the probabilistic modeling and focuses on the theoretical aspects of the EVT applicability. In this section the main steps of the algorithm proposed in this paper is described as well. Section 4 describes the experiments and their setup on the used ARM Cortex A5 platform. Section 5, 6, 7 and 8 provide subsequent details and the requirements for EVT applicability. Particularly, the proof of fitting the target distribution, estimation parameters and obtaining WCET estimators. Finally, Section 9 concludes this work.

2 RELATED WORK

The first complete overview of modern methods for timing analysis of computer task has been done by R. Wilheim et al. (Wilheim, 2007). In this work, the classes of existing methods have been firstly presented. Particularly, the investigation of the correctness and precision of SPTA for systems that use a cache with an evict-on-miss random replacement policy have been described.

F. Cazorla et al. in (Cazorla, 2013) establish principles and requirements to EVT with the MBPTA method to derive WCET estimates. Thereby they addresses WCET problem by introducing randomization into the timing behavior of the system hardware and software. The work (Abella, 2014) presents comprehensive comparison among timing analysis techniques SDTA, SPTA and MBPTA. These and others works by these authors have been performed within the PROARTIS and PROXIMA projects for artificial random systems (random replacement policies in cache memories).

The work by F. Guet et al. (Guet, 2016) proposes a DIAGnostic tool, which applies the MBPTA method without human intervention. Depending on the certain theoretical hypotheses of the EVT, the logical work flow of the framework derives its pWCET estimate of traces of execution times. Also considering the DIAGnostic tool, K. Berezovskyi et al. investigate both methods of EVT “Block Maxima” in (Berezovskyi, 2014) and “Peak over Threshold” in (Berezovskyi, 2016) for Graphical Processor Units (GPUs). These works outline the particular features of each method. The main results have showed that hardware time-randomization is not essential for the applicability of EVT and can be applied even to some non-time-randomized systems as GPUs.

A statistical approach based on EVT theory has also been used for optimal performance analysis. Radojković et al. in (Radojković, 2016). Authors have presented an approach for finding and predicting the performance of the thread assignment in multi-core processors, using statistical inference.

However, aforementioned approaches give little information about the sequences of checking statistical hypotheses and making safe decision on their basis. In this work, adopting probabilistic analysis techniques, we intend to develop a more coherent analysis of the timing behavior on embedded platforms (in particular, considering the certain task of time acquisition).

3 THE PROBABILISTIC MODELING OF EXECUTION TIME

The measurement-based methods produce estimates (for parameters of some distributions) by executing the given task on the given hardware or on a simulator and measuring the execution time of the task or of its parts. In particular, MBPTA approaches are interested in modeling extreme execution times and characterizing the worst-case. The probabilistic theory that focuses on extreme values and large deviations from the average values is the Extreme Value Theory (EVT) (Coles, 2001). This section evaluates EVT theory by applying it to all measurements of time acquisition and outlines main steps to obtain reliable pWCET estimates - the worst possible distribution of task execution times.

3.1 EVT Applicability

The safety of the probabilistic worst-case estimates relates originally to the EVT applicability. The EVT theory estimates the probability of occurrence of extremely large values, which are known to be rare events. More precisely EVT predicts the distribution function for the maximal (or minimal) values of a set of n observations, which are modeled with random variables. The main result of EVT is provided in the Fisher-Tippett-Gnedenko theorem (Embrechts, 1996). The theorem characterizes the max-stable distribution functions, where $\{X_1, X_2, \ldots, X_n\}$ is a sequence of n independent and identically-distributed (i.i.d.) random variables and $M_n = max\{X_1, X_2, \ldots, X_n\}$. According to the theorem, if F is a non degenerate distribution function and there exists a sequence of pairs of real numbers (a_n, b_n) such that $a_n > 0$ and $lim_{n\to\infty} P([M_n - b_n]/a_n \leq x) = F(x)$, then F is called an extreme value distribution and belongs to one of the following three classes: either Fréchet, Gumbel, or Weibull.

In fact, these three distributions are combined in a single family of continuous CDFs, known as the generalized extreme value (GEV) distribution. Then GEV is characterized by three parameters: $\mu \in R$ - location parameter, $\sigma > 0$ - scale parameter and $\xi \in R$ - shape parameter. Depending on the shape parameter ξ, GEV has 3 types of distributions depicting the following three CDFs:

Type I, Gumbel ($\xi = 0$), when the underlying distribution has a nonheavy upper tail:

$$F(x;\mu,\sigma,\xi) = e^{-e^{-(x-\mu)/\sigma}}; \quad (1)$$

Type II, Fréchet ($\xi = \alpha^{-1} > 0$), when the underlying distributions has a heavy upper tail:

$$F(x;\mu,\sigma,\xi) = \begin{cases} e^{-y^{-\alpha}} & y > 0 \\ 1 & y \leq 0 \end{cases}; \quad (2)$$

Type III, "reversed" Weibull* ($\xi = -\alpha^{-1} < 0$), when the underlying distributions has a bounded upper tail:

$$F(x;\mu,\sigma,\xi) = \begin{cases} e^{-(-y)^{-\alpha}} & y > 0 \\ 1 & y \leq 0 \end{cases}; \quad (3)$$

where x is the total amount and y stands for the excess over the threshold u, with $y = x - u$. Figure 1 gives examples of Gumbel, Fréchet and Weibull distributions:

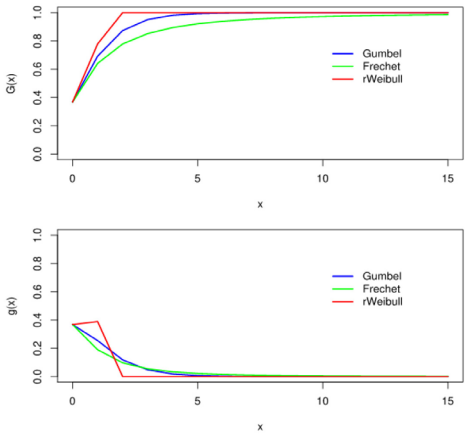

Figure 1: Examples of Gumbel, Fréchet and Weibull a) CDFs and b) PDFs with μ = 0 and σ = 1.

By estimating μ, σ, ξ parameters, we can prove the resulting GEV distribution: if the shape parameter $\xi = 0$, then the measured values in trace belong to a Gumbel distribution, which in most previous works (Cucu-Grosjean, 2012), (Hansen, 2009) has been assumed as applied to the pWCET distribution. Though there is no restriction on the values that ξ can take and resulting GEV distribution. Nevertheless, in order to be close to the accurate estimation of parameter, we intend to check all three distributions.

3.2 Selecting Extreme Values

Within the EVT context, there are two primary approaches to measure the extreme values: Block Maxima (BM) Models and The Peak over Threshold (POT). The approach of BM relies on deriving block maxima series. This is the traditional method, which comprises grouping the data into blocks, fitting the GEV distribution to the maxima of the blocks and estimating the risk measure from it. The second POT approach focuses on the observations, which exceed a given threshold. This is a more recent technique, which involves the following steps: select a threshold defining observations to include in modeling; calculate the exceedances; fit of the Generalized Pareto Distribution (GPD) to the exceedances and compute of the risk measure.

In fact, the Fisher-Tippet-Gnedenko theorem described above presents the EVT BM formulation where the tail distribution is the possible limit law characterizing the sequence of the maxima

* Within EVT the reverse (or negative) Weibull distribution is often referred to as the Weibull distribution, whereas the inverse Weibull is also known as type II or the Fréchet distribution

(Berezovskyi, 2014). Whereas in case of the BM approach the block size plays a central role, analogically the POT method models the law of the execution time peaks that exceed selected threshold. Nevertheless, the law of extreme execution times and the BM are closely linked to the law of peaks above the thresholds. Since the same value of ξ is shared, the equivalence of the distribution laws composing both the GEV and GPD distributions can be followed (Berezovskyi, 2016). The Pickands-Balkema-de Haan theorem presents the formulation of POT method (Balkema, 1974). Accordingly to it, for a large class of underlying distribution function F (which satisfies the conditions of Fisher-Tippet-Gnedenko Theorem) the conditional excess distribution function $F_u(x)$,

$$F_u(x) = F_u(y+u) = P(X-u \le y | X > u) \quad (4)$$
$$= \frac{F(x)-F(u)}{1-F(u)} \quad for\ 0 \le y \le x_0 - u,$$

is well approximated by the Generalized Pareto Distribution $G_{\xi,\sigma_u}(x)$:

$$\lim_{u \to x_0} \sup_{0 \le y < x_0 - u} |F_u(x) - G_{\xi,\sigma_u}(x)| = 0$$

$$G_{\xi,\sigma_u}(x) = \begin{cases} 1 - (1 + \xi \frac{y}{\sigma_u})^{-1/\xi} & \xi \neq 0 \\ 1 - e^{-y/\sigma_u} & \xi = 0 \end{cases} \quad (5)$$

where x_0 is either finite or infinite right endpoint of the underlying distribution F; $y \ge 0$ when $\xi \ge 0$, and $0 \le y \le -\sigma_u/\xi$ when $\xi < 0$; and $\sigma_u = \sigma_{u_0} + \xi(u - u_0)$;

As in recent studies have been followed, the POT is preferred over the BM, because data are used more efficiently, though the evident disadvantage is the selection of the suitable threshold value. Moreover, in the single-path case the POT appears to be more accurate (with respect to the measurements), but the increase of the threshold u can result into more pessimistic pWCET estimations. Further, we use the POT method to estimate the cost of time acquisition, based on the measured cost of the sample. However, the complexity due to threshold selection and its impact to the resulting pWCET has to be considered.

3.3 WCET Estimation Algorithm

The following algorithm for WCET estimation is suggested according to probabilistic theory described above:

Step 1. Selecting extreme values. The objective of this step is to collect, from the original distribution, the values, which fit into the tail, and hence can be modeled with the GEV distribution. Further, the POT method has been chosen to estimate extremes:

Step 1.1. Threshold choice. With the help of graphical diagnostic: mean residual life plot and parameter stability plot, choice the best fitted threshold.

Step 1.2. Retrieve the new sample data: filter values which are above the threshold.

Step 2. Fitting the GEV distribution: Gumbel, Fréchet and Weibull types. To ensure that the sample data correctly matches the distribution we fit, the certain goodness-of-fit tests as well as Chi-square, QQ-plot have been used. If none of three types distributions fits, then going back to Step 1.1 and increase the threshold value.

Step 3. Estimate the remaining parameters of fitted distribution: μ, σ and ξ.

Step 4. Verification of EVT hypothesis of independence and identical distribution. If both are verified, then the EVT distribution tail projection can be considered as a safe and good pWCET estimate.

Step 4.1. Checking that the data are identically distributed.

Step 4.2. Prove that samples are independent. That is ensured by a combination of hardware with suitable randomization properties.

Step 5. Return WCET estimation based on μ, σ and ξ parameter.

4 EXPERIMENTAL SETUP

Within MBPTA approach, complete runs of the test are made on the target hardware. For these experiments, we have collected timestamps of CPU cycle counter on the Atmel SamaA5D4 board. This board uses one ARM Cortex-A5 600 MHz core, which belongs to the ARMv7-A architecture generation. The common problem of most processors in SoCs is, that CPU cycle counter is not directly available from user-space. Thereby, the investigations of timing capabilities are being performed within the high performance *HighPerTimer* library (Fedotova, 2013). The main idea behind the *HighPerTimer* library is to simplify the timestamps acquisition process from the main cycle counter of different processors. During the library initialization step, a specific time register is assigned to the main library time source. The time counter has the channel size of 32-bit width and frequency 11 MHz. Thus, it wraps around in every 6.5 minutes. The said library provides means for correct dealing with such wrap-arounds and providing a global 64-bit fast ticks counter independently from the underlying timing hardware. A special device

driver within the library, which is loaded as a kernel module beforehand, enables proper operations with timers from the user-space. The main timing mechanism, which in its turn supports the procedure of handling overflows is processed by the user space library avoiding any system calls.

The platform is running with the standard Linux kernel of version 4.4.11 and the measured process is scheduled by the Normal scheduling policy, which is set by default. Within the context of this work, we estimate the timer cost, setting two consecutive timers of *HighPerTimer* library and calculating the time difference between them (further x_i.). The representation of complementary cumulative distribution function (CCDF) of the trace is shown in Figure 2 and basic statistics in Table 1.

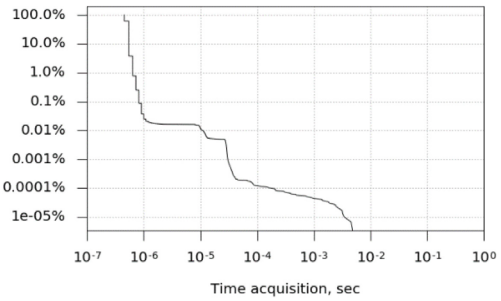

Figure 2: CCDF representation of time execution.

Table 1: Statistical properties of the original data set.

Number of samples	$30*10^6$
Trace length	27 min
Mean execution time	5.71 cycles = 0.519 µsec
Std. deviation	24.384 cycles = 2.217 µsec
Max value	65943 cycles = 5994.7 µsec
Min value	5 cycles = 0.455 µsec

The estimation part of a representative trace has been taken 27 minute and as can be seen from the graph, the distribution peaks near the mean and falls with rapidly decreasing probability density below 1 µsec.

5 GRAPHICAL DIAGNOSTICS FOR THE OPTIMAL THRESHOLD

The choice of an appropriate threshold u requires a compromise between precision and bias. If the threshold is too low, then the results will tend to be more certain. On the other hand, the analysis will only become practically valid, when the threshold is sufficiently high. Therefore, the goal is to find such a lowest possible threshold, that the extreme value model provides a reasonable fit to exceedances of it. Two graphical tools can be used for identifying an appropriate threshold for modeling extremes via the GPD: Mean residual life plot and Parameter stability plot (Scarrott, 2012).

a) Mean residual life plot.

In the mean residual life plot, for a range of candidate values for u the corresponding mean threshold excess has to be identified. Then this mean threshold excess is plotted against u. The plot should be linear above the threshold u_0 at which the GPD model becomes valid. On the Figure 3, the blue lines correspond to the lower and upper confidence limits respectively. The purpose is to find the lowest threshold where the plot is nearly linear, taking into account the 95% confidence interval. Though interpretation of these plots can be subjective, linearity in Figure 3 might be suggested above $u_0 \approx 2e\text{-}04$ *sec*, beyond which it is approximately linear until $u \approx 2.5e\text{-}04$ *sec*, whereupon it decreases sharply. These limits are dashed red lines on the plot. This way, the minimum and maximum possible thresholds, at which the model can be fitted have been firstly suggested as $u_{min} \approx 2e\text{-}04$ and $u_{max} \approx 2.5e\text{-}04$.

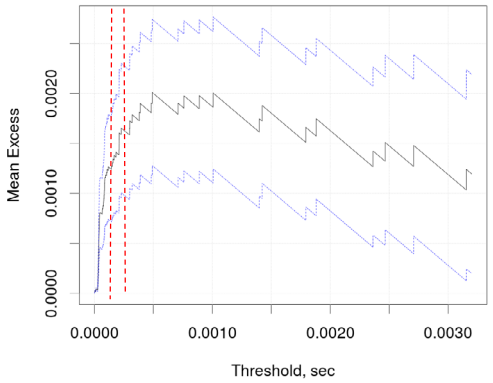

Figure 3: The empirical mean residual life plot.

b) Parameter stability plot.

For the next step, two parameter stability plots showing maximum likelihood estimates, confidence intervals of the shape and modified scale parameters over a range of thresholds are produced. Figure 4 represents plots from fitting the GPD and point process models to these data. Denoting the value of the generalized Pareto scale parameter σ_u for a threshold from $u > u_0$ in (5), the scale parameter changes with u unless $\xi = 0$. Thereby, we can better

express it as a constant scale parameter with respect to u (Coles, 2001):

$$\sigma^* = \sigma_u + \xi u, \quad (6)$$

Consequently, estimated of σ^* and ξ should be constant above u_0 or at least stable after sampling errors. Therefore firstly, comparing the parameter stability plot for the whole range of samples in Figure 4(a) with the mean residual life plot in Figure 3, the retrieved possible interval of u_{min} and u_{max} can be confirmed. At least for the case of Gumbel distribution with its shape parameter $\xi = 0$, the desired threshold is likely within this range. Figure 4(b) shows more accurately the desired range, where the dependence of ξ parameter can be better observed.

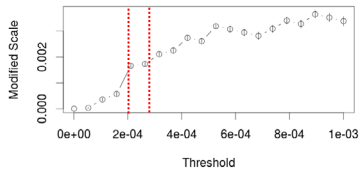

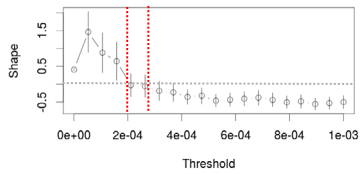

a)

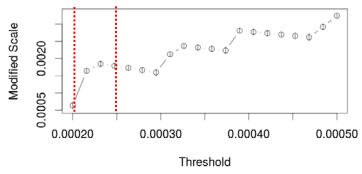

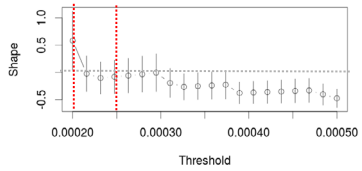

b)

Figure 4: Parameter stability plot a) for the whole trace and b) for the range with u_{min} = 2e-04 sec.

Though the threshold stability plots also does not provide very firm conclusions, together with the mean residual life plot, inconsistencies can be good observed. It lies between the estimated shape parameter at this level and higher thresholds around *u=2.3e-04* sec. Therefore, at the current stage it can be concluded that this is the best choice of threshold, which allows retrieving 24 extremes from the trace.

6 FITTING THE GPD DISTRIBUTION AND ESTIMATION THE PARAMETERS

Having determined the threshold value, the parameters of the GPD can be further estimated by maximum likelihood (MLE). In the following section we have tested the whole family of GPD distributions. The appropriate Goodness-of-fit statistics for Gumbel, Fréchet and Weibull distributions have been obtained and presented in Table 2. Each test is essentially a goodness of fit test and compares observed data to quantiles of the specified distribution. The null hypothesis for each test versus alternative is:

H_0: data follow an assigned distribution;

H_1: data do not follow an assigned distribution.

The resulting value is then checked against the following statistics to see if it is significant:

– the critical value from Chi-square test. Since we deal with the discrete data, the Chi-square test has been chosen against Kolmogorov Smirnov test. From the Chi-Square table we can find the critical Chi Square value for a level of significance p, which represents the probability that a Chi Square distributed random variable will exceed that critical value. Typically a match at the $p = 0.05$ is considered acceptable.

– the Bayesian (BIC) and Akaike (AIC) information criterion of (Burnham, 2004). AIC tries to select the model that most adequately describes an unknown one. Conversely, BIC aims to find the true model among the set of candidates. When comparing models fitted by maximum likelihood to the same data, the smaller the AIC or BIC, the better the fit.

– a QQ-plot (quantile plot). This is a plot of the empirical quantile values of observed data against the quantiles of the standard form of a target distribution. The slope and the intercept of the best-fit line through these points can be used as estimators ξ and σ parameters, respectively. A straight diagonal line of data points from the bottom left to the top right of the

Table 2: GPD parameters.

	p-value	AIC	BIC	σ	μ	ξ
Gumbel	0.346	534.240	536.596	12247.56	12968.35	0
Fréchet	0.065	531.211	534.745	10542.52	-1539.657	1.351

plot indicates that an exponential distribution is a relatively good fit to the tail.

Firstly, Chi-squared p-value for the Gumbel and Fréchet data ($p\text{-}value_G = 0.346$ and $p\text{-}value_F = 0.065$ respectively) > 0.05, hence both hypotheses can't be rejected. Secondly, the goodness-of-fit criteria for the Fréchet distribution is a bit less than for the Gumbel distribution: $AIC_F = 531.211 < AIC_G = 534.240$ and $BIC_F = 534.745 < BIC_G = 536.596$. Therefore, from the statistical tests the hypotheses that data fits Fréchet distribution is slightly preferred against the one, which checks Gumbel distribution. However, since the difference of statistics results is not significantly differed, it makes sense to retrieve the WCET estimate for both cases.

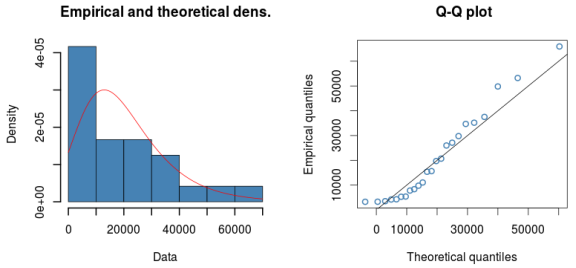

a)

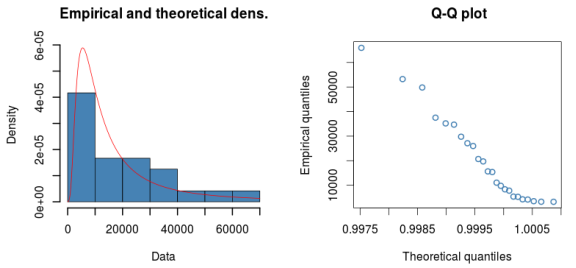

b)

Figure 5: The histogram against fitted density functions and theoretical quantiles against empirical ones of a) Gumbel and b) Fréchet distribution.

7 VERIFICATION OF EVT HYPOTHESIS

In order to apply the EVT, three hypotheses are required to verify: i) independent and ii) identically distributed execution time measurements from iii) a distribution, which belongs to the Maximum Domain of Attraction of the GEV with a shape parameter ξ (Guet, 2016). These proofs provide reliable and safe pWCET estimates. In the giving chapter, we intend to check the first two hypothesis. As follows from the definition, the sequence of random variables is independent and identically distributed if each random variable has the same probability distribution as the others and all are mutually independent (Coles, 2001), (Burnham, 2004), (Feller, 1996).

a) Identical Distribution.

It is worth to note that in the given application of EVT, the rule of identically distributed is obeyed since the analysis models the behavior of the system in the same execution context using the same set of parameters, including initial hardware and software state (Cazorla, 2013). However, to provide enough level of reliability, the property of identical distributed values are verified by the two-sample Kolmogorov-Smirnov (KS) test. The Kolmogorov-Smirnov statistic quantifies a distance between the empirical distribution functions of two samples. For the given experiment the null (H_0) and alternative (H_1) hypotheses are:

H_0: the both samples are identically distributed;

H_1: the samples are not identically distributed.

The test is performed by dividing the trace into subsets in order to verify if they have the same distribution function. By randomly taking elements from the original sample, three subsets of 100, 500 and 1000 values have been created. This ensures that the smaller samples maintain the same statistical properties as the original (Cucu-Grosjean, 2012), (Burnham, 2004), (Feller, 1996). Table 3 represents the p-value obtained by applying the KS test to the execution times. *P-value* is the probability of finding a situation more extreme than what in the data, assuming that $a_n = b_n$. The smaller this number is, the less likely that $a_n = b_n$ is true. *D value* of the KS test statistic means the maximum difference between the a_n & b_n probability mass function. The rule to accept H_0 is $p\text{-}value > 0.05$ - the predetermined significance level. Accordingly, from Table 3, the null hypothesis cannot be rejected, which allow concluding that samples are identically distributed.

Table 3: Statistics for identical distribution test.

m	D value	p-value
100	0.1	0.6994
500	0.012	1
1000	0.053	0.125

b) Independence.

From the definition, two random variables are considered to be independent if they describe two events such that the occurrence of one event does not have any impact on the occurrence of the other event (Coles, 2001), (Burnham, 2004), (Feller, 1996). To prove those properties, the Runs test (or Wald-Wolfowitz test) (Feller, 1996), (Wald, 1940), is used. In this context, a term "run" is a sequence of identical responses. The null and alternative hypotheses are:

H_0: elements of the sequence are mutually independent;

H_1: elements of the sequence are not mutually independent.

The following steps have to be accomplished to apply the Runs test:

Step 1: compute the sequential differences $d_i - d_{i-1}$, where positive values is related to increasing values and negative to a decreasing ones.

Step 2: compute the expectation of the number of runs $E(R) = 2mn/N$, where N is the total sample size, m is the number of positive values, and n is the number of negative ones.

Step 3: compute the variance of the number of runs $V(R) = 2mn(2mn - N)/(N^2(N-1))$. The minimum value of R is always 2. The maximum value is given by $2Min(m, n)-t$, where $t = 1$ for $m = n$, and $t = 0$ if not.

Step 4: estimate the test statistic $Z=(r-E(R))/\sqrt{V(R)}$. In Table 4, Z value and *p-value* are compared for a significance level $\alpha = 5\%$. At the given level, *Z-value* with an absolute value greater than 1.96 indicates non-randomness so the null hypothesis is rejected. Additionally, the rule to accept H_0 is if *p-value* is more than 0.05.

Since the $p\text{-value} = 0.247 > 0.05$ and $Z\ value = 0.684 < 1.96$, the hypothesis that each element in the sequence is independently drawn from the same distribution is accepted.

Table 4: Statistics for independence test.

V(R)	Z value	p-value
19.8	0.684	0.247

8 ESTIMATION PROBABILISTIC PWCET

The final step is to use the computed and verified GPD parameters and the exceedance probability of failure p to estimate the WCET. In fact, WCET thresholds are defined depending on the failue probability p such that $p = P(WCET_{safe} > WCET_{exact})$. In standard statistical language, this is a quantile estimate or for instance in finance, it is often referred as Value-at-risk (VaR) for measuring of market risk. Considering these application for our case, the WCET estimation is then derived on the basis of estimated parameters $\hat{\xi}$ and $\hat{\sigma}$ as following (Embrechts, 1996):

$$WCET = \begin{cases} u + \frac{\hat{\sigma}}{\hat{\xi}}((\frac{n}{k}p)^{-\hat{\xi}} - 1) \; if \; \hat{\xi} > 0 \\ u - \hat{\sigma} log(\frac{n}{k}p) \qquad if \; \hat{\xi} = 0 \end{cases} \quad (7)$$

where k - the number of peaks over the threshold standing for measurements that belong to the tail distribution. The initial probability of failure p defined as the likelihood the execution of a job exceeds its WCET for the current mode when previous jobs have not exceeded it. Different works on probabilistic WCET have claimed that values of p could typically be 10^{-16}, 10^{-9} or 10^{-4}. For our investigations, the failure probability at the level $10^{-9} < p < 10^{-7}$ (from hazardous class) provided by PED certification (Hsing, 1991), (ARP4761, 2001) has been chosen. PED certification is applied in the flight control system using portable electronic devices (PEDs). Further, Table 5 gives the modeling results of the extreme execution times and Figure 7, showing the distribution convergence for Gumbel and Fréchet scenarios.

In Figure 6 the x-axis shows the pWCET estimation and the y-axis shows the associated probabilities. The challenge of risk assessment is to assess the value that for each of the activities is not

Table 5: EVT Results for the Hazardous Class of p Considering GPD.

	σ	**μ**	**ξ**	**(WCET ; 10^{-7})**	**(WCET ; 10^{-8})**	**(WCET ; 10^{-9})**
Gumbel	12247.56	12968.35	0	27968.09 cycles = 2.54 msec	56169.13 cycles = 5.11 msec	84370.18 cycles = 7.67 msec
Fréchet	10542.529	-1539.657	1.351	124185.2 cycles = 11.3 msec	2898825 cycles = 263 msec	65126941 cycles = 5.921 sec

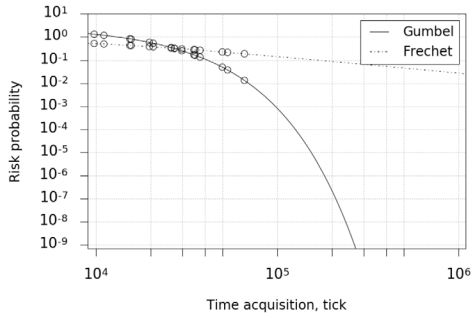

Figure 6: Estimate of upper bounds for the Gumbel and Frechet distribution.

able to be measured accurately. So we use a CCDF of General Pareto Distribution to predict these potential values. Finally, all tests are diagnosed as reliable regarding the EVT applicability and the pWCET estimate has been derived.

However, according to the Table 5 the WCET estimates for Gumbel and Fréchet distribution differ significantly. In fact, too pessimistic results of Fréchet are quite tight and practically less useful. On the other hand, the Gumbel distribution converges to 0 faster than the Fréchet one and it decrease the pessimism of the WCET thresholds. Nevertheless, having the access to the true values and capacity to run the experiment including the target risk probabilities, we can estimate the real max value and predicted WCET estimates. According to the Table 1, the max value on the examined range is 0.005 sec and whereas predicated upper bound using parameters for Gumbel distribution for failure probability $p = 10^{-9}$ gives 0.007 sec, which fits the assumption. For the case of Fréchet parameters, the estimate of 5.921 sec is obviously too pessimistic and less useful.

9 CONCLUSION

The contributions of this paper are: (i) proving optimality of the EVT theorems and verifying their applicability on the certain embedded platform ARM Cortex-A series of processors; (ii) introducing an approach of graphical diagnostic for selecting extreme values; (iii) considering several cases of GPD distributions for choosing reliable WCET estimation. Our results show that, for failure probability levels of 10^{-9} the single-path technique for time acquisition provides less pessimistic pWCET estimations about 7.67 msec using parameters for Gumbel distribution. This estimation can be taken as acceptable and considered during designing of time-critical applications on such SoCs. Therefore, the ongoing paper provides a useful guide of how to predict the upper bounds for the embedded single-core processor architecture. The future work should continue investigation of cache memory effects or impacts of scheduling tasks by Linux kernel. This can afford the improvement of the dependence metrics, reduce the pessimism of the pWCET estimation and as a result, make ARM processor more time-predictable.

REFERENCES

Wilhelm, R., Engblom, J., Ermedahl, A., Holsti, N., Thesing, S., Whalley, D., Bernat, G., Ferdinand, C., Heckmann R., Mitra, T., Mueller, F., Puaut, I., Puschner, P., Staschulat, J., Stenström, P., 2007, 'The Worst-Case Execution Time Problem — Overview of Methods and Survey of Tools', *ACM Trans. Embed. Comput. Syst.*, pp. 36–53.

Abella, J., Hardy, D., Puaut, I., Quinones, E., Cazorla, FJ., 2014, 'On the Comparison of Deterministic and Probabilistic WCET Estimation Techniques', *Proc. of the 26th Euromicro Conference on Real-Time Systems (ECRTS'14)*, Madrid, pp. 266–275.

Fedotova, I., Krause, B., Siemens E., 2017, 'Upper Bounds Prediction of the Execution Time of Programs Running on ARM Cortex-A Systems', Submitted at *IFIP AICT (Advances in Information and Communication Technology)* in press.

Altmeyer, S., Cucu-Grosjean, L., Davis, RI., 2015, 'Static probabilistic timing analysis for real-time systems using random replacement caches', *Real-Time Syst.*, vol. 51, no. 1, pp. 77–123.

Radojković, P., Carpenter, PM., Moretó, M., Čakarević, V., Verdú, J., Pajuelo, A., Cazorla, FJ., Nemirovsky, M., Valero, M., 2016, 'Thread Assignment in Multicore/Multithreaded Processors: A Statistical Approach', *IEEE Trans. Comput.*, vol. 65, no. 1, pp. 256–269.

Guet, F., Morio, J., Santinelli, L., 2016, 'On the Reliability of the Probabilistic Worst-Case Execution Time Estimates', *the 8th European Congress on Embedded Real Time Software and Systems (ERTS 2016)*, Toulouse, pp. 758–767.

Cazorla, F., Vardanega, T., Quinones, E., Abella, J., 2013, 'Upper-bounding Program Execution Time with Extreme Value Theory', *Proc. WCET workshop*, Paris, pp. 64-76.

Berezovskyi, K., Santinelli, L., Bletsas, K., Tovar, E., 2014, 'WCET Measurement-based and Extreme Value Theory Characterisation of CUDA Kernels', *Proc. of the 22nd International Conference on Real-Time Networks and Systems*, New York, , pp. 279-288.

Berezovskyi, K., Guet, F., Santinelli, L., Bletsas, K., Tovar, E., 2016, 'Measurement-Based Probabilistic Timing Analysis for Graphics Processor Units', Proc. Of *29th International Conference Architecture of Computing Systems – ARCS 2016*, Nuremberg, pp. 223-236.

Coles, S., 2001 ed, *An Introduction to Statistical Modeling of Extreme Values*. Springer.

Cucu-Grosjean, L., Santinelli, L., Houston, M., Lo, C., Vardanega, T., Kosmidis, L., Abella, J., Mezzetti, E., Quinones, E., Cazorla, JF., 2012, 'Measurement-Based Probabilistic Timing Analysis for Multi-path Programs', *Proc. of the 24nd Euromicro Conference on Real-Time Systems (ECRTS)*, pp. 91-101.

Hansen, J., Hissam, SA., Moreno, GA., 2009, 'Statistical-Based WCET Estimation and Validation', *Proc. of the 9th Intl. Workshop on Worst-Case Execution Time Analysis (WCET)*, pp. 123-133.

Embrechts, P., Klueuppelberg, C., Mikosch, T., 1996, *Modelling Extremal Events for Insurance and Finance*, Springer, Berlin.

Balkema A., Haan L., 1974, 'Residual Life Time at Great Age', *Annals of Probability*, vol. 2, no. 5, pp-749-791.

Fedotova I., Siemens E., Hu H., 2013, 'A High-precision Time Handling Library', *Journal of Communication and Computer*, vol. 10, pp. 1076–1086.

Scarrott, C., MacDonald A., 2012, 'A Review of Extreme Value Threshold Estimation and Uncertainty Quantification', *REVSTAT - Statistical Journal*, vol. 10, no. 1, pp. 33–60.

Burnham, KP., Anderson, DR., 2004, 'Multimodel Inference: Understanding AIC and BIC in Model Selection', *Sociological Methods & Research*, vol. 33, no. 2, pp. 261–304.

Wald, A., Wolfowitz, J., 1940, 'On a Test Whether Two Samples are from the Same Population', *Annals of Mathematical Statistics*, vol. 11, no. 2, pp. 147–162.

Hsing, T., 1991, 'On Tail Index Estimation Using Dependent Data', *Annals of Statistics*, vol. 19, no. 3, pp. 1547–1569.

ARP4761, 2001, '*Guidelines and methods for conducting the safety assessment process on civil airborne systems and equipment*'.

Computer Simulation Complex for Training Operators of Handling Processes

Rustam Fayzrakhmanov, Ivan Polevshchikov, Aydar Khabibulin
Department for Information Technologies and Computer-Based System,
Perm National Research Politechnical University, Perm, Russia
fayzrakhmanov@gmail.com, i.s.polevshchikov@gmail.com, shimakenshi@gmail.com

Keywords: Computer Simulation Complex, Training Operators, Handling Processes.

Abstract: The paper is dedicated to the development of the architecture of computer training simulation complexes (TSCs) for training operators of handling machineries as well as models and operation algorithms of their components. We introduce a unique training complex, Ganz TSC, for portal crane operators, developed according to the models and methods proposed. It demonstrates its effectiveness in the training process. In particular, our case study shows that operators trained with the use of Ganz TSC move cargoes 27% faster on average, preserving the required quality of work.

1 INTRODUCTION

There is a high need in increasing the effectiveness of the training of technological process operators with the aim of acquiring a required level of knowledge, abilities, and skills based on scientifically well-founded models and methods within a relatively short-time interval. Computer-aided training systems (referred to as CTSs) and training simulators of computer training simulation complexes (referred to as training simulation complexes or TSCs), leveraged for that, are addressed in research literature such as (Dozortsev, 2013; Chistyakova, Petin & Boykova, 2012; Lisitsyna & Lyamin, 2014; Bouhnik & Carmi, 2012; Zhuravlev & Shikov, 2015). CTSs are typically utilised for monitoring theoretical knowledge and for training the logics of professional thinking in various regular and extreme cases. Training simulators are, in turn, developed to simulate comprehensive technological processes and mould out necessary skills with the help of an instructor.

Contemporary training simulation complexes implement a limited set of specific training cases and have, therefore, a limited simulation environment. In contrast, in this paper, we present a comprehensive end-to-end system, Ganz TSC (Fayzrakhmanov & Khabibulin, 2014), with advanced full-fledged training simulator, Ganz, which has the following innovative advantages.

1) An instructor can control various configuration parameters of exercises and adapt the education process based on the knowledge and skills of the trainee.

2) On the example of the portal crane, with realistic simulation environment, the trainee can better understand the physics and peculiarities of the real working environment as well as the tools and objects he interacts with.

3) Ganz is a complex system with the software component used for simulating the virtual reality and the hardware component for simulation of the control panel of the portal crane. This therefore allows to reflect the environment with high precision. This system can be used as an independent system to simulate different kinds of portal cranes and various relevant objects of ports.

In this paper, we describe the architecture of training simulation complexes and their main functional components by example of Ganz TSC.

2 THE ARCHITECTURE OF GANTZ TSC

We developed a computer training simulation complex, Ganz TSC, for operators of the portal

crane, Ganz. It is intended for training future operators with the aim of acquiring professional knowledge and skills. A generic view of Ganz TSC is illustrated in Figure 1.

Ganz TSC comprises two interconnected components:

1) a training simulator for the handling process;

2) a computer-aided training system, which collects and analyses data related to performance of the trainees who are in the process of acquiring relevant knowledge and skills.

The training simulator models the real environment with all relevant aspects of the load-unload (handling) process and gives the trainee a unique experience which can be further used at the workplace. The trainee can acquire his experience of interacting with the system through visual, audio and tactile channels, i.e., with visual simulation of physical objects and processes, simulation of the background and foreground noises, and providing a physical control panel corresponding to a specific model of a crane, respectively. Thus, the training simulator consists of a module of mathematical modelling of physical processes, a visualisation module, a control panel, and input devices.

A modelling module implements the physics of all relevant objects of the environment related to the overall handling process; those are the modelling of the vibration of constructions (e.g., the tension of the cable, jerks, the vibration of the crane), external factors (e.g., wind, rain, light), collisions (e.g., the destruction of containers on impact, a breach of the cable), and friable cargoes.

A modelled environment of the port has the following types of key objects: static (a moorage, storage facilities, railroad tracks, accesses for motor vehicles) and dynamic (a ship on the moorage, cargoes in warehouses, holds, port personnel). An open source framework, Unity, is used for visualising 3D models of the key objects.

Figure 1: A generic view of Ganz TSC.

The high-quality visualisation of the environment allows the trainee to experience the whole picture of relations between all objects in the handling process as well as their features and functions. The simulator also realistically simulates all relevant background and foreground noises.

Our training simulator has mobile controls, an operator chair, joysticks, the keyboard as a control panel, and input devices.

Virtual simulation of the handling (load-unload) process, as it is seen by the trainee on screen, is represented in Figure 2.

An integrated CTS of Gantz TSC has extensive courses that allow the trainee to receive training both through theoretical (to obtain knowledge) and practical (to get required skills) phases, which are automatically controlled and monitored by the system. Gantz TSC also has a framework with a convenient user interface that is leveraged by the instructor to configure the system accordingly as well as the overall educational process. By setting the configuration parameters, the trainer takes into account the knowledge and abilities of the trainee as well as the goal that he wants to achieve in his training program.

The overall architecture of Gantz TSC is illustrated in Figure 3.

Figure 2: A screenshot of the virtual environment.

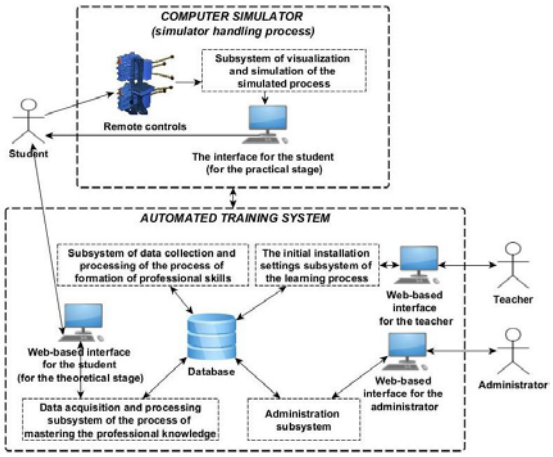

Figure 3: The overall architecture of Gantz TSC.

In the theoretical phase of the course, aimed at acquiring professional knowledge and implemented by CTS, a future operator studies the required theoretical material with the use of an electronic textbook and performs a control test afterwards.

Further in this section, we introduce models describing the structure, functional requirements, and functional peculiarities of the CTS based on our developed mathematical models of the computer-aided control system for acquiring skills, as well as the corresponding methods (Fayzrakhmanov & Polevshchikov, 2013, 2016).

We developed a mathematical model of the computer-aided control system for acquiring professional skills by operators (trainees) who perform exercises with the CTS. Each exercise forms specific professional skills, i.e., a proper action as well as reaction for a certain real situation. This model is a set-theoretic description of the input data and the functioning of each of the functional blocks, responsible for various constituents of the process of control. The set of these mathematical interdependencies is demonstrated in Figure 4.

Each exercise is associated with a planned performance trajectory that can be presented as a pair $T_{pl} =< M_{sost}^{pl}, M_{vozd}^{pl} >$, in which M_{sost}^{pl} is a set of planned states of the modelled environment, M_{vozd}^{pl} is a set of planned impacts affecting the modelled environment. The correlation between planned states and impacts can be presented as functions $M_{sost}^{pl} \times M_{vozd}^{pl} \to \{0,1\}$ and $M_{vozd}^{pl} \times M_{sost}^{pl} \to \{0,1\}$. The trainee interacts with the modelled environment with the use of physical simulators of control panel of the TSC with multiple levers $M_R = \{R_l \mid l = \overline{1, N_R}\}$, where $R_l = \{r_k \mid k = \overline{1, N_{pol}}\}$ is a set of positions of the l's lever. $V_{pl} \in M_{vozd}^{pl}$ can be represented as a set $V_{pl} = \{r_q(t_q) \mid q = \overline{1, N_{rych}}\}$, where $r_q(t_q) \in \bigcup_{l=1}^{N_R} R_l$ is a position in which the trainee should move a certain lever l in a specific time t_q. The quality assessment of performing a technological operation depends on the correlation between the planned T_{pl} and the actual T_{fct} task trajectories.

Figure 5 illustrates a use case diagram with functional requirements for the CTS to form necessary professional knowledge and skills in trainees, in their practical phase of the course.

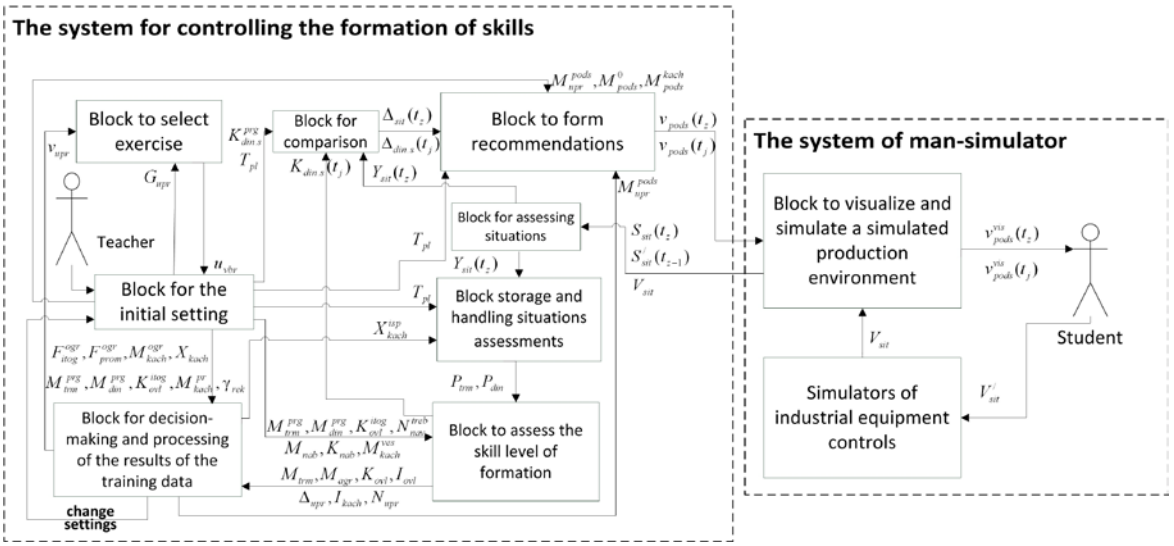

Figure 4: A schema of the process of computer-aided control.

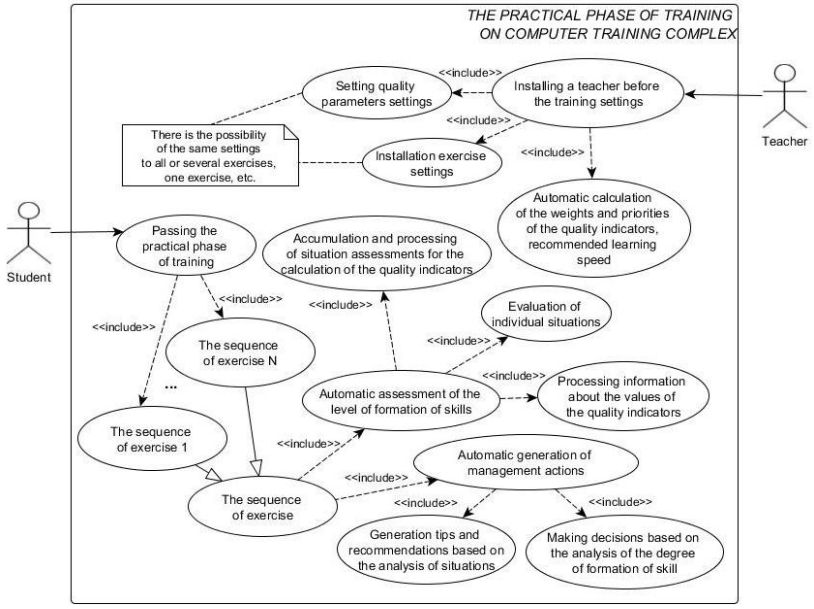

Figure 5: Use case diagram of the practical phase of the training course.

An activity diagram presented in Figure 6 reflects the algorithm of controlling the training process. This algorithm is based on mathematical models and methods described in (Fayzrakhmanov & Polevshchikov, 2016; Beiranvand, Khodabakhshi, Yarahmadi & Jalili, 2013; Mortaza Mokhtari Nazarlou, 2013).

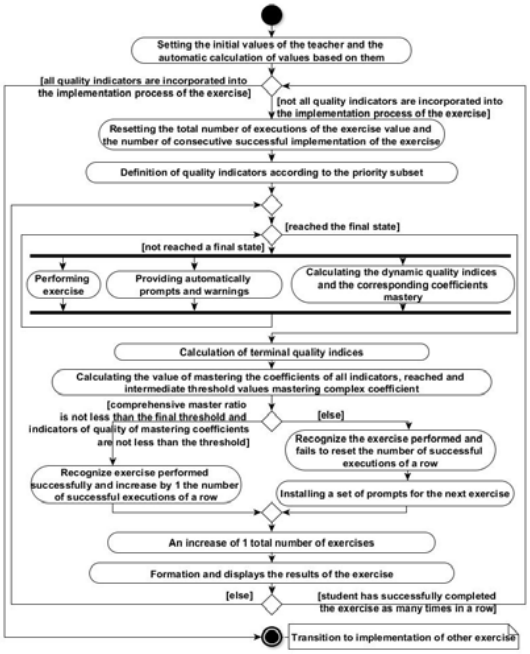

Figure 6: The algorithm of controlling the training process.

Figure 7 illustrates a quality assessment web form, one of interfaces of a rich Internet application developed for setting initial parameters.

The central database stores all information required for ensuring the effective training in consistent and systematic fashion, in particular: user profiles, initial configuration parameters, the progress trainees make as well as their results. Figure 8 represents a slice of the database schema, storing data of the process of acquiring professional skills by trainees, performing exercises in Ganz TSC.

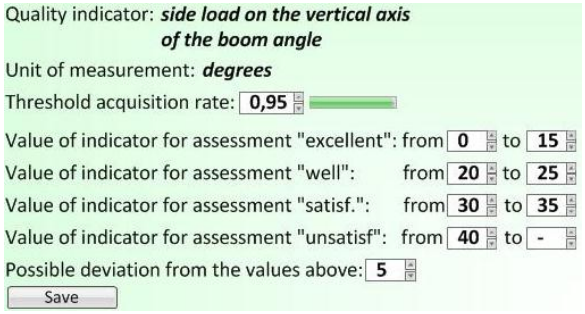

Figure 7: Configuration form for setting initial parameters of the quality assessment.

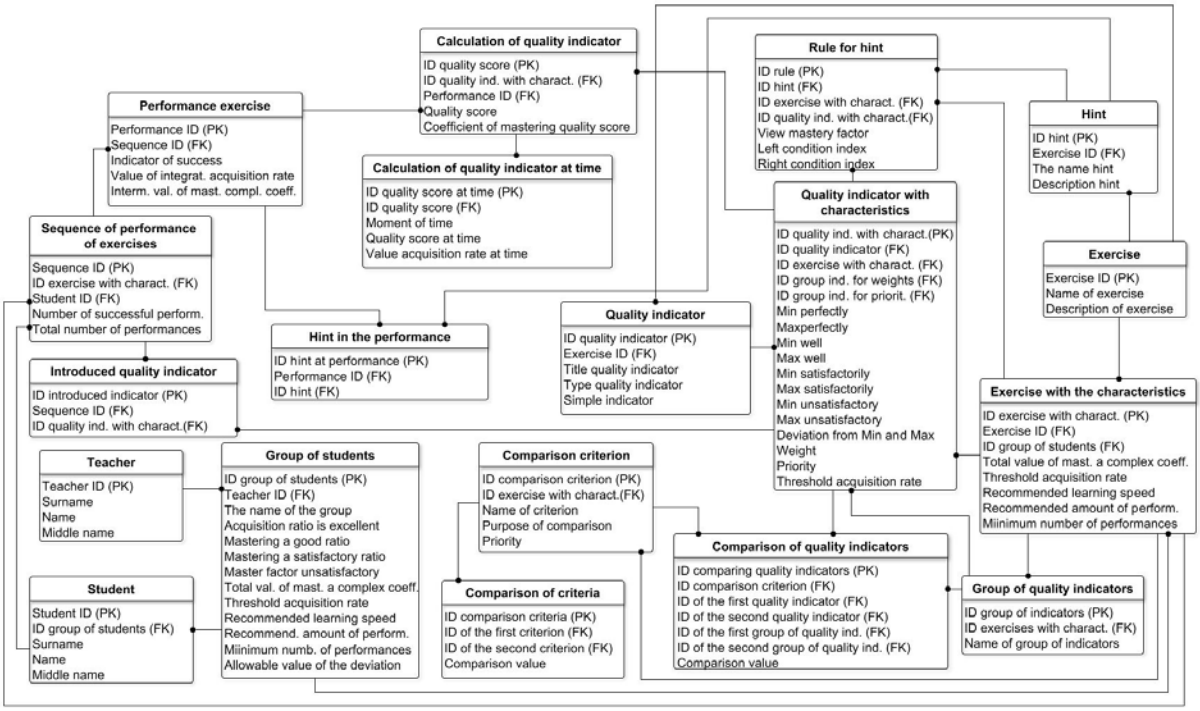

Figure 8: The logical database schema.

We also developed an educational program for trainees of the portan crane, Ganz, which includes exercises on the following main tasks:

1) lifting and pulling down a cargo in different realistic circumstances;

2) moving a cargo with different allowed movements of the derrick (e.g., only moving it back and forward or changing the angle);

3) loading and unloading the goods transport (water and land transport).

3 EFFECTIVENESS OF GANTZ TSC IN THE TRAINING

To evaluate the effectiveness of our training complex, we conducted a case study with two groups with 10 participants in each; the first group trained on a real portal crane, the second one trained on Ganz TSC. After the completion of their training course, we asked them to perform the following type of similar exercises 10 times: given the same conditions, move a cargo on a real portal crane. We measured the time they spend to successfully move a cargo on a real portal crane. The assessment of this criterion has a high importance as it reflects both the efficiency and accuracy of operators.

The second group was able to achieve better results, spending 27% less time than the first group on average. In particular, an average duration of the transfer for the second group was 48.6 sec., against 66.4 sec. for the first group.

We present detailed results of our study in Figure 9. As we can see, the overall time interval for the second group is within the range from 25 sec. to 75 sec., and with the frequency 0.4 (the highest bar in the histogram) they spent from 35 to 45 seconds. In contrast, the overall time interval of the first group is wider and ranges from 28 to 110 seconds, and with the frequency 0.27 they require more time to move the cargo — from 60 to 70 seconds. The frequency is a ratio of the quantity of measurements, in which the duration of the transfer has a specific value, to the total number of measurements.

The length of the time interval in the second group is smaller than in the first one, this indicates that Ganz TSC, training in a systematic and a goal-oriented fashion, greatly reduces the discrepancy in knowledge and skills obtained after the course.

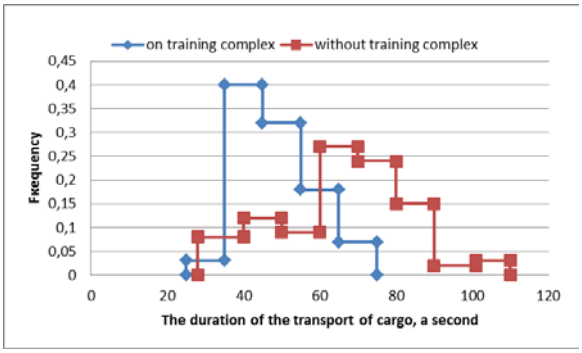

Figure 9: Graphs of the time required for moving cargoes in our case study.

Our experiment demonstrates the advantage of using Ganz TSC in training crane operators, that is reflected in a considerable reduction of the time required for transferring cargoes and more consistent and systematic training.

4 CONCLUSION

In this paper, we introduced a unique training simulation complex, Ganz TSC, which can help to effectively train professional crane operators and ensure the required level of knowledge and skills. It has an advanced training simulator, quite realistically modeling the environment of the process.

To conclude, the computer-aided training system of Ganz TSC has the following advantages.

1) It provides trainees with effective information support while doing exercises and success criteria, required for adequate self-control and self-assessment.

2) it is possible to schedule the process of acquiring the skill of manipulating every mechanism of the crane by gradual addition of individual quality factors into the training process.

3) All the exercises can be precisely reproduced with the same initial parameters that give the trainee the possibility to learn various peculiarities of the technological process and, thus, improve his skills considerably.

4) By leveraging the information provided by Ganz TSC about the progress of the trainee, an instructor can adapt the configuration parameters of the system in an according way to help him achieve better results in training.

5) All information regarding training processes and user profiles is collected, stored and processed by Ganz TSC to help instructors perform scheduling, accounting, monitoring, analysis, and control as the main constituents of the automated control process for acquiring professional skills.

The proposed system can be adapted for other machines and technological processes according to their specifics.

REFERENCES

Beiranvand, A., Khodabakhshi, M., Yarahmadi, M. & Jalili, M., 2013. Making a Mathematical Programming in Fuzzy Systems with Genetic Algorithm. *Life Science Journal*, N 10(8s), pp. 50-57.

Bouhnik, D. & Carmi, G., 2012. E-learning Environments in Academy: Technology, Pedagogy and Thinking Dispositions. *Journal of Information Technology Education: Research*, V. 11, pp. 201–219.

Chistyakova, T., Petin, K. & Boykova, O., 2012. Training operators at low-power electricity generating stations using trainer simulators. *Vestnik Saratovskogo Gosudarstvennogo Technicheskogo Universiteta*, V. 1, N 2 (64), pp. 263-269.

Dozortsev, V., 2013. Methods for computer-based operator training as a key element of training systems (present-day trends). *Automation and Remote Control*, V. 74, N 7, pp. 1191-1200.

Lisitsyna, L. & Lyamin, A., 2014. Approach to development of effective e-learning courses. *Frontiers in Artificial Intelligence and Application*, V. 262, pp. 732–738.

Mortaza Mokhtari Nazarlou, 2013. Research on Application of Hierarchy Petri-Net in Dynamic Workflow Modeling. *Life Science Journal*, V. 10, N 1, pp. 821–825.

Fayzrakhmanov, R. & Khabibulin, A., 2014. Designing and developing training complex of portal crane operator. *Vestnik Permskogo Nacionalnogo Issledovatelskogo Polytehnicheskogo Universiteta. Electronika, Informacionnie technologii, Sistemi Upravleniya*, N 1(9), pp. 80-92.

Fayzrakhmanov, R. & Polevshchikov, I., 2013. Increased of Efficiency in the Automated Training of Fuelling Machine Operators Using Iterative Simulation Learning. *World Applied Sciences Journal*, N 22 (Special Issue on Techniques and Technologies), pp. 70-75. URL: idosi.org/wasj/wasj22(tt)13/12.pdf.

Fayzrakhmanov, R. & Polevshchikov, I., 2016. Automated control simulation of professional skills formation for production system operator. *Nauchno-Tekhnicheskiy Vestnik Informacionnih Tekhnologiy, Mehaniki i Optiki*, V. 16, N 1, pp. 181–190.

Zhuravlev, A. & Shikov, A., 2015. Contemporary automated training systems with the use of playing form of education. *Innovacii v Obrazovanii*, N 4, pp. 111-119.

Development of the Detection Module for a SmartLighting System

Ivan Matveev[1], Eduard Siemens[1], Dmitri Dugaev[1] and Aleksey Yurchenko[2]
[1]*Department of Electrical, Mechanical and Industrial Engineering,*
Anhalt University of Applied Sciences,
Bernburger Str. 55, 06366, Köthen, Germany
[2]*Institute of Non-Destructive Testing, Tomsk Polytechnic University, Lenina Str. 30, Tomsk, Russia*
{i.matveev, e.siemens, d.dugaev}@emw.hs-anhalt.de, niipp@inbox.ru

Keywords: Smartlighting, Sensors, Detection, Human Detection, Detection Module.

Abstract: The research presented in this paper focuses at the human detection means for lighting areas. In particular, analysis of output sensors signal and software signal processing, analysis of ambient conditions influence on detectors functionality is given. The performed research is based on experiments, conducted at the Future Internet Lab Anhalt. The main goal of this paper is development of the human detection module for a SmartLighting system that satisfies a set of requirements of reliable human object detection. The given tests have been performed using ultrasonic, radio wave and infrared sensors. The analysis of the performed experiments allows us to define a degree of sensors conformance for the aimed SmartLighting applications. As the result of the performed experiments it is also shown that the combination of different detectors provides the most informative parameters about moving object in a control area than any considered single detection method. The hardware design and signal processing algorithm of the detection module have also been implemented in the course of this work. We found out that the sensors combination provides an error probability of less than 1% of human movement detection at distances up to 10 meters.

1 INTRODUCTION

According to International Energy Agency (2006), the street lighting is 53 % of worldwide outdoor energy consumption for lighting. Therefore, modern lighting systems have strict requirements for energy consumption and resource efficiency. These requirements can be satisfied by using smart lighting systems.

Smart lighting systems have a set of advantages in comparison to legacy ones. While conventional lighting systems have default lighting time that is independent from time of day and weather. In particular, lighting will not be activated automatically in required environmental conditions (e.g. at foggy or rainy weather). Also, switching on/off of conventional lighting systems do not depend on presence of pedestrians and moving cars, which leads to excessive energy consumption during all the dark time of day (Srivatsa et al., 2013).

The key element of smart lighting systems is a motion detection module. Accuracy and reliability of this unit have high impact on workability and efficiency of a smart lighting system. The registration of human motions in a controlled area by means of collection and processing of informative parameters is performed by a detection subsystem (Matveev et al., 2015).

Contemporarily existing detection means which are used in smart lighting systems have a number of significant disadvantages, particularly a high detection error rate. Their detection reliability heavily depends on operating conditions. Therefore, an approach for compensation of interfacing factors influence on detection reliability is studied in current work.

Currently, the prototype of a smart lighting system is being developed within *SmartLighting* project at the Future Internet Lab Anhalt of Anhalt University of Applied Sciences (Dugaev et al., 2014). The project is aimed at developing an autoconfigurable mesh networks across street lighting systems which passes motion detection messages across the network and performs intelligent handling on motion activities on the street. In particular, a specific routing scheme for

wireless mesh lighting networks along with a detection subsystem is there under development (Dugaev et al., 2014), (Dugaev and Siemens, 2014).

This paper is focused on experimental research of different sensors types which are acceptable for human movement detection. That includes investigation of sensors parameters as operating range, probability of detection errors, triggering error, informative signals.

2 RELATED WORK

Existing detection means, which are used in smart lighting systems, are usually based on single control method (Sung, 2013). Hereby, workability and accuracy of the detection system are limited by disadvantages of method, for example, false triggering or small working distance (Goponenko and Matveev, 2015).

Two kinds of widely spread motion sensors are passive infrared (PIR) and ultrasonic (US) sensors (Yavari et al., 2013). Passive infrared (PIR) sensors are compact, have low cost and low power (Zappi et al., 2007), however, they are highly dependent on the ambient temperature and brightness level (Fardi, et al., 2005). Ultrasonic technology enables obtaining distance information to the motion object, which can be used for the object motion speed calculation (Canali et al., 1982). One of the main disadvantages of these sensors is the multipath reception that could distort measurements of the distance between emitter and receiver. Also, these sensors are sensitive to temperature changes as it has a significant impact on the sound speed (Mainetti et al., 2014).

In contrary to the said two sensor kinds, radio wave (RW) sensors are commonly used for object detection in security or surveillance systems. RW sensors have high sensitivity (Yavari et al., 2013) that can cause incorrect work of a detector, for example, by vibrating equipment or small animals. The efficiency of RW sensors depends on the ambient conditions. Usage of RW detector requires resource demanding filtration, demodulation and processing algorithms due to specifics of the output signal (Matveev et al., 2016). However, it ensures large number of informative parameters, which can be used for motion analysis.

The hybrid systems based on US - PIR (Pfeifer and Elias, 2003) or RW - PIR (Bai et al., 2013) combination of sensors are focused on indoor object detection and localization that makes such systems hardly acceptable for street lighting related applications.

3 REQUIREMENTS FOR THE MOTION DETECTION MODULE

Given the significant role of the detection module as a part of SmartLighting system (Siemens, 2014), requirements and conditions for the following requirements of motion detection have to be fixed.

Requirements for error probability. One of the significant problems, which can appear during SmartLighting system operation is incorrect triggering of the detection module. Errors can be divided into two classes of errors:

Error of human detection. The error is occured when motion is not detected in presence of a human object. This error class has high influence on the reliability of the detection module therefore error probability has to be as low as possible. We believe that the value of the human detection error probability for the detection module has to be less than 1% in operational SmartLighting systems.

False triggering error. This error occurs when motion is detected while no human motion is present in control area. Such errors are typically caused by bad weather conditions and caused by non-human motion sources like trees oscillation etc. The value of the false triggering error is less critical than error of human detection, since it leads only to unnecessary energy consumption and doesn't negatively impact the public security, so we set the target threshold for the detection module to be less than 5%.

Detection range requirements. The human motion has to be detected early to provide necessary lighting area for a pedestrian. The taken detection distance is equal to 10 m and chosen based on analysis of street lighting systems parameters for pedestrian areas which are represented bellow.

The typical distance between lighting poles is 25 - 50 m. Lamp type is light emitted diode (LED), high-pressure sodium (HPS) or fluorescent (FL). Power of lamps varies in the range of 70 - 150 W. Lamps installation height is 5 - 8 m (Transport Canberra and City Services, 2007), (Lighting Orient Co., n.d.), (Standard Development Specification, n.d.).

Necessary informative parameters (status). The information about existence (movement or occupancy) of an object in area of lighting. The status is an obligatory information which is necessary for proper operation of the SmartLighting system.

Complementary informative parameters (speed). The parameter can be used with the aim of SmartLighting system reliability and accuracy increase, e.g. for calculation of object location between lighting units.

Flexibility of the system. The module is developed as integrated unit for SmartLighting system. The flexibility of the detection module assumes compatibility of interacting interfaces and system architecture which is convenient for further extensions and modifications.

4 EXPERIMENTAL RESEARCH

In this section the operation range and reliability of US, RW and PIR sensors are researched independently on each other. Acceptability of chosen detection means for usage in detection module has been defined experimentally.

4.1 Experimental Setup

In order to perform the analysis of dependence between human motion and the responses of sensors an experimental setup as follows has been designed. The positioning of sensors on the experimental board is shown on Figure 1. The board with sensors is installed on a tripod with 2 m height. The distance between sensors is 0.1 m.

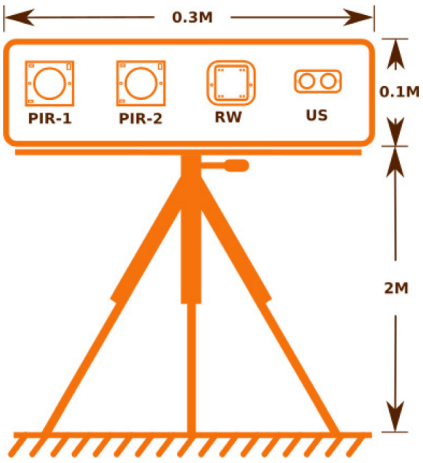

Figure 1: Location of sensors on the experimental board.

Three types of detectors have been used. Two PIR sensors: “PIR-1” - produced by SeedsStudio and “RK410RQ” - produced by Rokonet). A radio wave detector “X-band motion detector” produced by Parallax and an ultrasonic sensor “SRF08 ranger”. In further text, the “PIR-1” is referred as PIR-1, the “RK410RQ” as PIR-2, “X-band motion detector” as RW and “SRF08 ranger” - US.

The structure of the experimental setup is represented on Figure 2. A main control device of the test setup is a Beaglebone Black (BBB) microcomputer. The BBB provides power supply for detectors, executes the measurement program, polls the sensors, process received data, and transmits collected data to a workstation.

The mobile device is used for a remote system control and for starting the experiment. The application on mobile device simplifies the operation of the experiment - in particular, one person is able to control the system remotely and to be an object of sensors response. Also, the problem of timing of people's motion in the experiment is resolved by the mobile device.

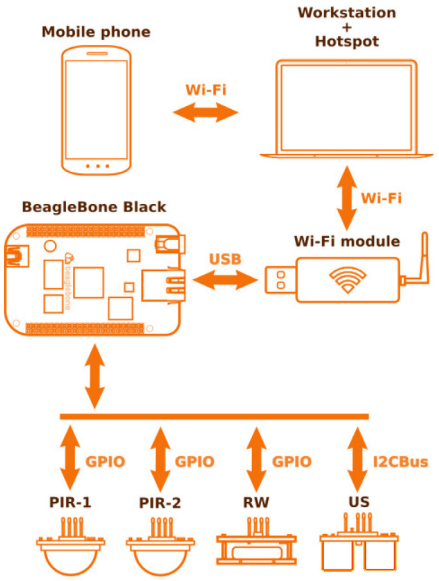

Figure 2: Diagram of the experimental setup.

A Wi-Fi hotspot has been deployed on a workstation that receives the data from the BBB at the end of experiment for further processing and analysis.

4.2 Methodology of the Experiment

The experiment has been performed under environmental conditions that are close to expected operational conditions of the detection module at a

street area with 10 m length and 14 m width. Motion vectors are oriented to sensors radiation direction with 1m grid density. Experiments have been performed at twilight and night time to avoid false triggering of PIR sensors during the day, because the level of brightness affects response time, sensitivity and operating range of sensors significantly.

The temperature range during experiments was 18–25° C, approximate wind speed range - 7–23 km/h.

Each experiment run takes 30 s: 0–5 s - no motion; 5–15 s - motion in one direction across control area; 15–20 s - no motion; 20–30 s - motion in opposite direction across controlled area.

4.3 Experimental Results

As a result of experiments, the feasibility of sensors usage in the human detection module has been analyzed. PIR-2, RW and US sensors were not able to cover the aimed detection range. The PIR-1 sensor detects movement at distances up to 10 m. However, PIR-1 can react on warm object outside the control area, that leads to increased triggering error probability.

4.3.1 Ultrasonic Sensor

The given experiments have revealed that the US sensor is not usable for the target application. The sensor responds only when significant motion occurs in the control area. The sensor is able to detect reliably an object on a distance which is less than 1.5 m with 30° angle of scanning.

However, such data, as a distance to the object, is an important information and can be used for an object speed calculation. The US sensor will be not used in the developed detection module, due to the given disadvantages.

4.3.2 Passive Infrared Sensors

Two PIR sensors have been used to define variation of detection parameters as range, angle, triggering delay and errors probability values, for different models of PIR sensors.

The PIR-1 and PIR-2 output signals are high when continuous motion is detected. This can be simply analyzed without need of further processing.

The detection graphs for PIR sensors are represented on Figure 3. These graphs show response of sensors while human motion is performed during of the experiment run.

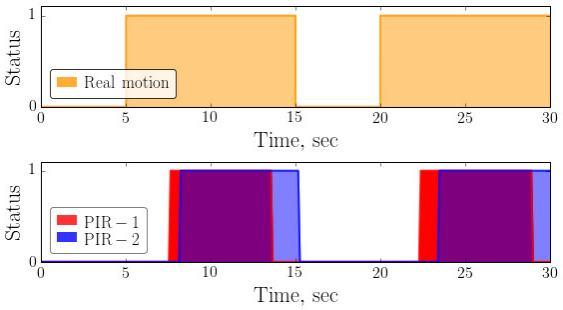

Figure 3: Motion detection diagrams for PIR-1 and PIR-2 sensors. Motion across control area on two meters distance to the experimental setup.

The time shift between real motion and detected signal can be explained by limited operation angle and triggering delay. So, it takes 2.5 s to overcome the distance from border of polygon to the area of detection, covered by PIR-1. Triggering delay value for the sensor was determined experimentally and equals to 0.3 s. The PIR-1 is able to detect movement on distances up to 10 m. The operating angle is 140°. The human detection error probability of the sensor was equal to 0% (according to 200 experiment samples). The disadvantage of the PIR-1 is that sensor can react on warm object outside the control area, such as cars, because the IR radiation intensity from engine of a car is more than IR radiation intensity from a human. Triggering of the detector caused by non-human sources of IR radiation leads to increase of triggering error probability.

The PIR-2 sensor is designed for alarm security systems. The sensor operates within 4 m range, which is low for typical IR based sensors. Triggering delay of the sensor is about 2 s, which is not acceptable for usage in the detection module because a lighting area for a pedestrian should be provided timely. The operating angle is equal to 140°. Due to the disadvantages, the PIR-2 sensor will be not used in the developed detection module.

4.3.3 Radio Wave Sensor

The output signal of RW sensor is a dependence of signal frequency and duty cycle from the size and speed of a moving object. The dirty cycle is defined as the ratio between the pulse duration and the time distance between the beginning of the current pulse to the next pulse. However, the raw RW signal needs further processing for being used for motion and speed detection. A segment of raw signal from RW sensor during 8 - 8.6 s of the experiment, when the person enters detection area of RW sensor, is represented on Figure 4.

The frequency transformation is performed as follows. Based on raw signal, the period of each impulse T_{imp} is defined, then inverse value $f_{imp} = 1/T_{imp}$ is calculated. The resulting impulse frequency is registered on y axis with corresponding time values on x. The signal frequency correlates with object speed - the higher frequency, the faster object is moving. This conversion allows plotting a frequency transformation graph and estimate object movement intensity (figure 4).

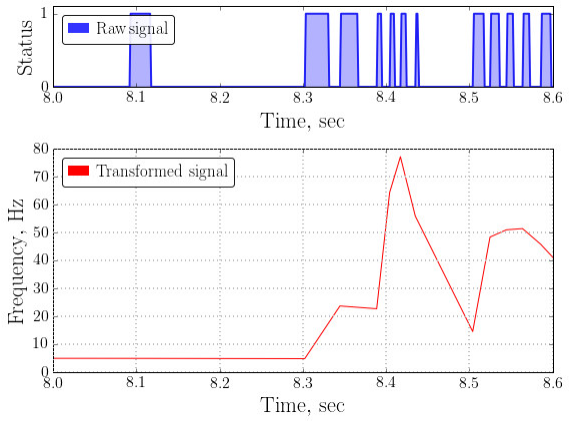

Figure 4: Raw and transformed signals from RW sensor.

Such signal conversion allows the definition of a frequency level, that is typical for a human motion, and set this value as a level for a human detection. Values of signal frequency higher than the defined level indicate the human presence in control area.

The performed tests have shown that the RW sensors reacts very sensitively on insignificant movements, for example, on trees or grass oscillations caused by a gust of wind. Also, electromagnetic interferences affect sensor performance significantly (Combined detectors for alarm systems, n.d.). The frequency filtering is based on calculating a mean and standard deviation values of the signal frequency:

Mean value of a sample allows to define average signal frequency during a defined window size. The sample is an array which contains calculated frequency values of impulses. Given the relation between signal frequency and movement intensity, mean value is used as first human detection criteria.

$$\bar{x} = \sum_{i=0}^{n} x_i \cdot \frac{1}{n} \qquad (1)$$

where $\bar{x}$ - mean value;
x_i - observed value of the sample items;
n - sample size.

Standard deviation is used to quantify the amount of variation or dispersion of a set of data values (Bland and Altman, 1996). This value allows filtering out of areas of rapid frequency changing.

$$\sigma = \sqrt{\frac{1}{n}\sum_{i=1}^{n}(x_i - \bar{x})^2} \qquad (2)$$

where σ - standard deviation
x_i - observed value of the sample items;
$\bar{x}$ - mean value of the observations;
n - sample size.

Human detection is performed only when the following conditions are satisfied: calculated mean signal value is more than established mean criteria value and standard deviation value is less than corresponding criteria value;

$$\bar{x} > m_{cr} \cup \sigma < st_{cr} \qquad (3)$$

where $\bar{x}$ - mean value of a sample;
m_{cr} - mean criteria;
σ - standard deviation value of a sample;
st_{cr} - standard deviation criteria;

Figure 5 represents mean and standard deviation plot of signal frequencies taken when motion occurred at two meters distance from the experimental setup. The standard deviation value in areas of human motion has gradual increase behavior therefore such areas are not subjected to be filtered. The result of detection for the RW sensor is shown on third graph of figure 4, where high levels correspond to a detected motion.

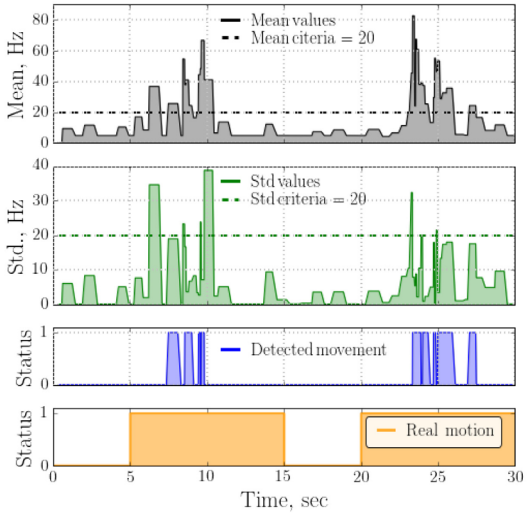

Figure 5: Processed signal for RW sensor. Motion across control area on five meters distance to the experimental setup.

A two-dimensional detection area for the RW sensor using given filtering is represented on Figure 6. The black spot at coordinates [0, 7] is the

position of the tripod with sensors. The blue elliptical shapes are the points where human motion is detected by the sensor. The highest level of detection is allocated within the gray elliptical area on the figure. The human detection error probability in the whole gray area is less than 3%, the triggering error probability is approximately 10%.

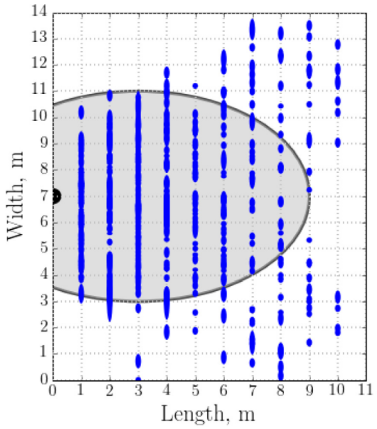

Figure 6: Detection area for RW sensor (m_{cr} = 20 and st_{cr} = 20).

The aimed human detection error probability of is less than 1%, are given when filter criteria are equal to m_{cr} = 30 and st_{cr} = 15 (Figure 7). The triggering error probability for these criteria is approximately 5%. The detection range for these parameters is up to 4 m. The triggering delay range is 0.1 - 0.2 s due to signal processing time.

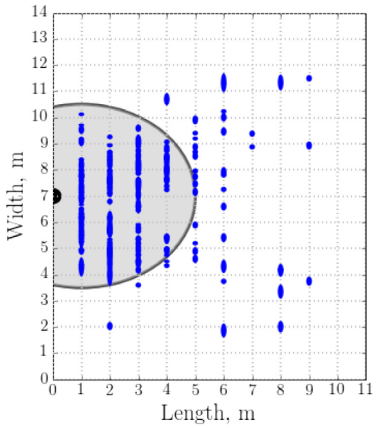

Figure 7: Detection area for RW sensor (m_{cr} = 30 and st_{cr} = 15).

However, a significant disadvantage of the senor is its high sensitivity to insignificant motions in a control area. Also, the detection distance, when 1% of the error probability is provided, is insufficient to the operating distance requirements for the detection module.

5 PROPOSED COMBINED DETECTION MODULE APPROACH

As experiment result, an improved combination of sensors for usage in the detection module has been found. This combination consists of the PIR-1 sensor and the RW sensor. Due to sensors disadvantages, obtained signals separately do not allow to estimate human motion or presence precisely.

One of the possible solutions is a dynamical filtering level adjustment of the RW detector. The concept is based on RW sensor signal level reduction for the filter, when a human motion is detected by the IR sensor. Such approach allows to compensate detectors disadvantages and to reduce errors probability. The human detection is only performed when both sensors detect human motion.

The chosen detectors have following informative parameters in respect to human detection purpose. Binary signal from the PIR detector identifying a warm object motion in the controlled area. Frequency and duty cycle data of the RW detector based on object movement intensity in a control area.

Application of dynamical detection criteria allow to increase sensitivity and detection distance of the RW sensor. Such approach allows to increase detection range of RW sensor and while avoiding false triggering errors of the PIR sensor. Also, the probability of false RW sensor triggering is reduced, because the sensor sensitivity is only increased when human motion is expected.

Usage of the sensors combination and efficient detection algorithm allow to detect human motion in a control area with approximate error probability of 0.5%.

False triggering probability of the detection module (due to interfering factors) depends on the environmental conditions. In the described experiments, the error value equals to 3%, when an approximate wind speed is up to 25 km/h.

Signals which are received from the detection module, when dynamical human detection criteria are applied for the RW sensor, are shown on Figure 8.

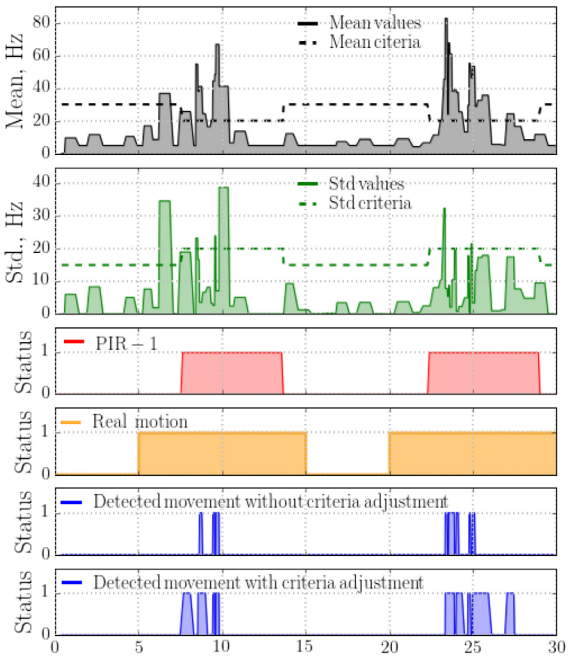

Figure 8: Dynamical human detection criteria adjustment.

The resulted detection area of the detection module is represented on Figure 9 as a gray elliptic area.

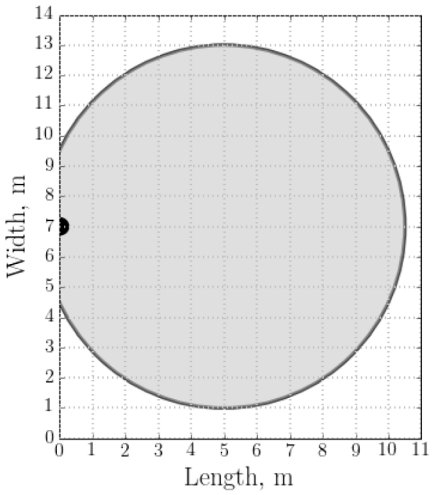

Figure 9: Operating area of the detection module.

6 CONCLUSION

The experimental research has been performed to test the feasibility of the given sensors for motion detection in the SmartLighting environment. It enables engineers to analyze detectors' responses, the investigation of areas of detection with its respective error rates. Using this, a significant improvement of the reliability of motion detection by using of a combination of PIR and IR sensors for a human detection could be tested and its benefits have been proven.

Using the combined methods with the given filter parameters the detection error probability can be reduced to 0.5% whereby false triggering error probability can be kept at 3%. Thus, resulted values of errors probability satisfy the error probability requirements for the detection module. Resulted detection range of the detection module is equal to 10 m. That satisfies the operating distance requirement.

The prototype's hardware provides extendibility and flexibility. The implemented approach allows to easily integrate the detection module to the SmartLighting system that satisfy flexibility requirement for the detection module.

The following research tasks to the detection module are supposed to be considered in further activities. Other models of US sensors are going to be considered with the aim of an object speed calculation. Development of improved filtering algorithm that allows to increase performance of the detection system has to be done. Also, of an algorithm for system adaptation to ambient conditions based on statistical data analysis could further improve the motion recognition reliability. Power consumption reduction via algorithm optimization (decrease of redundant calculations) is going to be performed. Integration of brightness detection elements that provides the SmartLighting system activation in required weather and climate conditions which influence on the ambient brightness level has to be done.

REFERENCES

Bai, Y.W., Cheng, C.C., Xie, Z.L., 2013. Use of ultrasonic signal coding and PIR sensors to enhance the sensing reliability of an embedded surveillance system. *Presented at the 2013 IEEE International Systems Conference (SysCon)*, pp. 287–291. doi:10.1109/SysCon.2013.6549895

Bland, J.M., Altman, D.G., 1996. *Measurement error and correlation coefficients*. BMJ 313, 41–42.

Canali, C., Cicco, G.D., Morten, B., Prudenziati, M., Taroni, A., 1982. A Temperature Compensated

Ultrasonic Sensor Operating in Air for Distance and Proximity Measurements. *IEEE Transactions on Industrial Electronics IE-29*, 336–341. doi:10.1109/TIE.1982.356688

Combined detectors for alarm systems. Part 1., n.d.. *Security systems*. [Online], Available from: https://polyset.ru/article/st1001.php (accessed 8.12.16).

Dugaev, D., Siemens, E., 2014. A Wireless Mesh Network NS-3 Simulation Model: Implementation and Performance Comparison With a Real Test-Bed, in: *Proceedings of 2nd Applied Innovations in IT International Conference*. Koethen, Germany, pp. 1–5.

Dugaev, D., Zinov, S., Siemens, E., 2014. A Survey of Multi-Hop Routing Schemes in Wireless Networks applied for the SmartLighting Scenario, in: *Proceedings of 5th Technologies and Equipment for Information Measurement International Conference*. Tomsk Polytechnic Univ., Tomsk, Russia.

Fardi, B., Schuenert, U., Wanielik, G., 2005. Shape and motion-based pedestrian detection in infrared images: a multi sensor approach. Intelligent Vehicles Symposium. *Presented at the IEEE Proceedings*., pp. 18–23. doi:10.1109/IVS.2005.1505071

Goponenko, A.S., Matveev, I.G., 2015. Overview of motion and presence detection systems used in smart lighting systems, in: *Proceedings of Information and Measuring Techniques and Technologies Conference*. Tomsk Polytechnic Univ., Tomsk, Russia, pp. 241–246.

International Energy Agency, 2006. *Light's labour's lost. Policies for energy-efficient lighting*. Paris, France: IEA.

Lighting Orient Co., n.d. *Project of LED Street Lights*. [Online], Available from:

http://www.ledlightsorient.com/docs/LEDStreetLightProjects.pdf (accessed 15.01.16).

Mainetti, L., Patrono, L., Sergi, I., 2014. A survey on indoor positioning systems, in: *Presented at the 2014 22nd International Conference on Software, Telecommunications and Computer Networks (SoftCOM)*, pp. 111–120. doi:10.1109/SOFTCOM.2014.7039067

Matveev, I.G., Goponenko, A.S., Yurchenko, A.V., Kovalev, M.V., 2015. Design of detection module based on BeagleBone Black microcomputer, in: *Polzunovsky Vestnik No.3 2015*. pp. 126–130.

Matveev, I., Siemens, E., Yurchenko, A., Kuznetsov, D., 2016. Development and Experimental Investigations of Motion Detection Module for Smart Lighting System. *IOP Conference Series: Materials Science and Engineering* 132, 1–6. doi:10.1088/1757-899X/132/1/012010

Pfeifer, T., Elias, D., 2003. Commercial hybrid IR/RF local positioning system, in: *KiVS 2003, 13. ITG GI-Fachtagung Kommunikation in Verteilten Systemen. Kurzbeiträge, Praxisberichte Und Workshop E-Learning*. pp. 119–127.

Siemens, E., 2014. Method for lighting e.g. road, involves switching on the lamp on detection of movement of person, and sending message to neighboring lamps through communication unit. DE102010049121 B4

Srivatsa, D.K., Preethi, B., Parinitha, R., Sumana, G., Kumar, A., 2013. Smart Street Lights, in: *India Educators' Conference (TIIEC)*, 2013 Texas Instruments. Presented at the India Educators' Conference (TIIEC), 2013 Texas Instruments, pp. 103–106. doi:10.1109/TIIEC.2013.25

Standard Development Specification., n.d. *Street Lighting Design Guide p 26*. [Online], Available from: http://www3.hants.gov.uk/street_lighting_design_guide__4th_edition_.pdf (accessed 15.01.16).

Sung, W.-T., Lin, J.-S., 2013. *Design and Implementation of a Smart LED Lighting System Using a Self Adaptive Weighted Data Fusion Algorithm*. Sensors 13, 16915–16939. doi:10.3390/s131216915

Transport Canberra and City Services, 2007. *Design Standards or Urban Infrastructure. Street Lighting, Section 12*. Edition 1, Revision 1,

Yavari, E., Jou, H., Lubecke, V., Boric-Lubecke, O., 2013. Doppler radar sensor for occupancy monitoring, in: 2013 IEEE Topical Conference on Biomedical Wireless Technologies, Networks, and Sensing Systems. *Presented at the 2013 IEEE Topical Conference on Biomedical Wireless Technologies, Networks, and Sensing Systems*, pp. 139–141. doi:10.1109/BioWireleSS.2013.6613701

Zappi, P., Farella, E., Benini, L., 2007. Enhancing the spatial resolution of presence detection in a PIR based wireless surveillance network. *Presented at the 2007 IEEE Conference on Advanced Video and Signal Based Surveillance*, pp. 295–300. doi:10.1109/AVSS.2007.4425326

Analysis of Outdoor Lighting Control Systems and Devices for the Creation of Outdoor Lighting Automatic Control System Using the Traffic Flow Value

Nikolai Pavlov[1], Andrei Bachurin[1] and Eduard Siemens[2]
[1]*Electrical Engineering Faculty, Perm National Research Polytechnic University, Komsomolskiy Prospect 29, Perm, Russia*
[2]*Anhalt University of Applied Sciences - Future Internet Lab Anhalt, Bernburger Str. 55, 06366 Koethen, Germany*
pavlov_v94@mail.ru, bachurin@ellips.ru, e.siemens@emw.hs-anhalt.de

Keywords: Lighting Automatic Control, Control System, Outdoor Lighting, Energy Efficiency, Quality Lighting, Traffic Flow.

Abstract: This article describes various automatic light control systems. The aim is to analyze existing luminous flux lighting installations with automatic control systems and propose some invention, which is able to eliminate some of their shortcomings. Disadvantages of existing systems are the increased power consumption due to the lack of the luminous flux flexible regulation depending on the traffic on the objects requiring illumination. The aim of invention is to optimize the power consumption by reducing its consumption in moments of significant traffic reduction. The known control systems are supplemented with a counter number of vehicles per unit of time and the controller of functional dependence, which controls the lighting installation luminous flux. The control signal for the lighting system is automatically generated depending on the intensity of vehicles, and sets the light amount as a percentage of the nominal value. The technical result is a significant reduction of power consumption of public lighting systems, the economic result - a reduction of electricity costs.

1 INTRODUCTION

About 14% of all generated electricity is spent on public illumination (Klykov, 2011), therefore increasing the lighting systems energy efficiency plays an important role in energy savings.

The application of the electronic ballasts and lighting control systems makes it possible to bring savings up to 60%.

The main contribution to this effect is created by light management systems (40%), while the share of electronic ballasts in the magnitude of this effect does not exceed 20% (Liping Guo, 2008).

Components of a lighting installation, determine its energy efficiency are shown in Table 1.

Table 1: Components of lighting installations and their functions.

Components of the lighting system	Functions
Lighting sources	Luminous flux generation
Lighting appliances	Luminous flux distribution
Ballasts	Performs supply electrical energy to light sources
Lighting control systems	Lighting Mode Control

2 ANALYSIS OF AUTOMATIC LIGHTING CONTROL

We know that economic efficiency during operation of lighting installations is inversely proportional to their power consumption, power consumption, in turn, is determined by the nominal value of the luminous flux produced by the lighting installation.

It is also known that different situations require different quantities of illumination and, under otherwise identical lighting installations parameters, different luminous flux quantities.

Generally, these situations are divided depending on the work complexity performed by the operator and the irritant (distractions) factors intensity.

Lighting systems project in a specific location (room, area, street section) is calculated on the operation for a long time (at least 5 years) (GOST, 2013).

Usually, the situation in the illuminated spot changes over the lifetime of the lighting system: the intensity of the movement throughout the day and over the year is changing, etc.

There are many technical solutions with automatic lighting control systems application.

Lighting load control is carried in two main ways: disconnection of all or of part of luminaires or change in the lamp luminous flux (for all the group of lamps or individually) (Branislav, 2016).

There are cases where the project specifications for the illuminated object is selected initially overestimated (excessive light flux, increased operation of lighting installations time limits) from various reasons (historical city center, theoretical streets capacity, movement of public transport, etc.) that additionally increases electric power consumed in the absence of regulation in real time.

The moment of illumination mode change in known systems is determined by signals from a light barrier, timers, motion sensors. Classification of outdoor lighting control system is shown in Figure 1.

Disadvantage of the existing control systems with motion sensors is reduction of lamp life due to switching on and off and the lack of luminous flux regulation.

Disadvantage of other control systems is the inability of automatic lighting control in real time depending on lighting needs in a specific situation (Boyce, 2009).

3 POWER CONTROL DEPENDING ON THE TRAFFIC FLOW

The aim of new lighting control system is to optimize the power consumption by reducing its consumption in the moments of a significant reduction in traffic on the objects which require illumination.

The control system taken as a basis is able to adjust the light flux of lighting installations in groups, depending on the time of a day according to the formula:

$$J = f(T), \tag{1}$$

where J - is the light flux level in the percentage of its nominal value, %; T - a variable indicating the current time, take one of four values: "Day", "Night", "Morning" or "Evening"; f - control function.

But it lacks switching of the lighting on and off due to flexible schedule. It is necessary that the schedule does not have only three states during the day - when the light is switched on, when light is switched on not at full power and when the light is switched off, but allows adjustments according to the traffic intensity within a few minutes.

This objective is achieved by the fact to be considered as a prototype of the control system with fixed time zones, the principle of which is shown in Figure 2, supplemented by: the number of vehicles per unit of time counter and the controller, which in turn controls the lighting system luminous flux by functional dependency:

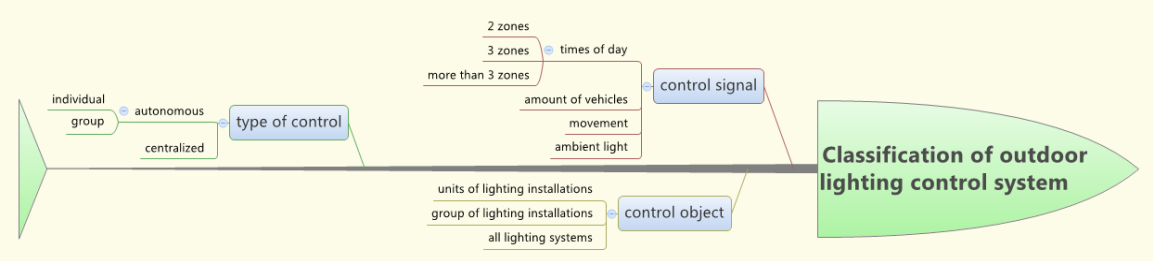

Figure 1: Classification of outdoor lighting control system.

$$J = f(N), \qquad (2)$$

where J - is the light flux level in the percentage of its nominal value, %; N - number of vehicles in the percentage of the maximum average annual value, %; f - control function.

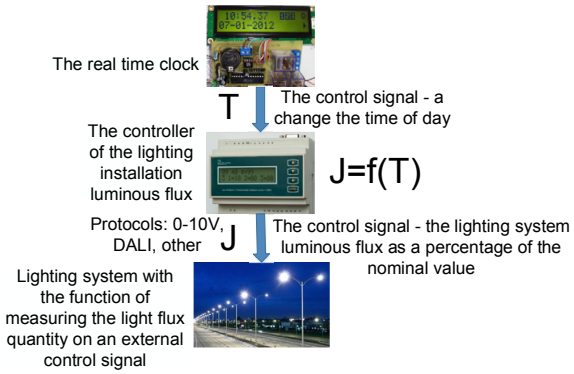

Figure 2: The operating principle of the control system with fixed time zones.

To develop the control algorithm, were calculated traffic flows on several typical streets of the city. The calculation was performed manually by counting the number of vehicles over one day per every 5 minutes on the site of interest. Counting was carried out on the previously recorded video.

For operation in the proposed control system can be applied automatic counters (based on infrared, ultrasonic or video technology). Figure 3 shows the operating principle of the new control system.

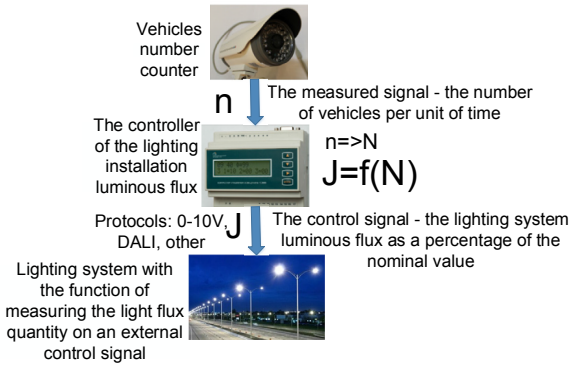

Figure 3: The operating principle of the new control system.

Features of the proposed operating principle - control signal for the lighting installation is automatically generated depending on the traffic of vehicles per unit of time.

The control signal sets the light amount as a percentage of the luminous flux nominal value. The dependence can be determined in tabular form or as a continuous function.

The application effectiveness of electronic ballasts with a hard regulation within 8 range shown in Figure 4 (Bachurin, 2016).

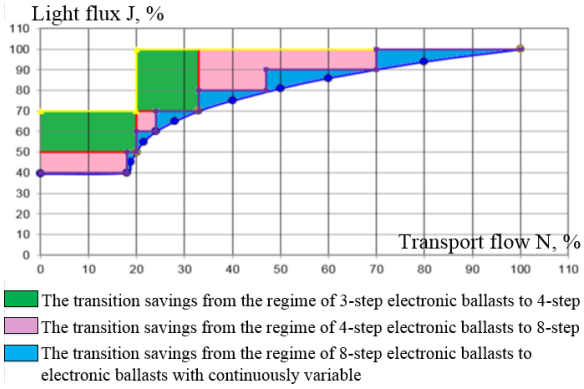

Figure 4: The application efficiency of electronic ballasts.

Specific functional dependencies must be consistent with the technical possibilities of lighting systems and applicable regulatory documents (GOST, 2013).

Example timetable of vehicles in conjunction with the operating schedule of the existing lighting system and the operating schedule of the system with an 8-step control principle is shown in Figure 6. The luminous flux is directly proportional to the traffic flow, so these values on the graph shown in the same coordinate axis.

In the daytime artificial lighting is not required. The principle of signal shaping in the form of tabular dependence is shown in Table 2.

Table 2: Example of control by 8-step tabular function.

№ step	Amount of light flux J, %	The boundaries of the traffic flow changes N, %
1	100	100-70
2	90	70-47
3	80	47-33
4	70	33-24
5	60	24-20
6	50	20-18
7	40	18-1

Values for the function are calculated in proportion to the value of the traffic flow - 100% of the light flux corresponds to 100% annual average movement intensity of vehicles, while reducing traffic volume - decreases the value of lighting

installations luminous flux. Figure 5 shows the operation of this principle.

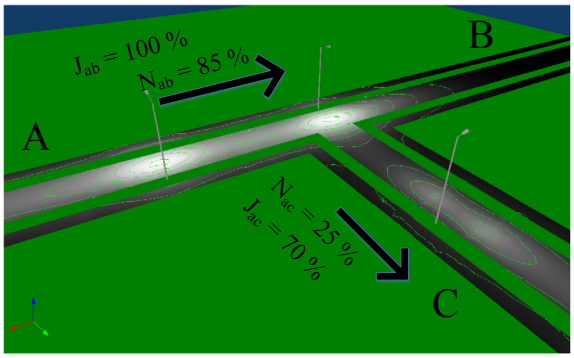

Figure 5: Operating of the new control system.

The dependence can be determined 2nd order function so as to fit in key points of standard documents (GOST, 2013).

These tables can be represented as a continuous function as shown in Figure 4. The coefficients in this case is calculated by method of least squares:

$$J = -0{,}0052N^2 + 1{,}208N + 31{,}522 \qquad (3)$$

where N - is the traffic flow, %; J - the luminous flux, %.

Schedule automatic control system is shown in Figure 7. The figure also schematically marked energy savings by using functional and table control functions. Next, to evaluate the effectiveness of the lighting control proposed method is necessary to perform a quantitative assessment to save electricity.

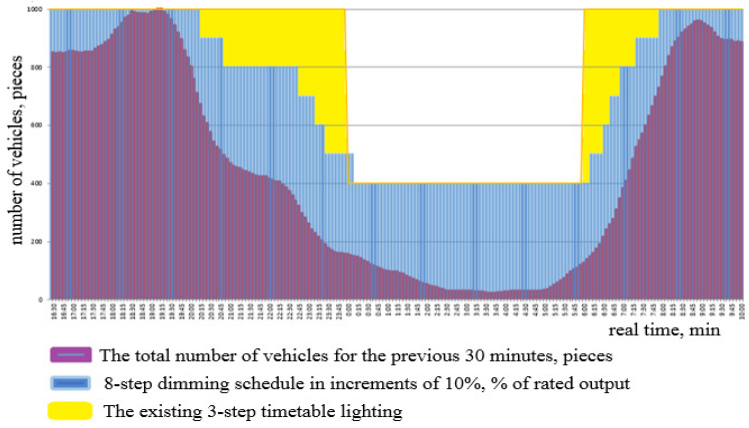

Figure 6: Vehicles movement schedule in conjunction with the operating schedule of the existing lighting system and the operating schedule of the system with 8-step regulation principle presented in tabular form.

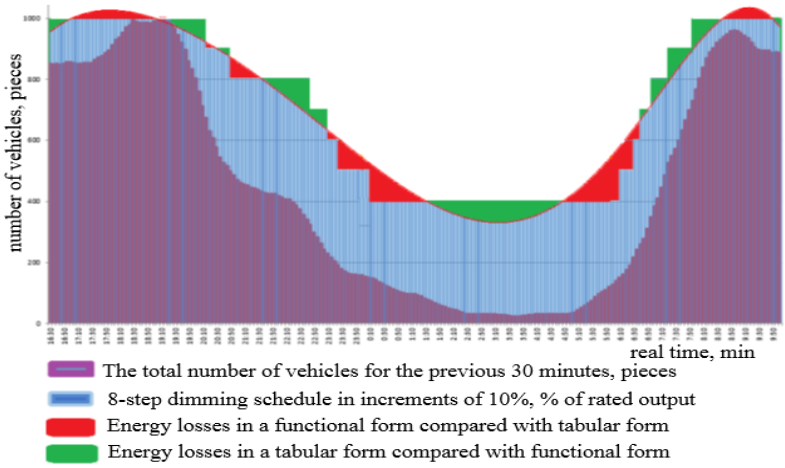

Figure 7: Vehicles Movement schedule in conjunction with the operating schedule of the existing lighting system and the operating schedule of the system with 8-step regulation principle presented in tabular form and continuous function form.

4 CALCULATION OF ELECTRIC ENERGY CONSUMPTION WITH OUTDOOR LIGHTING SYSTEM

To evaluate the effectiveness of the proposed lighting energy control system must calculate power consumption before and after its application. The estimation is made for Perm's outdoor lighting systems.

The integration of power consumption carried out for the year, since it is the smallest time interval at which the outdoor lighting power schedule more accurately shows the change in energy consumption, therefore, the annual consumption of outdoor lighting installations should be calculated according to the formula:

$$W_{year} = \int_{year} P \cdot dt \quad (4)$$

Schedule of power consumed by the outdoor lighting installation with the existing control system is shown in Figure 8.

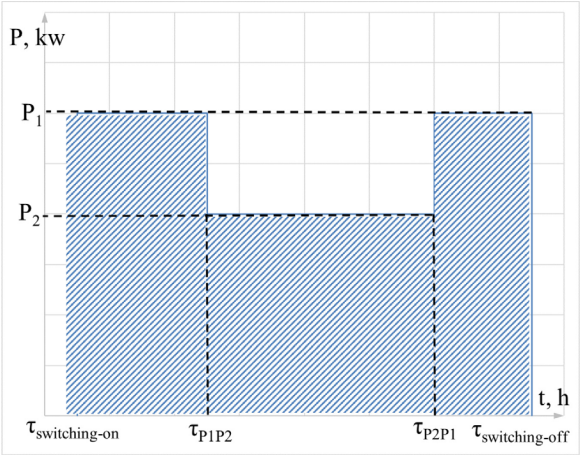

Figure 8: Schedule of power consumed by installations with the existing outdoor lighting control system.

Having defined time limits, you can count the number of inclusion hours by the formulas:

$$\tau_{P_1} = \sum_{i=1}^{m}((\tau_{P_1P_2} - \tau_{switching-on}) + (\tau_{switching-off} - \tau_{P_2P_1}) \quad (5)$$

$$\tau_{P_2} = \sum_{i=1}^{m}((\tau_{P_2P_1} - \tau_{P_1P_2}), \quad (6)$$

The results of the annual outdoor lighting operating time calculation are presented in Table 3.

Table 3: Annual operating time for the existing regime of outdoor lighting.

№ step	Site length τ, h	Power consumption on site P, kW
1	1856,04	6970
2	1928,38	4879

Schedule of power consumed by outdoor lighting installations with a new control system with 8-step operating schedule is shown in Figure 9.

The inclusion hours number of each of the 8 new control regimes, at certain time intervals, is analogous to the existing control system calculation.

The results of the annual outdoor lighting operating time calculation are presented in Table 4.

Table 4: Annual operating time for the new 8-step regime of outdoor lighting.

№ step	Site length τ, h	Power consumption on site P, kW
1	1960,03	1600
2	308,4	3485
3	146,93	4182
4	163,25	4879
5	561,7	5576
6	237,4	6273
7	406,7	6970

The total values of energy consumed by the outdoor lighting installations shown in Table 5.

Table 5: Annual energy consumption of the existing and the new control system.

The control system	Energy consumption per year, GW per h
existing	22,345
new 8-step	8,841

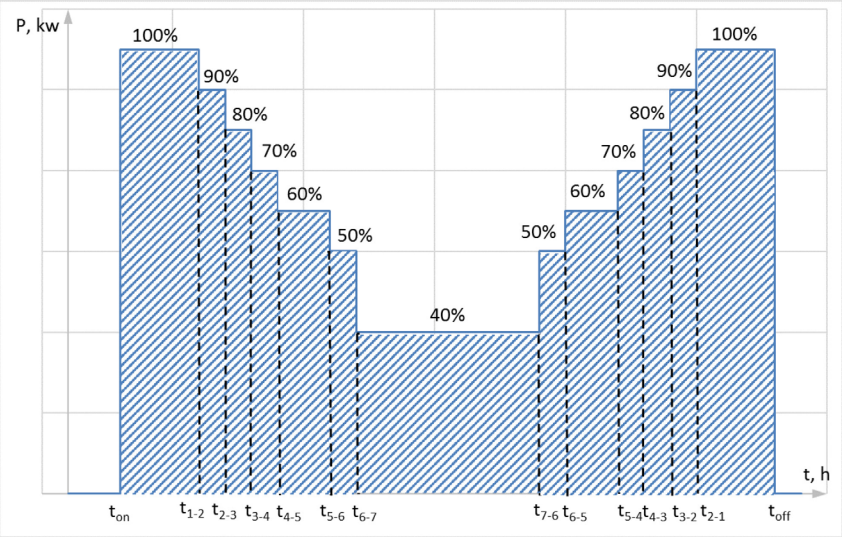

Figure 9: Schedule of power consumed by outdoor lighting installations with 8-step control.

5 CONCLUSION

The proposed automatic control system of lighting installation differs from the existing ones, that is provided with number of vehicles per unit of time counter, transmitting the measured signal in the luminous flux controller.

The controller, in turn, generates a control signal based on the functional dependence of the illumination level of the intensity of vehicle traffic, and then transmits the control signal to lighting system as a percentage of its nominal value in accordance with the one of standard interfaces (0-10V, the DALI, etc).

Implemented control principle allows to provide reduction in the value of the power consumption, reduce electricity costs and improve illumination uniformity of urban spaces and eliminate the need to switch off the lighting at night.

The estimated efficiency of the proposed new control system is 60%, compared to existing lighting systems.

It should be noted that the proposed control system will also improve the efficiency of modern lighting systems based on LED-lamps, the efficiency will not be less than 10%.

The next steps in this direction should be devoted to features of the technical implementation, the development of techniques and accurate energy calculation with system application for a particular facility, the development of control functions with maximum energy efficiency.

REFERENCES

Klykov M.E., Ju.B. Ajzenberga, 2011. Electronic ballasts for discharge lamps and automatic lighting control systems. PROON.

Liping Guo, Marjukka Eloholma DSc & Liisa Halonen D.Sc, 2008 Lighting Control Strategies for Telemanagement Road Lighting Control Systems, LEUKOS, 4:3, 157-171

GOST R 55706-2013, 2013 Outdoor lighting utilitarian. Classification and standards

Branislav M. Todorović, Dragan Samardžija, 2016. Road lighting energy-saving system based on wireless sensor network. Springer Science+Business Media Dordrecht

Boyce PR, Fotios S, Richards M, 2009. Road lighting and energy saving. Lighting Research and Technology; 41: 245–260.

Bachurin A, 2016, Improving the energy efficiency of outdoor lighting systems using the SmartLight technology Proceedings of the 4th International Conference on Applied Innovations in IT (2016). Jg. IV. Koethen : Hochschule Anhalt, pp. 9-13

Multidimensional Monitoring System of State Machines

Bogdan Zoltowski[1], Leonel F. Castaneda, Mariusz Zoltowski[2], Krzysztof Napieraj, Jacek Wachowicz[3], Ryszard Bielski[4]

[1]*Faculty of Mechanical Engineering, UTP University of Science and Technology in Bydgoszcz, al. prof. S. Kaliskiego 7 85-796 Bydgoszcz, Poland*

[2]*Faculty of Management, UTP University of Science and Technology in Bydgoszcz, al. prof. S. Kaliskiego 7 85-796 Bydgoszcz, Poland*

[3]*BOLS Institute, WSB University in Gdańsk, al. Grunwaldzka 238A, 80-266 Gdańsk, Poland*

[4]*Faculty of Management and Economics, Gdańsk University of Technology, ul. Traugutta 79, 80-233 Gdańsk, Poland*

bogzol@utp.edu.pl, mariusz.zoltowski@utp.edu.pl, jacek_wachowicz@o2.pl, ryszard.bielski@zie.pg.gda.pl

Keywords: Diagnostics, Monitoring, System of Exploitation, Reliability, Damages

Abstract: Technical systems are more complex every day as their electronics and mechanics. Technological advances tend to be autonomous in its performance and perform an auto-diagnosis that allows determining an abnormality existence in a component or subsystem and deciding if the system has to be stopped or not. The conventional maintenance does not allow an integrated diagnosis analysis of a system. Among the factors, that generated condition can be found a lack of communication between units: bad information of management, ignoring relevant of information, a lack of a clear monitoring policy and variables measurement tendency.

1 INTRODUCTION

Technical systems are becoming more complex when talking about their mechanic, and electronic. Technological advances tend to be more auto sufficient, and able to auto diagnose themselves, what allow to determine if any anomaly is present in any subsystem, or component, to finally decide whether the system must or not be stopped (Bongers 2004, Cempel 1999, Formenti et al. 1986, International union of railways 2003, National Instruments 2004).

The conventional maintenance with some factors such as the lack of communication between dependencies, a not proper management of information, not having a clear monitoring policy nor variables trends among other, don't not allow the performance of an integrated diagnose of the system (Natke et al. 2001, Potter et al., 1984, Żółtowski et al. 2006a, Żółtowski et al. 2006b, Żółtowski et al. 2007b, Żółtowski et al. 2007c) .

Due to the previous factors, it is necessary to implement new methodologies of technical diagnostic, in order to satisfy all of the company's needs, getting as result, an integrated diagnose through computing simulation, tools, analysis methods and information evaluation from the machine's technical state (Cempel 1999, Natke 1997, Żółtowski 2007a, Żółtowski 2011).

The energy processors theory is based on a main energy flow analysis, where a system balance arises between input energy N_i, dissipated energy N_d and useful energy N_u (Cempel 2003, Natke 1997).

Through a residual process series as vibration, noise and heat the input energy is dissipated in one of these phenomena, that reflect the technical system wear (accumulated dissipated energy), therefore the dissipated energy study through the system provides inference about the artefacts wear and therefore determining the system technical condition is of interest. Figure 1 shows the methodology followed by the mini-central technical diagnosis. This process involved the next diagnosis stages (Richardson 1995, Tournay 2001, Żółtowski 2006c, Żółtowski 2011):

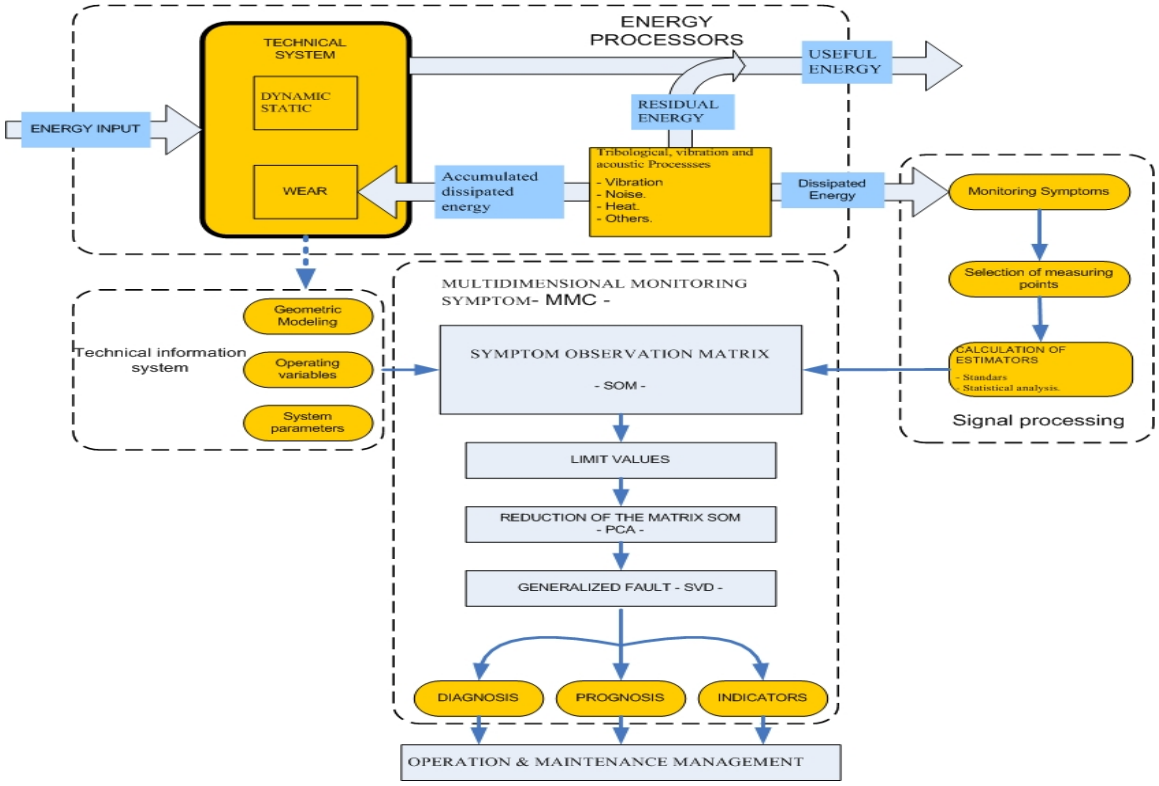

Figure 1: Technical diagnosis methodology for a water turbine .

- Register and acquisition of residual energy (reception and selection points of vibration signals and operation variables).
- Signal processing.
- Statehood monitoring of Francis turbine.
- Multidimensional Monitoring Condition.
- Maintenance ratios establishment.

2 STUDY CASE

As study case for presented methodology is La Herradura's Mini-central Hydroelectric property of Empresas Públicas de Medellín, which is located in the municipality of Frontino, north-east of Medellín, Antioquia. The Mini-central has two water type turbines of horizontal axis, each one with a rated power of 10.4MW and a $5m^3/s$ flow, with a rotation speed of 900rpm and a design net jump of 230.6m. Figure 2 shows up a general scheme of parts forming the turbine.

The Mini-central has two systems able to obtain information of technical condition. The first one is the vibration monitoring system and the second one - is the Mini-central monitoring and control system. The permanent vibration monitoring system for the generator is based on an instrument with the serial number "VDR-24" (Vibro Diagnostics Recorder – 24 channels), in the VDM data module and in the "ATLANT" diagnosis program. The vibrations measurement chain is showed on Figure 3.

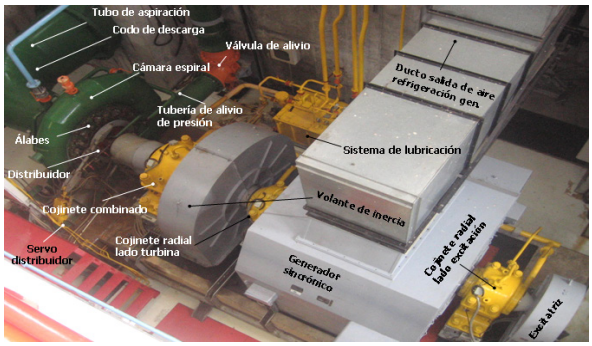

Figure 2: The view of the studied water turbine.

Through this system the r.m.s signals vibration value is monitored (speed and displacement) in points presented on Figure 4.
The system used to central monitoring and control from operation station is the V7 Monitor Pro from Schneider Electric (Figure 5), this allows the data acquisition, monitoring and real time control and has a setting Server-Client and an unlimited number of TAG's (variables).

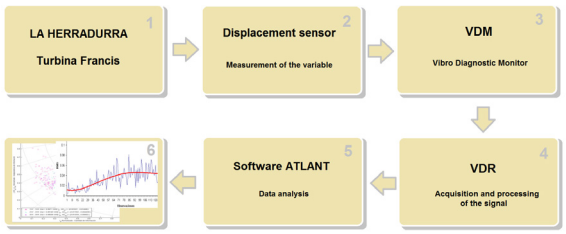

Figure 3: Measurement chain of vibration analysis system.

[symbols: 1) La Herradura's Mini-central. 2) Sensors – Variable Measurement. 3) VDM – Data Module. 4) VDR – Processing and signal acquisition.. 5) ATLANT Software. 6) ATLANT signal and analysis transformation]

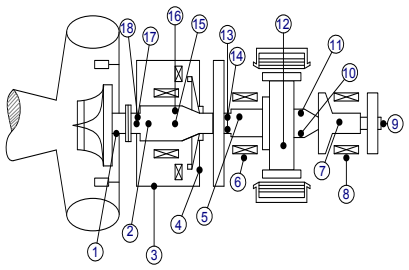

Figure 4: Acquisition point scheme of variables related to vibration.

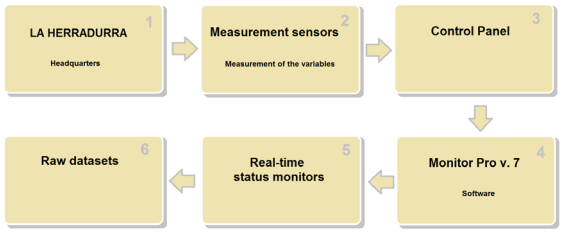

Figure 5: Measurement chain of the monitoring and control system.

[symbols: 1) La Herradura Mini-central. 2) Variables measurement sensors (Pressure, temperature, current, voltage). 3) Control panel. 4) V7 Monitor Pro Software. 5) General deployments of generation and monitoring units. 6) Historical board and reports]

3 MEASUREMENT POINTS SELECTION

Based on measurement points algorithm the mechanical vibration signal is analyzed, received from the three hydro-dynamical bearings based on independence criterion and information quantity. Fort the first case the information independence will be given by inverse area under the curve of coherence $\gamma_{xy}^2(f)$ between two signals measured at the same place, for the current study the signals are taken from vertical and horizontal speed in every bearing therefore, there will be a greater information independence when the maximum area, according to the next expression [5]:

$$AC_{xy} = \frac{1}{\int_0^F \gamma_{xy}^2(f)dF}$$

To determine the information quantity the coherence values are taken between signals depending on certain frequencies (system characteristic frequencies) and a criterion under the following expression [5]:

AC_{xy} and In_{xy} values are registered in a data base, given the data volume to analyse, an optimization problem is set out, which aims to determine the generation bearing in which the independence and information quantity are the highest.

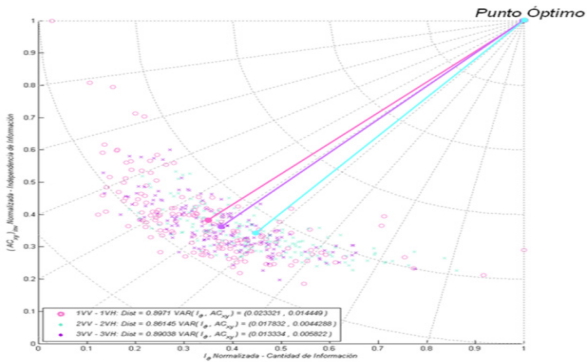

Figure 6: Reception point analysis from diagnosis signal.

According to Figure 6, the reception points of diagnosis signal are located almost at the same distance from the optimal point. This means that has reliable information for the technical diagnosis of the generation unit.

4 SYMPTOMS CALCULATION

During the diagnosis model implementation, a series of new symptoms were calculated to make a follow up of registered signals by the vibration monitoring system, Figure 7 shows up an example of the Amp. Espectro (225Hz):2VV symptom: this refers to the vibration speed amplitude of impeller blades frequency flow (225Hz), in vertical direction of 2 bearing. A data tendency was observed during monitoring time, which indicates the evidence of a system abnormality, thus the evidence the real system statehood condition, allows detecting, locating and evaluating failures in the system. On (Natke 1997) is showed up the symptom definition and some examples are suggested.

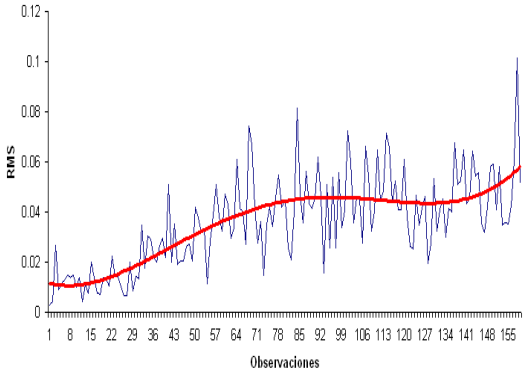

Figure 7: Vibration speed frequency from impeller blades flow (225Hz), in a vertical direction of 2 bearing.

5 OBSERVATION MATRIX ELABORATION

To elaborate the symptom matrix 25 generation and control variables were considered, corresponding to specific average values registered during the monitoring day. This selection was made along with the systems operators, seeking to include the variables that in a certain case can provide abnormality evidence in the system. Regarding to vibration monitoring signals, 210 symptoms were calculated each monitoring day, also based on operators experience and appropriate literature. Among them highlights scalar estimators as: average, RMS value, peak value, peak to peak value, shape factor, standard deviation, bias, among others. In this way a new observation matrix of symptoms will contain 235 variables and 157 observations. The symptoms observation matrix from a system is represented on Figure 8, where columns are different measured symptoms and rows are observations or measurements made for every symptom in different life cycle times of technical system.

6 LIMIT VALUE ESTABLISHMENT FOR ESTIMATORS

Symptoms limit value of diagnosis systems were calculated according to the following relation [5]:

$$S_{\lim} = \overline{S} + \sigma_P \sqrt{\frac{G}{2A}}$$

Where: $\overline{S}$ is the symptom average value during θ machine operation time

$$O_{pr} = |S_{ij}| = \begin{bmatrix} S_{1,1} & S_{1,2} & \cdots & S_{1,j} & \cdots & S_{1,r} \\ S_{2,1} & S_{2,2} & \cdots & S_{2,j} & \cdots & S_{2,r} \\ \vdots & \vdots & \ddots & \vdots & & \vdots \\ S_{i,1} & S_{i,2} & \cdots & S_{i,j} & \cdots & S_{i,r} \\ \vdots & \vdots & & \vdots & \ddots & \vdots \\ S_{p,1} & S_{p,2} & \cdots & S_{pj} & \cdots & S_{pr} \end{bmatrix} \overbrace{\quad}^{\text{Síntomas Varaibles}} \begin{pmatrix} -\theta_1 \\ -\theta_2 \\ \vdots \\ -\theta_i \\ \vdots \\ -\theta_p \end{pmatrix} \overbrace{\quad}^{\text{Observaciones Mediciones}}$$

$$i = 1, 2, \cdots, p$$
$$j = 1, 2, \cdots, r$$

Figure 8: Symptoms observation matrix.

and the symptom standard deviation, σ_P , ^{A} - is the tolerable level of unnecessary established repairs and G is the machine availability.

Figure 9 shows up the relation between the manufacture established limit and the previous calculated method. The set limit observed can be found way above from normal data behaviour therefore do not show variable changes evidence. On the other hand, the calculated limit can identify subtle variable changes being in an historical behaviour range.

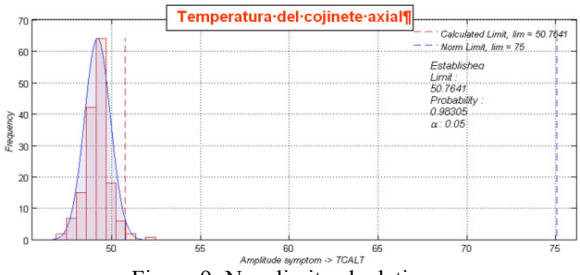

Figure 9: New limit calculation.

6 SINGULAR VALUE DECOMPOSITION

Following the proposed methodology, symptoms observation matrix, its dimensions are reduced through PCA. Then the Singular Vale Decomposition (SVD) is applied with the purpose of extracting different failure modes that evolve in a system, assessing the wear advance used en new indexes and ratios. The SVD application for sizing the symptoms observation matrix can be expressed as follows (Potter 1984):

$$O_{pr} = U_{pp} * \sum_{pr} * V_{rr}^{T}$$

U_{pp} : dimension orthogonal matrix. p , are the left singular vectors. : V_{rr} is an r dimension orthogonal matrix of right singular vectors. : $\sum_{pr}$ is a diagonal matrix of singular values.

The failures profiles are determined using singular values and vectors found with SVD, obtaining a condition evolution interpretation of technical system. These failures are given by (Richardson 1995):

$$SD_t = O_{pr} \times v_t = \sigma_t \cdot u_t$$

Where SD_t is the left singular vector amplified by a respective singular value σ_t . Hence this value leads as bug and information about intensity of failures due to the inclusion of σ_t (Richardson 1995).

The total generalized failure profile $P(\theta)$ or $SumSD$, which represents the general evolution of condition of technical system is determined through (Tournay 2001):

$$P(\theta) = SumSD = \sum_{i=1}^{z} \left| SD_i(\theta) \right|$$

7 IMPLEMENTATION METHODOLOGY

During the implementation methodology at La Herradura's Mini-central an evolving failure on Francis turbine was detected, which is showed up on Figure 10.

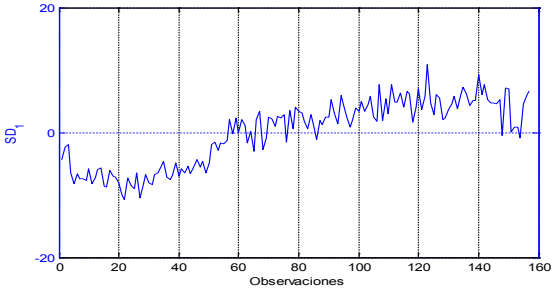

Figure 10: First water turbine failure evolution.

The technical diagnosis showed up that the evolution profile of machine was strongly correlated with variables that describe the technical condition of first Francis turbine bearing. The temperature, the relative axis displacement with respect to combined bearing and the 225 Hz spectral component are part of diagnosis parameters that dominate in this first evaluation unit. The observed frequency corresponds the pitch frequency of blades of the Francis turbine. A continuous component increase was observed during the machine operation time. This occurs as a consequence of interaction between impeller blades and distributor moving blades, a pulse is generated due to the frequency flow pressure of impeller blades (225 Hz, this pulse is labyrinths transported from turbine seals causing an axis push in axial sense, generating a vibration at the same frequency level. With the turbine seals wearing increase, the pulse effect increases, hence, the axial push increases generating vibrations increase.

On Figure 11 the diagnosis parameters tendencies are showed up for Francis turbine operating time related to identify failure.

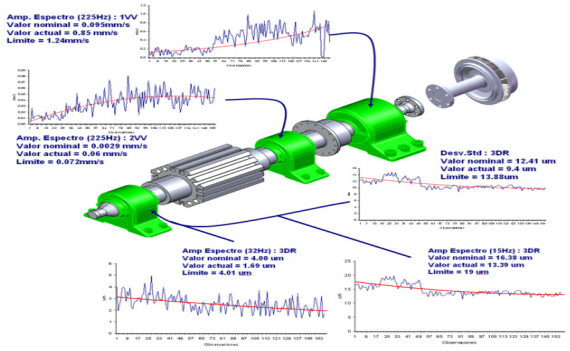

Figure 11: Vibrations evolution related to failure profile.

The probabilistic decision model (Figure 12) and reliability symptoms function (Figure 13) of Francis turbine were determined with important information in any strategy of critical operating systems maintenance. These machine's behaviour patterns allow making correct decisions just in time and reducing risk. It is important to remember the implemented methodology during this project, which is based on real data of Francis turbine condition during utility time.

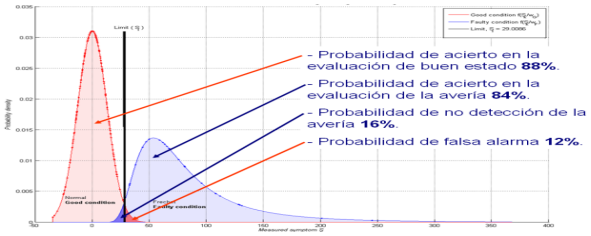

Figure 12: Probabilistic diagnosis model.

8 CONCLUSIONS

Techniques and algorithms used in different branches of science can be applied to technical condition monitoring, as the case of main components analysis and the singular values decomposition.

The multidimensional symptoms monitoring allows identifying changes in the system technical condition and establish possible causes from that condition.

This kind of monitoring in the specific analysed case generate a maintenance decision-making support, which impacts in cost reduction related to maintenance and optimal personal use besides, it generates an increase in the system's availability and reliability.

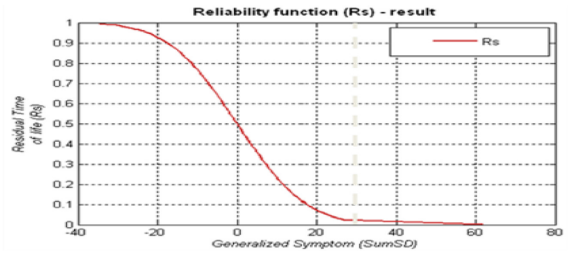

Figure 13: Reliability symptoms function of Francis turbine.

The study was made in real exploitation conditions, considering dynamic variables of generators with the purpose of obtaining information about the general technical condition of system.

REFERENCES

Bongers D. R., 2004. Development of classification scheme for fault detection in long wall systems. Brisbane, Australia.

Cempel C., 1999. Innovative Developments in Systems Condition Monitoring. Key Engineering Materials, vol 167-168, Poznan, Poland, pp. 172-188.

Cempel C., 2003. Multi - fault condition monitoring of mechanical system in operation. XVII IMEKO, Dubrovnik, Croatia. pp.1-4 .

Formenti D., Richardson M.H., 1986. Global Frequency & Damping from Frequency Response Measurements. 4th International Modal Analysis Conference, Los Angeles, CA.

International union of railways, 2003. Testing and approval of railway vehicles from the point of view of their dynamic: behaviour – safety – track fatigue – ride quality. UIC 518, Paris, France, 212p.

National Instruments, 2004. DAQ, Quick Start Guide, Austin, USA. 144p.

Natke H. G., Cempel C., 1997. Model-aided diagnosis of mechanical systems. Fundamentals, Detection, Localization, and Assessment. New York: Springer-Verlag. 248 p. ISBN 3540610650.

Natke H. G., Cempel C., 2001. Symptom observation matrix for monitoring and diagnosis. In: Journal of sound and vibration. Hanover, Germany University of Hanover. pp.609 - 613.

Potter J., Richardson R., 1984. Identification of the Modal Properties of an Elastic Structure from Measured Transfer Function Data. 20th International Symposium, Albuquerque, New Mexico.

Richardson, M., 1995. Modal Analysis Using Digital Test Systems. Seminar on Understanding Digital Control

and Analysis in Vibration Test Systems, Shock and Vibration Information Center Publication, Naval Research Laboratory, Washington D.C.

Tournay H., 2001. Guidelines to best practices for heavy haul railway operations: wheel and rail interface issues. International Heavy Haulage Association – IHHA, Missouri, USA.

Żółtowski B., Castaneda L., 2006a. Portable diagnostic system for the metro train. Diagnostyka, nr 1(37), Olsztyn, pp.39-44.

Żółtowski B., Castaneda L., 2006b. Sistema Portail de Diagnostico para el Sistema Metro de Medellin. VIII Congresso International de Mantenimiento, Bogota, Columbia.

Żółtowski B., 2007a. Diagnostic system maintenance the ability of machines. Eksploatacja i Niezawodność, Nr 4 (36) pp.72-77.

Żółtowski B, Castañeda L, Betancourt G., 2007b. Monitoreo Multidimensional de la Interfase Vía-Vehículo. Congreso Internacional de Mantenimiento, ACIEM, Bogotá, Colombia.

Żółtowski B., Castañeda L., Betancur G., 2007c. Monitoreo multidimensional de la condición (MMC) basado en la descomposición en valores singulares (SVD) Caso de estudio: sistema ferroviario. En: Revista Universidad EAFIT. Julio - Agosto - Septiembre, vol. 43, no. 147, pp. 81-94. ISSN 0120-341X.

Żółtowski M., 2011. Management information systems in fabrication engineering. ITE - PIB, Radom ISBN 978-83-7204-919-3, 271 p. (in Polish).

Projection Method for Solving Systems of Linear Equations Using Wavelet Packet Decomposition of the Residual

Vasily Esaulov and Roman Sinetsky
Platov South-Russian State Polytechnic University (NPI)
Prosveschenia Str. 132,, Novocherkassk, Rostov Region, Russia
esaul_va@mail.ru, rmsin@srspu.ru

Keywords: Systems of Linear Equations, Projection Methods, Wavelet Packet Decomposition, Entropy Criteria.

Abstract: The work is devoted to the problem of solving large systems of linear algebraic equations with irregular structure matrices. To solve them the variant of the projection method in the Petrov-Galerkin form is proposed. Most of the known projection methods is based on the use of bases of Krylov subspaces. The main difference of the proposed method is the choice of the basis from coefficients of wavelet packet decomposition of the residuals. In general, the wavelet transform can be adaptive due to the entropic criteria for the evaluation of elements of the wavelet tree. This distinguishes the proposed method from the known FOM method, the GMRES algorithm and other projection solvers. Conducted a series of computational experiments comparing the proposed algorithm with the main existing projection methods. The experiments showed that the proposed algorithm is competitive with the major existing projection type methods, and in some cases can exceed them.

1 INTRODUCTION

The development of computer technology causes transition to more complex models (three- and multi-dimensional geometry in arbitrary areas) in the form of systems of differential equations in partial derivatives and to their discrete analogues on unstructured grids. This leads to the necessity of solving large sparse systems of linear algebraic equations with irregular matrices, for example, in the analysis of three-dimensional scanning of complex shapes, tomography, etc.

The most efficient and robust among the iterative methods for the solution of such systems of equations are projective techniques, especially the class that is associated with the projection on the Krylov subspace (Saad, 1981). These methods have a number of advantages: they are stable, allow effective parallelization, works with different row and column formats and different types of preconditioners.

2 BACKGROUND

Consider the system $Ax = b$ and formulate the following problem. Let set some two subspaces $K \subset R^n$ and $L \subset R^n$. Is required to find a vector that would provide a solution to the original system optimum with respect to the subspace L, i.e. to satisfy the Petrov-Galerkin condition (Reddy, 2006):

$$\forall l \in L : (Ax, l) = (b, l) \qquad (1)$$

Grouping both sides of the properties of the scalar product, and noting that $b - Ax = r_x$, condition (1) can be rewritten as:

$$\forall l \in L : (r_x, l) = 0 \qquad (2)$$

i.e. $r_x = b - Ax \perp L$. This problem is called ***the problem of designing the solution x on the subspace K orthogonal to the subspace L***.

In a more general formulation of the problem is as follows. For the original system is known an approximation x_0 to the solution x_*. Required to clarify its amendment $\delta_x \in K$ so that $b - A(x_0 + \delta_x) \perp L$. The condition of Petrov-Galerkin (2) in this case takes the form:

$$\forall l \in L:\ (r_{x0+\delta x},\mathrm{l}) = ((b - Ax_0) - A\delta_x,\mathrm{l}) = (\mathrm{r}_0 - \mathrm{A}\delta_x,\mathrm{l}) = 0\ . \quad (3)$$

Let $\dim K = \dim L = m$. Let's enter in subspaces K and the L bases $\{v_j\}_{j=1}^m$ and $\{w_j\}_{j=1}^m$ respectively. It is easy to see that (3) holds if and only if:

$$\forall j(1 \le j \le m):\ (r_0 - A\delta_x,\mathrm{w_j}) = 0 \quad (4)$$

Introducing matrix notations $V = [v_1 \mid v_2 \mid ... \mid v_m]$ and $W = [w_1 \mid w_2 \mid ... \mid w_m]$ for bases, we can write $\delta_x = Vy$ where $y \in R^m$ – the vector of coefficients. Then (4) takes the form:

$$W^T(r_0 - AVy) = 0\ , \quad (5)$$

from whence $W^T AVy = W^T r_0$ and

$$y = (W^T AV)^{-1} W^T r_0\ . \quad (6)$$

Thus, the decision should be specified in accordance with the formula:

$$x_1 = x_0 + V(W^T AV)^{-1} W^T r_0\ , \quad (7)$$

from which immediately follows an important requirement: ***in practical implementations of projection methods subspace K and L and their bases should be chosen so that the matrix*** $W^T AV$ ***were either low dimensions, or had a simple structure, easy to inversion***.

Formula (7) comprises a wide class of iterative methods. The simplest situation is when the space K and L are one-dimensional. Let $K = span\{v\}$ and $L = span\{w\}$. Then (7) takes the form:

$$x_{k+1} = x_k + \gamma_k v_k\ , \quad (8)$$

and γ_k is easily found from the orthogonality conditions $r_k - A(\gamma_k v_k) \perp w_k$:

$$(r_k - \gamma_k Av_k,\ w_k) = (r_k, w_k) - \gamma_k (Av_k, w_k) = 0\ ,$$

from whence:

$$\gamma_k = (r_k, w_k) / (Av_k, w_k)\ .$$

Let $v_k = w_k = r_k$. Then (8) takes the form:

$$x_{k+1} = x_k + \frac{(r_k, r_k)}{(Ar_k, r_k)}\ .$$

Since the expression in the denominator represents the quadratic form $r_k^T Ar_k$, the process of convergence is guaranteed if the matrix A is symmetric and positive definite.

The main problem of all these methods is the choice of the dimension m of the space K.

3 SOLUTION

In (Esaulov, 2015) proposed an iterative algorithm using wavelet solutions. In the paper we propose to implement (7) using the basis V of elements different from that used in Krylov subspaces.

As a variant of the construction of the basis V can be the basis of containing levels of decomposition the R_0-residuals obtained using the wavelet transform (Chui, 1992). Wavelet theory offers a more flexible signal processing technique than the Fourier transform (Bracewell, 2000). It provides the possibility of analysis of the signal not only by its frequency components, but also localizes them. By using wavelet analysis for signal processing it is advisable to use the methods of multiresolution analysis and fast algorithm for finding the wavelet coefficients. Multiscale representation makes it possible to review the signal at different levels of decomposition.

One of the most well-known algorithms for multiresolution analysis is Mallat algorithm (Resnikoff, 1998). In this algorithm, two filters, a smoothing A and detailing the D, recursively used to obtain data for all available scales. As a rule, filters are of finite impulse response in which the samples of the analysed signal, trapped in a small window, are multiplied by a predetermined set of coefficients, the resulting values are summed, and the window is shifted to calculate the next value of the output. Flowchart of the Mallat algorithm shown in Figure 1.

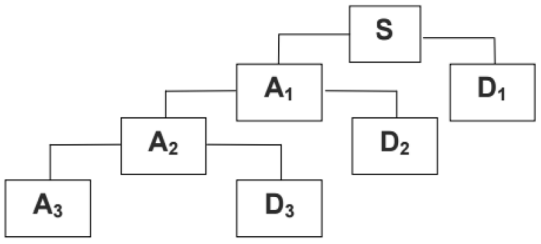

Figure 1: Flowchart of the Mallat algorithm wavelet analysis of a signal S.

It is also known wavelet packet decomposition (Coifman, 1992), which is characterized by repeated filtering of the detailing coefficients. Wavelet packet decomposition allows better control of the separation process of the original signal spectrum into parts, but significantly increases the computational complexity. In addition, the wavelet packet decomposition contains an excessive number of wavelet coefficients, which can be reduced if to

organize the search for "best tree". Wavelet packet decomposition is adaptive, and is widely used for the signal compression and noise reduction. It can adapt more accurately to the characteristics of signals by selecting the appropriate optimal form of the tree decomposition, which provides a minimum number of wavelet coefficients for a given accuracy of reconstruction of the signal, and, thus deliberately excludes from the inverse wavelet transform insignificant, redundant information or unnecessary signal details.

A measure of optimality usually is the number of wavelet coefficients to reconstruct the signal with a given accuracy. It can be performed by entropy, evaluated as:

$$E = \exp(-\sum_n p_n \cdot \log(p_n)) \ , \ p_n = |x_n|^2 \|x\|^{-2} \qquad (9)$$

Any averaging of coefficients increases the entropy. While tree analysis calculates the entropy of a node and its split parts. If the entropy is not reduced, when splitting a node, then further branching from this node does not make sense.

In accordance with the proposed working hypothesis the algorithm of solving of the system of linear equations, using wavelets may be formulated as following steps:

1. Set an initial approximation x_0.
2. Generate wavelet tree of residuals r_0 in accordance with the selected type of wavelets tree building algorithm and (9).
3. On the basis of the wavelet-tree builds subspaces *K* and *L*.
4. In accordance with (6-7) the clarification of solutions is carried out.

There are many ways to build bases *V* and *W*. Using of these methods in solving test problems does not give positive result, due to the bad conditioning of the main matrix in the (5). This occurs because of the proximity of the values of individual rows. In view of smoothing and detailing properties of the wavelet transform has been proposed the following approach.

Let there is a wavelet tree Ω. The basis of the subspace *K* is the set of nodes corresponding to the coefficient of approximation Ω_L. As the basis *W* of the subspace *L* selects the set of nodes Ω_r corresponding to detailing coefficients. This choice can be explained by the fact that in view of the approximation properties of the elements of the basis *V* it will display the most relevant information about the structure of residuals r_0.

The vectors corresponding to the elements of the basis of the subspace *W* of *L* are sparse in many cases. This fact can avoid orthogonalization of the basis *V*.

4 EXPERIMENTS

As test problems was used examples from the Regularization Tools library for MATLAB (Hansen, 2007). The maximum number of iterations was set to 500, convergence error was assumed to be 10^{-9}.

As the first test problem was taken the system of linear algebraic equations of Fox & Goodwin problem (Baker, 1977). The order of the main matrix was set to 100. Table 1 shows values of relative errors of solutions for Fox & Goodwin problem: Transpose-free quasi-minimal residual method (tfqmr), Generalized minimal residual method (gmres), Conjugate gradients squared method (cgs), Quasi-minimal residual method (qmr).

Table 1: Solution of the Fox & Goodwin problem by MATLAB solvers.

Solver	Error, %
tfqmr	0.027
gmres	0.029
cgs	0.025
qmr	0.029

Table 2: Solution of the Fox & Goodwin problem by the proposed algorithm

Wavelet type	Error, %			
	Using the one-dimensional decomposition basis		Using the one-dimensional reconstruction basis	
	$V=A\Omega_L$, $W=\Omega_r$	$V=\Omega_L$, $W=\Omega_r$	$V=A\Omega_L$, $W=\Omega_r$	$V=\Omega_L$, $W=\Omega_r$
db1	0.085	0.066	0.018	0.087
db2	0.064	8.773	0.329	5.197
db8	0.324	5.911	0.125	7.485
sym2	0.064	4.378	0.329	0.356
sym8	0.324	6.172	0.335	6.167
coif5	0.136	23.527	0.427	6.415

Table 3: Solution of the Shaw problem by MATLAB solvers.

Solver	Error, %
tfqmr	0.592
gmres	0.644
cgs	0.602
qmr	0.650

Table 4: Solution of the Shaw problem by the proposed algorithm

Wavelet type	Error, %			
	Using the one-dimensional decomposition basis		Using the one-dimensional reconstruction basis	
	$V=A\Omega_L$, $W=\Omega_r$	$V=\Omega_L$, $W=\Omega_r$	$V=A\Omega_L$, $W=\Omega_r$	$V=\Omega_L$, $W=\Omega_r$
db1	0.920	0.901	31.117	31.117
db2	3.130	2.050	1.992	1.992
db8	1.828	7.002	3.299	3.269
sym2	3.130	3.276	0.570	0.570
sym8	2.869	5.125	3.115	3.115
coif5	1.923	5.141	3.236	3.225

Table 5: Solution of the Baart problem by MATLAB solvers.

Solver	Error, %
tfqmr	0.110
gmres	0.110
cgs	0.110
qmr	0.109

Table 6: Solution of the Baart problem by the proposed algorithm

Wavelet type	Error, %			
	Using the one-dimensional decomposition basis		Using the one-dimensional reconstruction basis	
	$V=A\Omega_L$, $W=\Omega_r$	$V=\Omega_L$, $W=\Omega_r$	$V=A\Omega_L$, $W=\Omega_r$	$V=\Omega_L$, $W=\Omega_r$
db1	1.017	0.054	0.083	0.083
db2	0.522	0.522	4.325	2.143
db8	4.741	11.96	3.858	3.687
sym2	0.522	0.522	3.079	1.254
sym8	6.463	3.670	4.252	24.235
coif5	4.726	4.086	4.531	4.795

The solution by the proposed algorithm using different types of wavelets shown in Table 2: Daubechies (db1, db2, db8), Symlets (sym2, sym8), Coiflets (coif5).

As the second test problem was taken the system of linear algebraic equations of Shaw problem (Shaw, 1972). The order of the main matrix was set to 256. Table 3 shows values of relative errors of MATLAB solvers solutions for Shaw problem. The solution by the proposed algorithm using different types of wavelets shown in Table 4.

As the third test problem was taken the system of linear algebraic equations of Baart problem (Baart, 1982).The order of the main matrix was set to 100. Table 5 shows values of relative errors of MATLAB solvers solutions for Baart problem. The solution by the proposed algorithm using different types of wavelets shown in Table 6.

5 CONCLUSIONS

The paper shows that projection methods using Krylov subspace is a promising method for solving systems of linear equations. Based on conducted analysis, it was formulated the hypothesis about the possibility of using elements of the wavelet decomposition and wavelet reconstruction of the residuals as an alternative to Krylov subspaces. Principles of wavelet analysis of one-dimensional signals using entropy criteria are formed.

Conducted computing experiments have shown that the proposed algorithm is competitive with the major existing projection type methods, and in some cases can exceed them. It is also shown that accuracy of the solution depends on the type of wavelet.

REFERENCES

Saad, Y., 1981. Krylov subspace methods for solving large unsymmetric linear systems. *Mathematics of Computation*, 37:105-126.

Reddy, J. N., 2006. *An introduction to the finite element method* (3rd ed.), Mcgraw–Hill.

Esaulov, V, 2015. An iterative method for solving a system of linear equations using wavelet filters. *Engineering journal of Don*, No. 4, 2015. http://ivdon.ru/ru/magazine/archive/n4y2015/3372 (In Russian)

Chui, C. K., 1992. *An Introduction to Wavelets*. San Diego: Academic Press.

Bracewell, R. N., 2000. *The Fourier Transform and Its Applications* (3rd ed.), Boston: McGraw-Hill.

Resnikoff, H. L., Wells, R. O. Jr., 1998. *Wavelet Analysis*. Springer.

Coifman R.R., Wickerhauser, M.V., 1992. Entropy-Based Algorithms for Best Basis Selection. *IEEE Transactions on Information Theory*, 38(2).

Hansen, P. C., 2007. Regularization Tools Version 4.0 for Matlab 7.3, *Numerical Algorithms*, 46 (2007):189-194.

Baker, C. T. H., 1977. *The Numerical Treatment of Integral Equations*, Clarendon Press, Oxford.

Shaw, C. B. Jr., 1972. Improvements of the resolution of an instrument by numerical solution of an integral equation. *J. Math. Anal. Appl.* 37:83–112.

Baart, M. L., 1982. The use of auto-correlation for pseudo-rank determination in noisy ill-conditioned linear least-squares problems. *IMA J. Numer. Anal.*, 2:241–247.

Data Analysis and Visualization for Industrial Enterprise Water Supply System

Vladislav Noskov, Aleksey Kychkin
Microprocessor Means of Automatization Department, Perm National Research Polytechnic University
Komsomolsky Prospect 29, 614990, Perm, Russia
noskov_v_v_@mail.ru, aleksey.kychkin@gmail.com

Keywords: Water Supply System, Energy Monitoring, Data Analysis and Visualization, OpenJEVis.

Abstract: In this article the method of the industrial enterprises water supply system data analysis based on search of dependences of emergencies number on environmental parameters is considered. The example of water supply system with a standard structure is given, possible places of accidents are shown. The mathematical models of the monitoring results analysis in order to identify the relationship of accidents in knots, piping lines, consumer systems for water supply and sanitation by external factors are proposed. Calculation of correlation function showed dependence of the accident number on water temperature. Histograms of distribution of water temperatures in system and quantities of emergencies, graphics of the average values with use of the smoothing filters, dependence of temperature in the giving system of water from the number of accidents are constructed. Data visualization is carried out with using the OpenJEVis information system. The received results can be used for forming of observations statistics, an impact assessment of other parameters of system, accident rate forecasting. Research has been completed under the PNRPU grant No.2016/PI-2 «Methodology development of monitoring and heat flow utilization as low potential company energy sources».

1 INTRODUCTION

Today industrial enterprises are using a large amount of water except energy resources. Water at the enterprise is used in production processes, for washing and drinking needs, on ensuring fire safety, including fire extinguishing, etc.

Strict requirements are imposed to quality of water that together with requirements for ensuring stable water supply determines both product quality, and overall performance of all enterprise. The permanency in water supply and it`s quality are provided due to use of an effective engineering water supply system, standards and regulations, the supplied system of monitoring of emergencies with functions of control and forecasting (Hong et al., 2013). Such engineering system, which includes a subsystem of water treatment and water disposal (sewerage), is represent the geographically distributed network with a huge number of consumers, nodes and complex pipeline topology (Jacobsen, 1985).

Despite daily control and elimination of various emergencies, for example, breaks of the pipeline, leakages in systems of consumers or in nodes, etc., time periods when the number of accidents considerably exceeds average values we be observed (Seem, 2007). Usually such time frames fall on the summer period when it becomes difficult to find a leakage. Besides, there can be several emergencies at the same time that leads to a stop of production process or brings big water losses as a resource. That`s why data analysis and visualization for the production enterprise water supply system based on the searching dependences of accidents number on external factors, including water temperatures of a source and the environment is an urgent task (Lyakhomskii, Perfil'eva, Kychkin and Genrikh, 2015).

2 WATER SUPPLY SYSTEM

Production of concrete designs, silicate blocks and other construction materials requires the large volume of water therefore the engineering water supply system of such production represents by the big territorially distributed network. The purified

water on system of pipelines arrives to consumers, who are divided on large consumers. For example it can be a production of materials, cooling systems for compressors and power units, small consumers, including various processing equipment, economic, etc.

At the entity the closed water use cycle implying its reuse at the expense of the developed sewer system and cleaning is realized. The main volume of water is concentrated into the accumulation system. For maintenance of the set water level exist an additional water source.

Large engineering system of water supply geographical distribution, outdated technologies of water supply and pipeline systems, high pressure on sites of technological processes, lead to emergence of emergencies in various positions are shown in the figure 1. Such data can be collected using the energy monitoring system (Kychkin, 2016).

On the scheme the following designations are used:

$n_{p_{1..j}}$ – the accidents number on large consumers per day, where j – the number of large consumers;

$n_{p_{j+1..i}}$ – the accidents number on small consumers per day, where i – a total quantity of consumers at the entity;

$n_{L_{1..q}}$ – the accidents number on water supply pipelines per day, where q - the number of lines of a supply of water;

$n_{L_{q+1..e}}$ – the accidents number on water disposal lines per day, where e - total of lines;

$n_{U_{1..k}}$ – the accidents number in water supply nodes per day, where k - the number of water supply nodes;

$n_{U_{k+1..m}}$ – the accidents number in water disposal nodes per day, where m – total of nodes.

Total quantity of emergencies in an engineering water supply system of the construction materials production during a day is N:

$$N = n_{p_{1..i}} + n_{L_{1..e}} + n_{U_{1..m}}, \quad (1)$$

where $n_{p_{1..i}} = n_{p_{1..j}} + n_{p_{j+1..i}}$ – total accidents number per day on the party of consumers; $n_{L_{1..e}} = n_{L_{1..q}} + n_{L_{q+1..e}}$ – total accidents number per day on pipelines; $n_{U_{1..m}} = n_{U_{1..k}} + n_{U_{k+1..m}}$ – total accidents number per day in distribution knots.

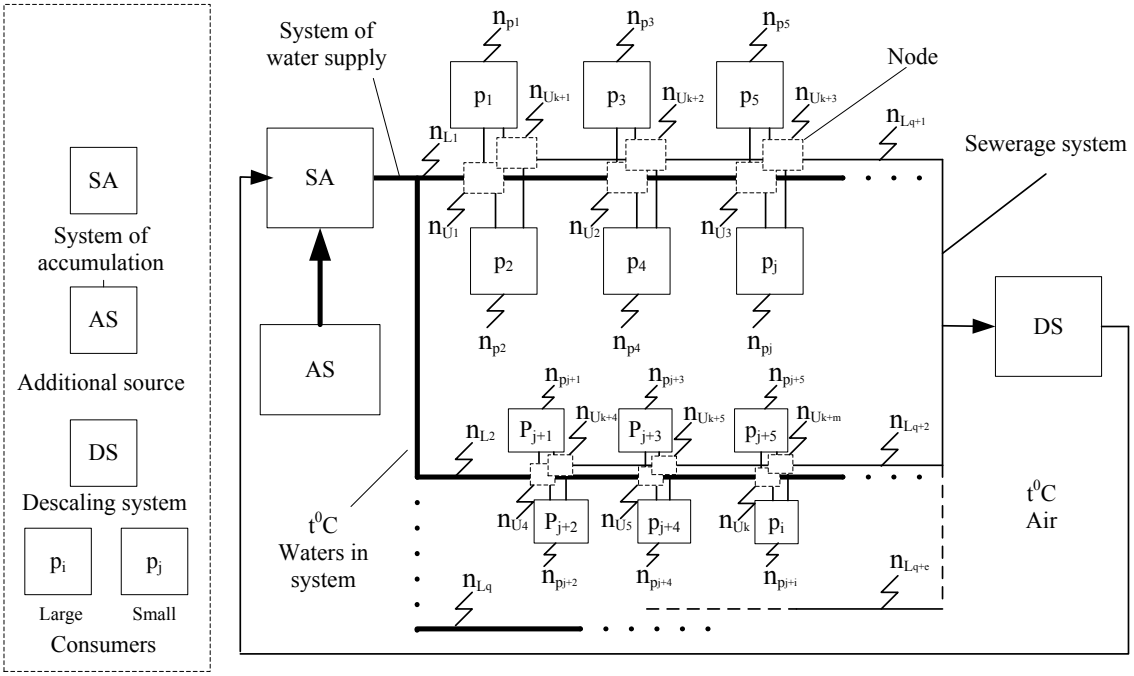

Figure 1: Water supply system structure and emergence accidents places.

3 DATA ANALYSIS

For dependence assessment of accidents number in engineering water supply system from external factors it is necessary to carry out the mathematical analysis of the ambient temperature and water temperature in a source observations results (Kychkin and Mikriukov, 2016). To find the values of the degree of temperature influence on the number of accidents it is necessary to analyze the behavior of the function f (Kychkin, 2013):

$$N = f(t_1^0, t_2^0), \tag{2}$$

where $t_1{}^0$ – air temperature in the period of emergencies; $t_2{}^0$ – source water temperature in the pipeline.

Correlation coefficients for couples of observations (N, $t_1°$) and (N, $t_2°$) can be found using formulas:

$$r_{N,t_1^0} = \frac{\sum(\overline{N}-N)\cdot(\overline{t_1^0}-t_1^0)}{\sqrt{\sum(\overline{N}-N)^2}\cdot\sqrt{\sum(\overline{t_1^0}-t_1^0)^2}}, \tag{3}$$

$$r_{N,t_2^0} = \frac{\sum(\overline{N}-N)\cdot(\overline{t_2^0}-t_2^0)}{\sqrt{\sum(\overline{N}-N)^2}\cdot\sqrt{\sum(\overline{t_2^0}-t_2^0)^2}}, \tag{4}$$

where $\overline{N}$ – the average number of accidents in engineering water supply system in one day; $\overline{t_1^0}$ – average value of air temperature in the period of emergencies; $\overline{t_2^0}$ – average value of source water temperature in the pipeline.

The correlation coefficient for couples of observations (N, $t_1°$) has made 0.35. This value means that there is weak dependence between two of these parameters. For couples of observations (N, $t_2°$) it has made 0.62 that corresponds to average degree of dependence. On the basis of these results we will choose dependence between the number of accidents and value of temperature in system of water supply.

To evaluate the frequency of origin abnormal a situation and the frequency of appearance of values of temperatures in the giving system of water-supply, it is necessary to construct the distributed histogram for a summer season for 2015 and 2016. In a figure 2 the distributed histogram of number of accidents in two years is shown. On a graphics asymmetry to the left – offset of the histogram in the left part is watched. It is visible that there is a mean value of number of accidents which makes 3 accidents for 2015 and 6 accidents for 2016.

In the figure 3 the temperature values distribution histogram for the source system in two years is constructed. The data bimodalness can be observed. It means that distribution isn't normal.

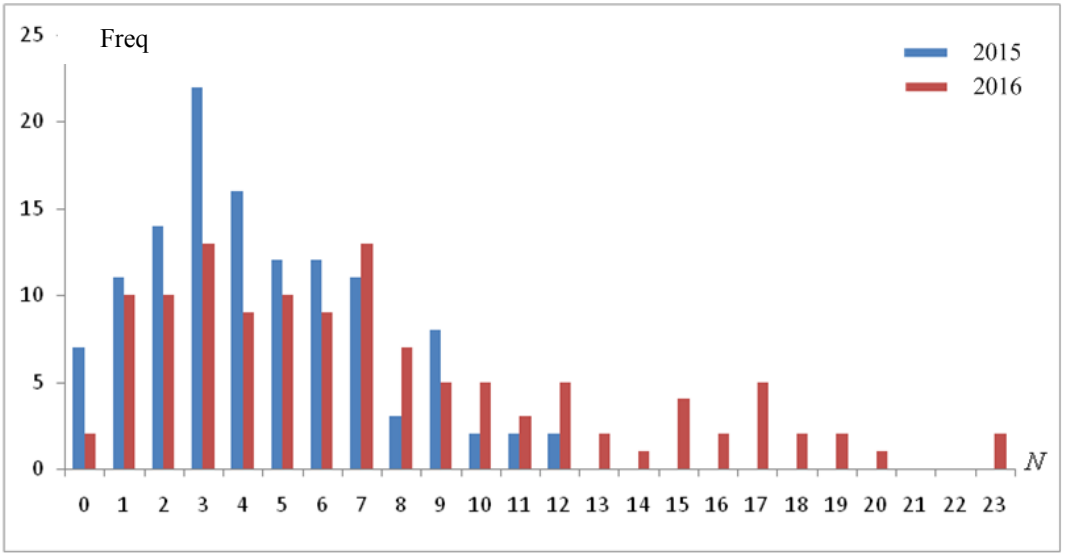

Figure 2: The accidents number distribution histogram.

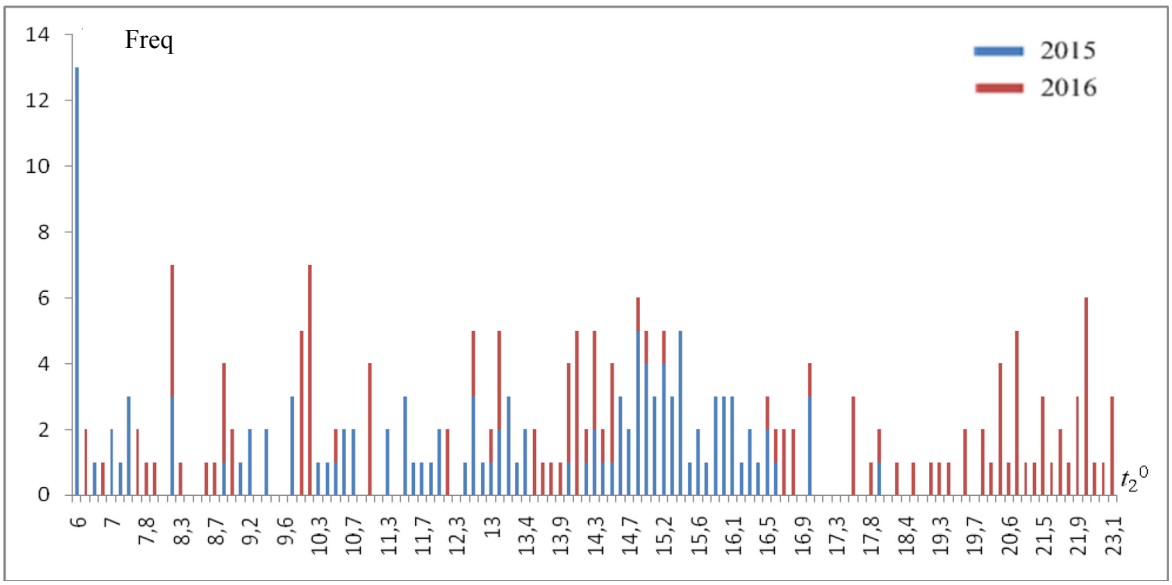

Figure 3: The temperature distribution histogram for water supply system.

Moving average is proposed to use for the data smoothing. It will allow to show the hidden changes on graphics.

For creation of moving averages will be used three types:

- simple (simple moving average, SMA);
- exponential (exponential moving average, EMA);
- weighted (weighted moving average, WMA).

For the construction of the simple average sliding it is necessary to use a formula (Prerez-Lombard, Ortiz, Pout, 2008):

$$SMA(k,n)=\frac{1}{n}\sum(x_1+x_2+\ldots+x_{k-(n+1)}), \qquad (5)$$

where $EMA[k, n]$ — the simple sliding n period average at the time of k; $x_{k-(n+1)}$ – the current value at the moment k-(n+1).

For the construction of sliding weighed it is necessary to use a formula:

$$WMA[k,n]=\frac{n\cdot x_k+(n-1)\cdot x_{k-1}+(n-2)\cdot x_{k-2}+\ldots+x_{k-(n+1)}}{\left(\frac{n\cdot(n+1)}{2}\right)} \qquad (6)$$

where $WMA[k, n]$ — the weighed sliding n period average at the time of k.

For the construction sliding exponential it is necessary to use a formula:

$$EMA[n]=q\cdot x_n+(1-q)\cdot EMA[n-1], \qquad (7)$$

where $EMA[n]$ — the exponential sliding average with n period; q – weight coefficient in the range from 0 to 1, reflecting the speed of aging of last data; $EMA[n\text{-}1]$ – value of the exponential sliding average calculated for the previous period.

4 RESULTS VISUALIZATION

For data visualization will be used open software OpenJEVis by Envidatec GmbH Company (Faizrakhmanov, Frank, Kychkin and Fedorov, 2011) and RapidMiner software.

Water supply system temperature and environment air temperature for 2016 schedules are shown in the figure 4.

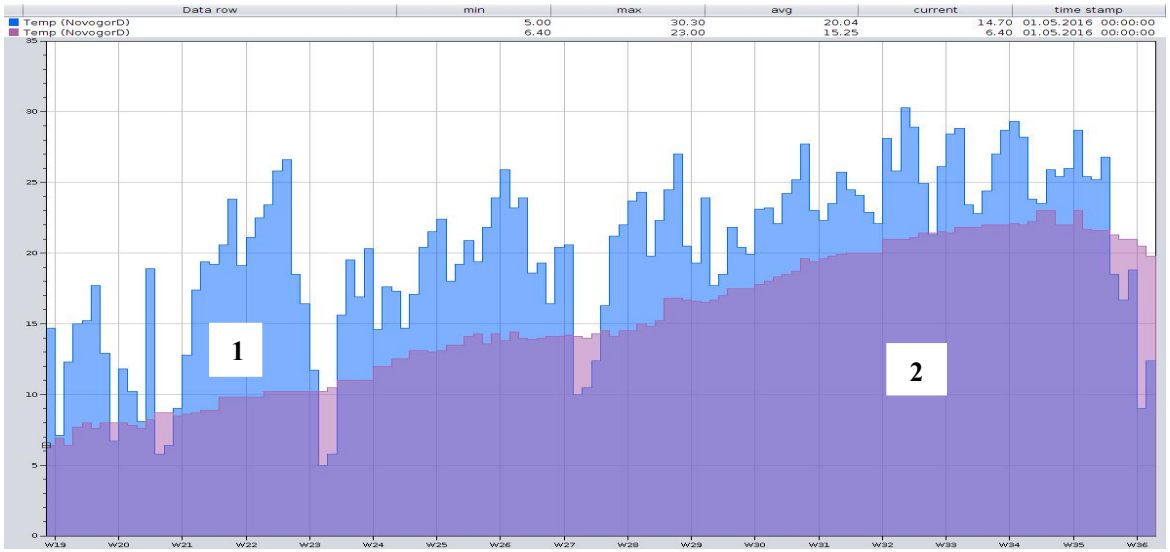

Figure 4: Environment air temperature (1) and temperature in water supply system (2).

In the figure 5 accidents number schedule in water system for 2016 is shown. After 28 week the accidents number was increased. This period coincided with the onset of warm weather in a region.

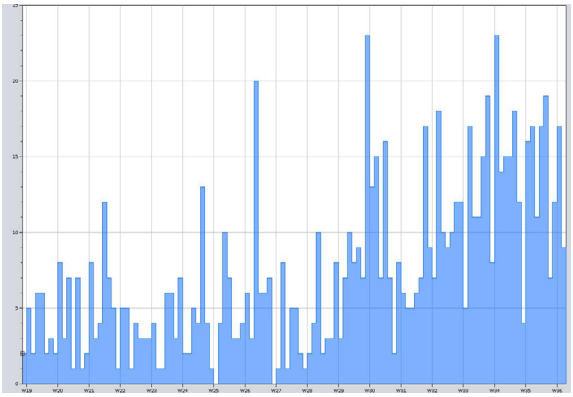

Figure 5: Accidents number in the water supply system.

In the figure 6 the simple moving average for accidents curve and water supply system temperature is shown. Accidents number increased in those days when water temperature in system was more than 15 degrees (t_2>15 °C).

The curves can be divided into two areas. Area *I* corresponds to area in which the number of accidents remains invariable.

Area *II* is an area in which the accidents number increases with increasing water temperature. Areas *I* and *II* are divided by temperature value t_2=15 °C.

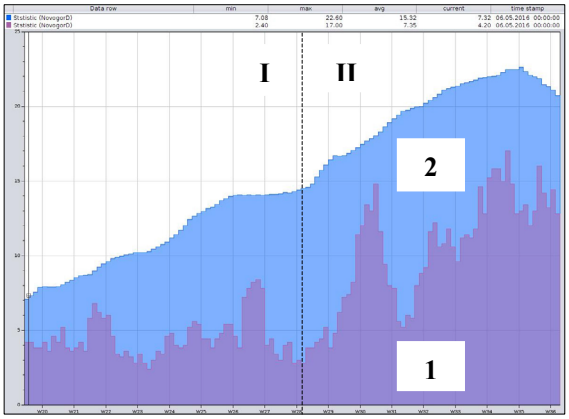

Figure 6: The moving average for accidents curve (1) and water supply system temperature (2).

It is possible to assume that function *f* can be piecewise determinate using statistic analysis (Claridge, 1998). The main results of calculations are given in table 1.

Table 1: Calculations results for 2016 year.

Parameter	t_1, °C	t_2, °C	*N*
Total accidents	-	-	930
Average value per day	20	15.3	7
Min	5	6.4	0
Max	30.3	23	23
Correlation coefficient	N, t_1°	N, t_2°	-
	0.35	0.62	-

5 CONCLUSIONS

The carried-out analysis and visualization of an engineering water supply monitoring results of the industrial enterprise specializing in release of construction materials are showing relation between numbers of emergencies and water temperature in system. This dependence is observed in case of excess of water temperature 15 ^{0}C. According to specialists this relation can be caused by increase in concentration of dissolved oxygen in water that is in turn leads to corrosion processes speed increasing. At the same time relation between water and air temperature is observed. In order to prevent the growth of emergencies it is proposed to realize water accumulating system based on isolated reservoirs, which are located at a depth of 1-2 meters of soil freezing level. In this case the level of ambient temperature influence on water temperature in the system during the season periods of year is minimal. The proposed analysis can be used for accident forecasting in the water supply system of other manufacturing and municipal services of the city.

REFERENCES

Claridge, D. E., 1998. *A Perspective on Methods for Analysis of Measured Energy Data from Commercial Buildings,* Journal of Solar Energy Engineering. 120(3).

Jacobsen, F.R., 1985. *Energy signature and energy monitoring in building energy management systems,* Proceeding of CLIMA 2000 World Congress, vol. 3: Energy Management.

Lyakhomskii, A.V., Perfil'eva, E.N., Kychkin, A.V., Genrikh, N. A., 2015. *A software-hardware system of remote monitoring and analysis of the energy data*, Russian Electrical Engineering. 86 (6), pp. 314-319.

Hong, T., Feng, W., Lu, A., Xia, J., Yang, L., Shen, Q., Im, P., Bhandari, M., 2013. *Building energy monitoring and analysis,* Lawrence Berkeley National Laboratory.

Seem, J.E., 2007. *Using intelligent data analysis to detect abnormal energy consumption in buildings*, Energy and Buildings, vol. 39, no. 1, pp. 52–58.

Prerez-Lombard, L., Ortiz, J., Pout, C., 2008. *A review on buildings energy consumption information*, Energy and Buildings, vol.40, no. 3, pp. 394–398.

Kychkin, A.V., 2013. *Intelligent information and diagnostic system for examining blood vessels*, Journal of Computer and Systems Sciences International. T. 52(3), pp. 439-448.

Faizrakhmanov, R.A., Frank, T., Kychkin, A.V., Fedorov, A.B., 2011. *Sustainable energy consumption control using the My-JEVis energy management data system*, Russian Electrical Engineering. 82 (11). pp. 607-611.

Kychkin, A.V. 2016. *Synthesizing a System for Remote Energy Monitoring in Manufacturing*, *Metallurgist*, Vol. 59 (9-10), pp. 752-760.

Kychkin, A.V., Mikriukov, G.P., 2016. *Applied data analysis in energy monitoring system*, Regional Energy Problems, 2 (31) / 2016.

Using Cluster Analysis in the Synthesis of Electrical Equipment Diagnostic Models

Ksenia Gnutova, Denis Eltyshev
Electrotechnical Department, Perm National Research Polytechnic University,
Komsomolsky Ave. 29, 614990, Perm, Russia
{lis, pab}@msa.pstu.ru

Keywords: Electrical equipment, Cluster analysis, Quality criteria, Fuzzy logic, Diagnostics.

Abstract: The article investigates the issue of improving the methods of diagnostics of electrical equipment conditions to ensure the effective assessment of equipment needs for repairs and its trouble-free, safe and economical operation. The possibility of taking advantage of different cluster analysis methods enables us to form the structure of fuzzy models of electrical equipment diagnostics. The method of synthesis of this class of models takes into account various ways to implement clustering algorithms and criteria for assessing its effectiveness. The software, which we use to study the applicability of methods for the analysis of data on temperature parameters data of transformer equipment, utilises methods such as k-means and fuzzy c-means.

1 INTRODUCTION

The reliability and quality of power supply systems of both industrial and civil use is largely determined by the ability of their constituent electrical equipment (EE) reliably perform specified functions. To solve this problem, it is necessary to organize an effective system of maintenance and repair of the EE with timely prevent potential accidents. An objective method of assessing the needs of the EE to be repaired involves the periodic (discrete) or permanent (continuous) controlling of its technical condition at the moment, at some point in the future (forecasting) and in the past (Solodyankin, 2015, Kychkin, 2016). Such control can be achieved through an integrated approach to improve the methods and technical diagnostics tools in order to ensure a safe, trouble-free and economical operation.

Construction of automated or automated information systems that will reliably diagnose the various elements of the EE and form recommendations to engineering and technical personnel, requires a specific methodology for the creation of models that can detect signs of defect states. The problem of constructing EE diagnosis models is usually quite complex, as it requires taking into account a variety of factors, including changes in the dynamics of equipment parameters and criteria for assessment of its condition, as well as the environment in which it operates (Semenov, 2004). That is why the development of effective methods of diagnosing EE in recent years increasingly applies intelligent technology such as fuzzy logic, in combination with various methods of representation of expert knowledge. To create a fuzzy model, EE diagnosis must perform the procedure and its structural parametric identification. The primary objective in this case is the right choice of parameters that affect the condition of the equipment and the formation of knowledge as well as the construction of the respective membership functions for each variable, and act as input variables of the model. To perform these operations in an automated or automatic mode, which significantly extends the capabilities of diagnostic information systems you can use EE data mining methods in particular, cluster analysis.

2 SETTING GOALS AND OBJECTIVES OF THE STUDY

The aim of this study is to investigate the possibilities of using different methods of cluster analysis to form a fuzzy diagnosis model structure - (FDM) EE.

The main tasks of the research are the following: to develop an algorithm of data clustering analysis for FDM; to perform clustering analysis of the quality assessment criteria; analysis of the influence on the quality of clustering changing the number of clusters and different ways of finding the distance between the clusters and centroids; formation recommendations.

3 ALGORITHM

Let's consider the following EE data clustering procedure in order to use the results for the synthesis of FDM (Figure 1).

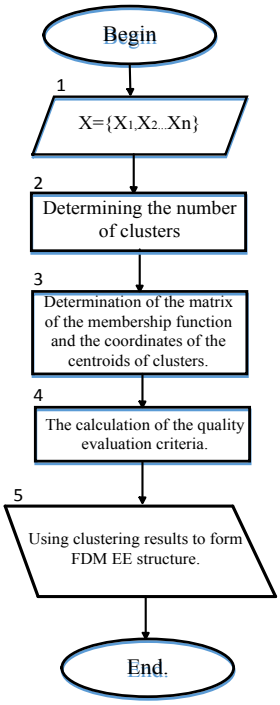

Figure 1: Clustering algorithm.

Initially, the set X input data is given, where n-number of key technical parameters of EE is controlled during its operation and affects the actual state (block 1). The next determined number of clusters is C, which is divided by the test data set. The C parameter can be set by an expert, or calculated in accordance with the established quality of the clustering criterion (block 2) (Kychkin, 2016). Using different methods of cluster analysis, we determine the matrix of membership functions and can find the cluster centroid (block 3). The last stage involves the comprehensive assessment of the cluster analysis quality (block 4).

For the comprehensive evaluation of the cluster analysis quality we will consider the following known criteria (Elizarov, 2009, Khoroshev, 2016, Eltyshev, 2016):

1. The partition coefficient:

$$PC = \frac{\sum_{i=1}^{|X|}\sum_{j=1}^{|C|} u_{ij}^2}{|X|} \quad (1)$$

where Uij is the corresponding element of the matrix accessories, X is the number of elements of the set input, C is the number of elements of the plurality of clusters. This ratio is $1 / C \le PC \le 1$. The closer it is to 1, the clearer the maximum partition is. We must not forget that for a small number of clusters, the partition coefficient gives an incorrect result. To do this without changing the nature of the test, its range has been shifted so that this dependence on the number of clusters C is not associated with the beginning of a specified length, and to its end. Let's perform the experiment by taking the ratio of the partition $1/(|C|)$. The value range of the ratio is in the range $0 \le PCM \le |C| - 1 / (|C|)$. The modified partition coefficient is as follows:

$$PC_M = \frac{\sum_{i=1}^{|X|}\sum_{j=1}^{|C|} u_{ij}^2}{|X|} - \frac{1}{|C|} \quad (2)$$

2. Partition entropy is as follows:

$$PE = -\frac{\sum_{i=1}^{|X|}\sum_{j=1}^{|C|} u_{ij} \ln(u_{ij})}{|X|} \quad (3)$$

where Uij is the corresponding element of the matrix accessories, the X is the number of elements of the set input, C is the number of elements of the plurality of clusters. This ratio takes the value $0 \le PE \le \ln |C|$, the best one what partition corresponds to a value close to 0. This ratio should not be used to compare solutions as well as a range of values for each clustering method will be different. Therefore, a more efficient use of the modified partition entropy is ensured (Khoroshev, 2016). The range for this criterion is not linked to the number of clusters and lies on the interval [0, 1]. The modified partition entropy is as follows:

$$PE_M = -\frac{\sum_{i=1}^{|X|}\sum_{j=1}^{|C|} u_{ij}\ln(u_{ij})}{|X|\ln|C|} = \frac{PE}{\ln|C|} \quad (4)$$

3. The effectiveness partition is as follows:

$$PI = \sum_{j=1}^{|C|}\sum_{i=1}^{|X|} u_{ij}^2\left(d^2(c_j,\bar{x}) - d^2(x_i,c_j)\right) = \sum_{j=1}^{|C|}\sum_{i=1}^{|X|} u_{ij}^2 d^2(c_j,\bar{x}) - \sum_{j=1}^{|C|}\sum_{i=1}^{|X|} u_{ij}^2 d^2(x_i,c_j) \quad (5)$$

where Uij is the corresponding element of the matrix accessories, the X is the number of elements of the set input, C is the number of elements of the plurality of clusters, Cj is cluster center j, $\bar{\mathbf{x}}$ is the arithmetic mean of the input elements of the set, the set Xi is the input set, d is a distance between the elements, which can be defined in different ways (Euclidean distance, Manhattan distance, etc.) (Eltyshev, 2016).

The algorithm provides for the possibility to set the different ways of finding the distance (metric) between the clusters and their centroids when calculating the clustering options. The best known ones are the following: Euclidean distance, Manhattan distance, cosine and correlation, as well as the Hamming distance (Petrochenkov, 2015).

Automatic selection of possible metrics is in accordance with the clustering quality criterion.

4 RESEARCH RESULTS

The research of the cluster analysis algorithm (Figure 1) is carried out using the power characteristics data of a power oil-filled transformer (POT) of the average power. The object of this type is one of the defining elements of the power supply systems of any configuration, and it is important to ensure reliability of power supply to consumers, and to are a come the difficulty in determining damages and defects at an early stage of development (Solodyankin, 2015, Kychkin, 2016, Semenov, 2004). To test the algorithm, we have selected the most popular cluster analysis methods, such as fcm and k-means (Petrochenkov, 2015, Shtovba, 2007). The initial data uses real settings POT, X = {X1, X2}, where X1 is excess temperature contact of live parts, X2 is temperature difference on the surface of the tank POT and cooling system components. The initial data distribution diagram is shown in Figure 2.

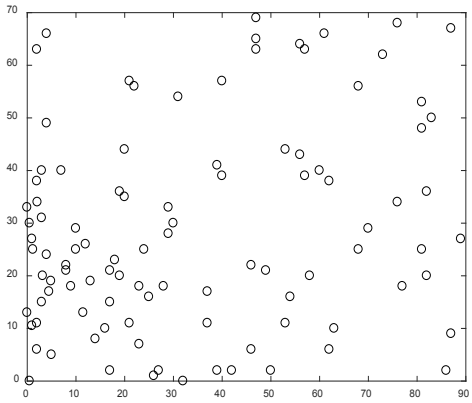

Figure 2: Distribution of raw data.

a)

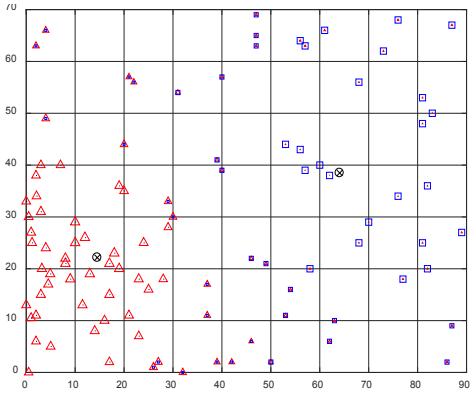

b)

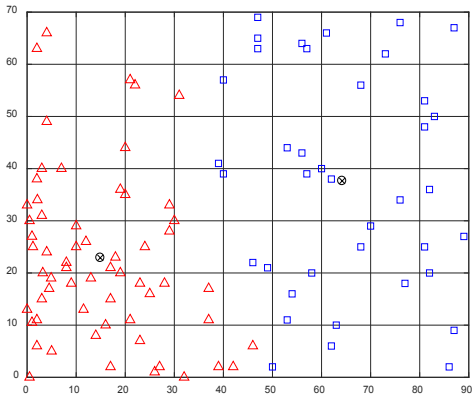

Figure 3: Results of clustering with C = 2, k-means (a) and fcm (b).

a)

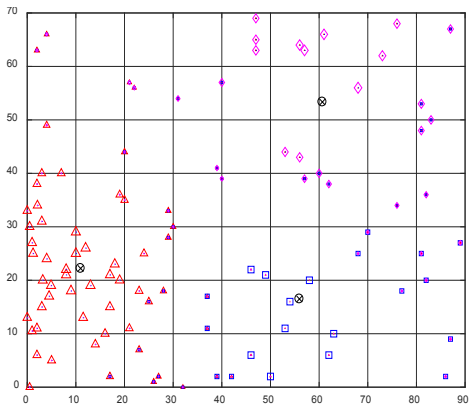

b)

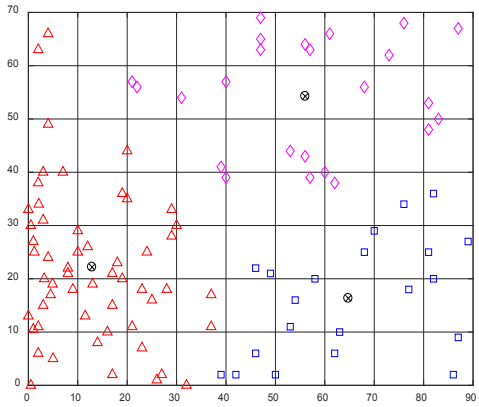

Figure 4: Results of clustering with C = 3, k-means (a) and fcm (b).

As seen in Figure 3 and Figure 4, the centroids belong to two methods when the number of clusters = 2 coincide, and when the number = 3 are different, and there are several elements that are found on the border of another cluster. The silhouette-plot (Figure 5) displays a measure of how close each point in the same cluster is to the points in the neighbouring clusters (Shtovba, 2007, Tosei Hator, 2014).

a)

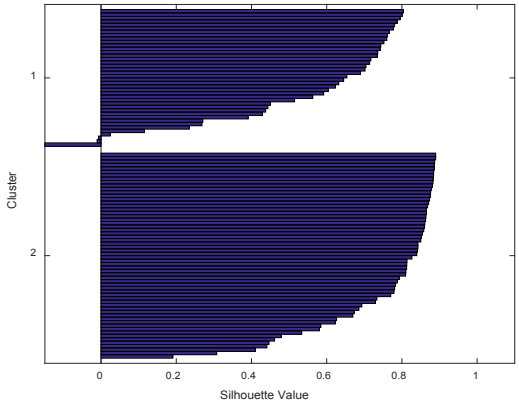

b)

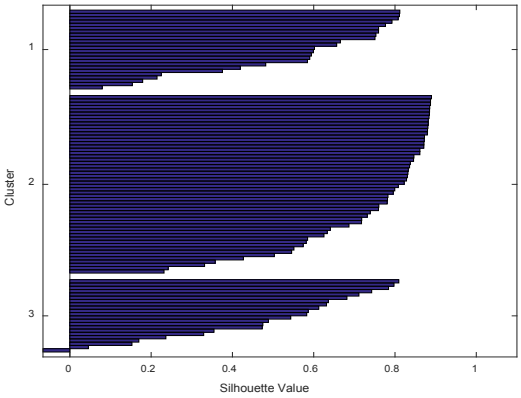

Figure 5: Silhouette-plot for C = 2 (a), C = 3 (b).

Figures 6,7 and 8 presents the results of using the quality criteria for the fcm method. We have obtained familiar indicate adequate quality evaluation data of the cluster analysis method. All the criteria are acceptable in the area. The image shows that the best decomposition occurs when the number of clusters equals to 5.

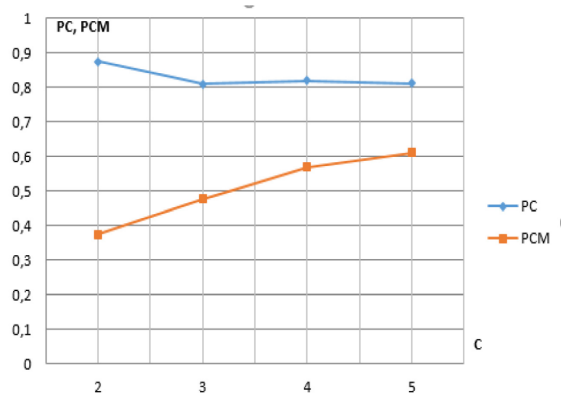

Figure 6: Graph PC, PCM = f (N).

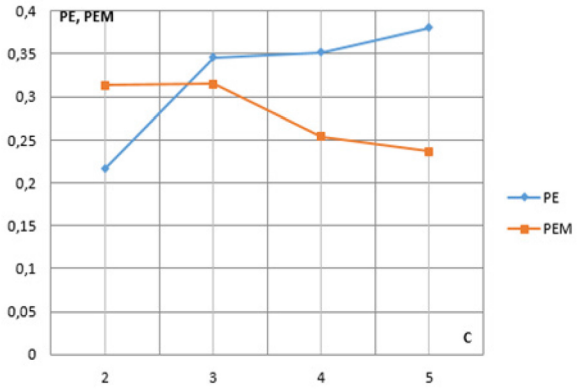

Figure 7: Graph PE, PEM = f (N).

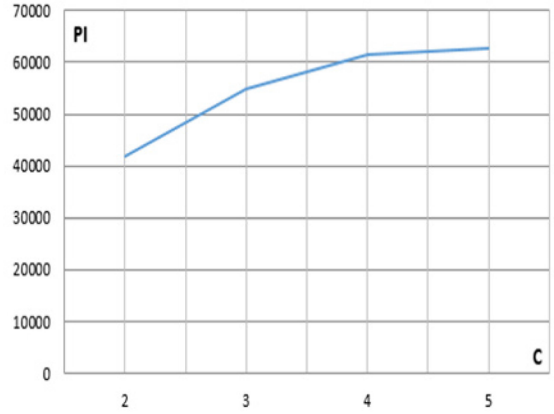

Figure 8: Graph PI = f (N).

Figures 9 and 10 presents the results of the quality criteria for the k-means method, which indicate the complexity of unambiguous assessment of the quality of the selected criteria aggregate. The belonging cluster matrix method, ranging from 0 or 1, makes it impossible to clearly and understandably assess the rate of decomposition and entropy decomposition (Petrochenkov, 2015, Shtovba, 2007). Changes in the clusters centers of coordinates affects the decomposition efficiency. The most adequate assessment method can be provided, based on the data obtained for the modified partition coefficient.

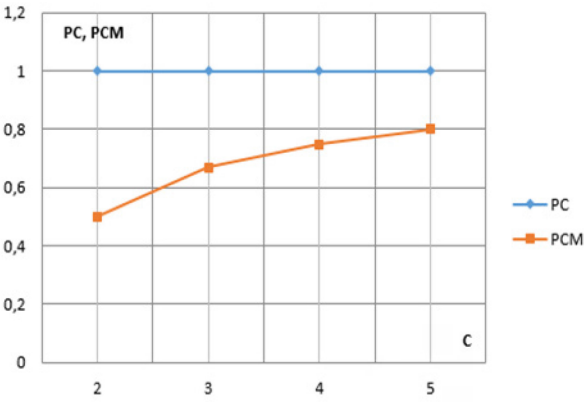

Figure 9: Graph PC, PCM = f (N).

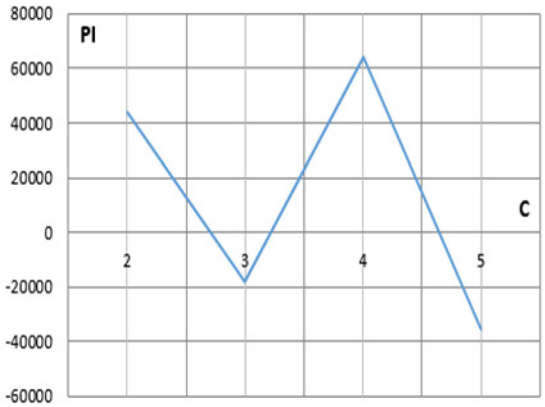

Figure 10: Graph PI = f (N).

5 CONCLUSION

The proposed article technique can be used in the construction of membership functions and rules of the knowledge base FDM. On the basis of a software implementation of clustering techniques in the analysis of known methods (k-means and fcm) made the following conclusions:

1) to determine the FDM structure use fcm method (or modifications thereof), and other methods that allow to evaluate the degree of membership of the input plurality of data items to each of the found clusters during the formation of the partition;

2) to select clustering algorithm and use the advantages of known methods of cluster analysis can

be used existing adaptive methods (Khoroshev, 2016);

3) the use of different criteria for assessing the quality of clustering does not allow an unambiguous conclusion about the optimal partition in terms of building FDM, therefore in order to find the desired number of clusters is necessary to take into account its impact on the accuracy of the classification performed using FDM.

Practical application of the methods, taking into account these factors will allow to formalize the procedure for constructing FDM and use them in automated and automatic control systems technical condition of the EE periodically, or on-line mode.

REFERENCES

Solodyankin A.A., Kolesnikov A.A., Grisha B.G., Nazarov A.A., Yanovich I.M. (2015), 'Modern methods of diagnostics and technical state assessment of the high-voltage electric power equipment', *Journal of Science and Technology*, 2, pp. 70-72.

Kychkin A.V., Mikriukov G.P. (2016), 'Applied data analysis in energy monitoring system', *Journal of Problems regional energy*, 2(31), pp. 84-92.

Semenov V.V. (2004). *Diagnosis and monitoring of high-voltage oil-filled electrical equipment.* Ufa. Ufa State Aviation Technical University.

Elizarov S.I., Bargesyan A.A., Kupriyanov M.S., Holod I.I., Tess M.D. (2009). *Analysis of the data and processes.* 3rd edition, Saint-Petersburg: BHV-Petersburg.

Khoroshev N.I., Pogorazdov R.N. (2016), 'Adaptive Clustering Method in Intelligent Automated Decision Support Systems', *Proceedings of the 19th International Conference on Soft Computing and Measurements.* SCM`2016, pp. 296-298.

Eltyshev, D.K., Boyarshinova, V.V. (2016), 'Intelligent Decision Support in the Electrical Equipment Diagnostics', *Proceedings of the 19th International Conference on Soft Computing and Measurements*. SCM 2016, pp. 157-160.

Petrochenkov A.B. (2015), 'Management of Effective Maintenance of the Electrotechnical Complexes of Mineral Resource Industry's Enterprises Based on Energy-information Model', *Proceedings of International Conference on Soft Computing and Measurements*. SCM 2015, pp. 122-124.

Shtovba S.D. (2007). *Design of fuzzy systems tools MATLAB* // S.D. Shtovba., Moscow: Telecom.

Tosei Hatori, Mika Sato-Ilic. (2014), 'A fuzzy clustering method using the relative structure of the belongingness of objects to clusters', *Journal of Procedia Computer Science*, 35, pp. 994 – 1002.